NOTICE

The quality of this microform is heavily dependent upon the quality of the original thesis submitted for microfilming. Every effort has been made to ensure the highest quality of reproduction possible.

If pages are missing, contact the university which granted the degree.

Some pages may have indistinct print especially if the original pages were typed with a poor typewriter ribbon or if the university sent us an inferior photocopy.

AVIS

La qualité de cette microforme dépend grandement de la qualité de la thèse soumise au microfilmage. Nous avons tout fait pour assurer une qualité supérieure de reproduction.

S'il manque des pages, veuillez communiquer avec l'université qui a conféré le grade.

La qualité d'impression de certaines pages peut laisser à désirer, surtout si les pages originales ont été dactylographiées à l'aide d'un ruban usé ou si l'université nous a fait parvenir une photocopie de qualité inférieure.

ISBN 0-315-53818-X

ANALYSIS OF STRAIGHT, CONTINUOUS PLATE-GIRDER BRIDGES

A Computer Analysis by Finite Strip Method

by

Wilson W. S. Lau, B.ASc.

A thesis
Submitted to the School of Graduate Studies
in partial fulfillment
of the requirements for the degree of
Master of Applied Science

Department of Civil Engineering
Faculty of Engineering
University of Ottawa
December, 1987

ACKNOWLEDGEMENTS

The work described in this thesis was conducted under the supervision of Dr. M. S. Cheung during the course of study for the degree of Master of Applied Science in the Civil Engineering Department at the University of Ottawa.

The author wishes to express his deepest gratitude for the constructive advice and guidance of Dr. M. S. Cheung.

Thanks are due to the assistance of Mr. W. Li and the generous support of the computer facilities provided by the computer center at the University of Ottawa.

The assistance and criticism of Miss I. Leung, Miss P. Ho and Mr. H. Hachem in the course of the writing stage of this thesis are greatly appreciated.

The author would like to thank his girl friend, Eva for her understanding, patience and encouragement.

The author also wants to give thanks to his parents and family for their loving, caring and financial support.

Mostly, thanks God for this opportunity and His blessings.

ABSTRACT

In this thesis, the linear analysis of straight simply supported, continuous plate-girder bridges is discussed. There are numerous methods which can be used for the analysis, but the two most widely employed ones are the Finite Element Method and the Finite Strip Method. When the two methods are compared with each other, the Finite Strip Method is chosen because of its advantages – such as easier in programming, less core storage, more economical, and suitable for micro-computers – over the Finite Element Method.

In the past, similar analysis has been carried out by using the Finite Strip Method with conventional approach (i.e. the combination of the finite strip analysis and the flexibility method). However, the convergency of the solution is very slow. In order to improve the rate of the convergency, a new continuous strip is developed for the Finite Strip Method. The displacement function of this new strip is approximated by the solution of the free vibration equation of a continuous beam in the longitudinal direction and an appropriate polynomial function in the transverse direction. This continuous beam vibration function is employed because it can well describe the displacement patterns and satisfy all the boundary conditions in the longitudinal direction. Also, it is a continuously differentiable smooth function and possesses the valuable properties of orthogonality.

The formulation of the continuous finite strip is developed in terms of the curvilinear coordinate system so that bridges with non-uniform girder depth can be analyzed. Case studies showed that these formulation can accurately predict the structural response of such haunched bridges. As a result, a computer program –

the strip program – has been written for the analysis by using the new approach of the Finite Strip Method.

Finally, a number of examples including beams, plates and actual bridge model are given to demonstrate the general applicability of the strip program. The accuracy of the theoretical solutions obtained from the Finite Strip Method is shown by comparing the results solved by the beam theory and/or the Finite Element Method (ADINA). The rapid convergency of the new approach has also been demonstrated by these numerical examples.

Contents

List of Figures

List of Tables

NOMENCLATURE

A	=	cross-sectional area
$A_{i,j}$	=	mode shape
b	=	the width of a strip
b_1	=	the actual width of the haunched web (strip)
b_f	=	the width of a flange strip
b_h	=	a fraction of the actual width of the haunched web
$[B]$	=	strain shape function
$[B_{fm}]$	=	the $[B]$ matrix for the flange strip in curvilinear coordinates
$[B^f_{ip}]$	=	the in-plane bending matrix for flange strip
$[B^w_{ip}]$	=	the in-plane bending matrix for web strip
$[B_{wm}]$	=	the $[B]$ matrix for the web strip in curvilinear coordinates
$[C]$	=	the coefficient matrix for displacement function
$[D]$	=	the material porperties matrix
E	=	the modulus of elasticity
$f_m(x)$	=	polynomial function in transverse direction (x-direction), subscript m indicates the m th term
$f(\xi)$	=	a general function of any degree

F = inertia force

$\{F\}$ = load matrix

G = shear modulus

I = moment of inertia

l_i = span length,
subscript i indicates the i th span

L = length of a strip

M = bending moment

$q(x)$, $q(y)$ = loading functions in x and y direction respectively

$\{q\}$ = loading matrix

$[S]$ = stiffness matrix

t = thickness of a finite strip

$[T_r]$ = transformation matrix

u = displacement in x-direction

U = force in x-direction

U_s = strain energy of a finite strip

U_p = potential energy of a finite strip

U_t = total potential energy of a finite strip

v = displacement in y-direction

V = force in y-direction

V_s = shear force

w = displacement in z-direction

w_{im}, w_{jm} = displacement parameters of a bending strip

$w(x,y)$ = displacement function

W = force in z-direction

$\mathcal{W}$ = weight coefficient

Y_m = harmonic series in longitudinal direction, subscript m represents the mth term

x, y, z = cartesian coordinates

ρ = density

ω = angular frequency of beam

μ = eigen solution of Y_m

θ = rotation about x-axis

θ_{im}, θ_{jm} = transverse slope of a bending strip

ψ = the curvature (or strain of a bending strip)

ν = possion ratio

ξ = abscissae for gaussian integration

α = the angle between the local and the global coordinate system

ζ, η = curvilinear coordinates

$\{\delta\}$ = displacement parameters matrix

$\{\varepsilon\}$ = strain matrix

$\{\sigma\}$ = stress matrix

CHAPTER 1

INTRODUCTION

Nowadays, the great increase in traffic, population, and the extensive growth of metropolitan urban areas result in the continuing expansion of the highway network. In most developed countries, this expansion has led to many changes in the use and up-grading of various kinds of bridges. The major types of bridges that have been used in canadian transportation system can be summarized as follows: arch bridge, cantilever girder bridge, cable-stayed bridge, suspension bridge, plate girder (or slab and girder) bridge and box girder bridge. Among those bridge types, plate girder bridges and box girder bridges have been widely proposed and used due to economic and aesthetic reasons for the overpasses, undercrossings, separation structures and viaducts in today's modern highway systems. These structures can be constructed to follow any desired alignment. In this thesis, the emphasis is placed on the linear analysis of straight simply supported, continuous plate girder bridges. There are a number of methods that can be used for such analysis. A review of these methods is given in the next chapter.

In recent years, the rapid increase in the computing power allows the bridge designer or researcher to do certain analysis which require extensive computation. Of major importance in this context is the numerical methods such as the Finite Element Method [51,16] and the Finite Strip Method [10] which, by virtue of its adaptability, enables a wide range of bridge loading, geometry and support conditions to be taken into account in analysis. In spite of the suitability of both methods

for the analysis discussed in this thesis, the Finite Strip Method is the one being chosen and concentrated (the review of this method is given in chapter 2, while the formulation of the Finite Strip Method is detailed in both chapters 3 and 4). It is because when the two methods are compared, the Finite Strip Method requires less number of equations and hence the computer storage capacity. Moreover, the reduced matrix band width in the Finite Strip Method results in significant saving in computing time which is known to be directly proportional to the square of the band width multiplied by the total number of equations solved. In most cases, the longitudinal moment and displacement variations are greater than those in the transverse direction; therefore, in the Finite Element Method, a good approximation of the displacement and moment variations in the longitudinal direction usually requires a large number of divisions (elements) in that direction. However, if the Finite Strip Method is used, then only one basic function is needed to describe the variations of these parameters in the longitudinal direction. Once again, the advantage of the Finite Strip Method is observed. In terms of programming, it is much easier to write the finite strip program than the finite element program. This is due to the fact that in the Finite Element Method, a nodal point depending on the physical location can be connected to a number of elements; while in the Finite Strip Method, at the same location, a less number of finite stripes (i.e. elements) are connected because the nodal point is replaced by a nodal line. In addition, the input data preparation for the Finite Element Method is much more complicated than that for the Finite Strip Method. Besides these, the Finite Strip Method, unlike the Finite Element Method in which a huge computer system is needed, can be easily carried out by a micro-computer. This is one of the main advantages because

micro-computer is now so common that most of the consulting companies or even individual engineers may have their own personal micro-computer. Another great advantage is the saving on the total cost of the analysis due to the reduction in computing time. However, at this moment, the Finite Strip Method seems to be mainly used for analyzing simply supported bridge structures.

The study of the continuous slab and girder bridges by the Finite Strip Method has been carried out by Cheung [1]. In his analysis, the conventional approach (i.e. combining the finite strip analysis with the flexibility method) is employed for the continuous bridge with intermediate columns. The same idea is used to solve the continuous plate with line supports by Ghali and Tadros [23]. It was noticed that the convergency of the solution from those analyses were very slow which prevented from wide use of this method by design engineers. The other objective of this thesis is therefore to investigate this problem and to find ways to improve it. In order to improve the rate of the convergency, a different approach is considered. In this approach, the free vibration equation of a simply supported, continuous beam is solved and treated as the longitudinal shape function [4]. The derivation and the eigen solution of the series is described in chapter 3. This series will then be combined with a suitable transverse polynomial function to form the complete displacement function (chapter 4) for the finite strip analysis of continuous bridges with intermediate line supports. The continuous beam vibration function is used because it can sufficiently describe the displacement pattern and satisfy all the required boundary conditions in the longitudinal direction. Furthermore, this function is continuously differentiable and possesses the valuable properties of orthogonality.

In chapter 4, the stiffness matrix and the load matrix of a rectangular folded plate strip are given. In order to cover the analysis of continuous haunched bridges, a folded plate strip with variable width is also derived. The formulation of this variable width strip is done with the help of the curvilinear coordinates system which is considered one of the most accurate approximation for this kind of strips.

Consequently, a computer program, the strip program [2], has been written according to the above theories. The strip program has been verified by a number of examples given in chapter 5. These examples, including beams, plates and actual bridge sections, are mainly divided into two categories: (i) structures with constant cross-sections and (ii) structures with variable cross-sections. The results are checked with either the beam theory or the Finite Element Method (ADINA which is a finite element program for Automatic Dynamic Incremental Nonlinear Analysis). As expected, structures with constant cross-section give more accurate results, although all solutions obtained by the strip program are in good agreement with the results solved by the beam theory or the finite element program.

CHAPTER 2

REVIEW OF LITERATURE

In the past, numerous methods have been developed for the structural analysis. Some of them are very effective in the bridge analysis. In this chapter, a brief review of some commonly used analyses about the plate girder bridges is given. These available methods include the Folded Plate Analysis [41], the Line Solution Technique [40] and some numerical analyses such as the Finite Element Method [28] and the Finite Strip Method [8,34].

(I) Folded Plate Analysis

Several methods have been established for analyzing folded plate structures. Two main methods of such analysis are the Elasticity Method [18,24] and the Ordinary Method [14,21,42]. Both methods can be readily adapted for the analysis of girder type bridges (i.e. plate girder, slab and girder, and box girder etc.), because these bridges may be regarded as a special type of folded plate in which the plates are arranged so as to form the given bridge section. The detail of each method is given in the listed reference. The attempt here is only to give a basic description of both methods.

(Ia) The Elasticity Method

In this method, girder type bridges may be modelled analytically as a folded plate system consisting of an assembly of longitudinal plate elements interconnected at joints along their longitudinal edges and transversely between designated joints on the cross-section. The bending of each plate normal to its plane and the bending

in the plane are analyzed by plate flexure theory and plane stress theory respectively. These classical theories necessitate the representation of the external loads. An analysis of such loads with any arbitrary longitudinal distribution for straight bridges may be performed using a direct stiffness harmonic analysis. The applied loads are first resolved into Fourier series components. The analysis is made for the component of each particular harmonic and then the final results are obtained by summing the results for all harmonics used to represent the load.

The analysis of each harmonic load has the advantage that loads and displacements have the same variation and thus a single characteristic value may be used to describe any force or displacement pattern. This makes it possible to treat an entire joint as a single nodal point and to operate with single forces and displacements instead of functions. Furthermore, if the geometric compatibility and static equilibrium at a nodal point are maintained, then both conditions along entire longitudinal joint will be automatically satisfied. Each longitudinal joint usually has four characteristic degrees of freedom: displacement in vertical and horizontal plane of the cross-section, translation in longitudinal tangent to the joint and rotation about an axis tangent to the joint. Those directions define a global coordinate system for displacements and forces. Finally, the structure stiffness matrix of the system is obtained by applying direct stiffness method. If the continuous bridge is concerned, then an additional force method of analysis is needed and used in combination with the direct stiffness harmonic analysis. Both direct stiffness method and force method can be found in many textbooks.

(Ib) The Ordinary Method

This is an approximated method of analysis because it assumes a simplified

structural behavior. The assumption significantly reduces the amount of computation required. The errors introduced by these simplifying assumptions has been shown [19] to be small for uniformly loaded folded plates, provided that the length-width ratio of the component plates exceed three. Usually, most bridge girders will have a much bigger ratio than three. Therefore, the Ordinary Method can be safely employed.

The Ordinary Method has been extended by Johnson and Lee [30] to the analysis of folded plates containing tapered plates, provided that the plate taper is not excessive. This restriction on taper arise from the fact that the length-width ratio of each plate must be greater than three before the Ordinary Method can be applied. Once again in the point of view of bridge girder, the limitation is not too serious because in many practical cases the taper will be considerably less than this limiting value.

The Ordinary Method is started with the following assumptions:

(1) Homogeneous and linearly elastic material.

(2) Small deflection with respect to structural dimension.

(3) Fully monolithic connections between plates.

(4) Infinitely stiff in its plane and flexible normal to its plane at each supporting end diaphragm.

(5) Similarity of the in-plane action between an individual plate and a simple beam spanning between the end diaphragms.

(6) Similarity between the action of each plate normal to its plane and the same action of a transverse one-way slab strip.

The folded plate may behave in the same way as the action of a series of transverse one way slab strips supported elastically at the ridges by a series of interconnected plate-girders spanning longitudinally between the end diaphragms. The slab strips which only transmit shears and moments in transverse direction are analyzed by considering as a continuous beam, the equilibrium of transverse moments and the compatibility of rotations being satisfied at the ridges; while the plate-girders which only transmit forces in their plane are analyzed as a simply supported beam spanning between the end diaphragms, the connection between the adjacent plates being taken into account by ensuring the equilibrium of longitudinal shear forces and the continuity of longitudinal strains at the ridges.

Since the slab system is elastically supported by the plate-girder system, so the displacements of the plate-girder system are produced by the slab reactions while these reactions themselves depend partly on the plate-girder displacement. Under this circumstance, the analysis is not straight forward. Several convenient solution techniques have been proposed. One of them is the Method of Particular Loadings which is developed by Yitzhaki [48]. In this method, the slab system of the structure, under the action of the externally applied loads, is analyzed by assuming to be rigidly supported by the plate-girder system and thus the displacement set up in the plate-girder system are calculated. These plate-girder displacements lead to relative joint displacement in which the additional sway moments in the transverse slab system are set up. These additional moments are taken into account by carrying out a subsequent correction analysis. Consequently, the final results are found by superposition of the individual parts of the analysis.

On the other hand, if the Ordinary Method is applied to a conventional folded

plate structures in which all plates are rectangular and the loading on each plate has a similar distribution in the longitudinal direction, then it is sufficient to consider the satisfaction of equilibrium and compatibility conditions between adjacent plates at one point only on their common edge because both conditions are automatically satisfied all along the ridge if they are satisfied at this one point. As a result, only one transverse slab strip has to be considered and the longitudinal shear forces and stresses have to be calculated at one cross-section only of each longitudinal plate beam.

(II) Line Solution Technique

The analysis of plate and shell structures by the line solution technique was first discussed by Jenkins and Tottenham [29]. Applications to the plane stress problem by Coull and Kazmi [31] were successfully proven. Moreover, Coull and Rao [12] showed that the technique could be used for a wide range of problems, such as uniformly distributed, block and concentrated loads, continuous decks and decks of variable thickness etc. in the analysis of right isotropic bridge decks. On the other hand, Das [13] extend the technique to cover the curved isotropic decks with or without edge stiffening beams. The technique was limited to the isotropic material only until the first investigation on the orthotropic slabs was carried out by Trockalakis [46].

The method of line solution is a mean of reducing a partial differential equation to a set of simultaneous ordinary equations. However, the method was of limited value due to numerical instability. The basic idea of the method is quite simple. For some required function $f(x, y)$ which must satisfy some partial differential equation, it is assumed that along the lines $y = y_k$ $(k = 1 \cdots n)$ the solution has the values

$f(x, y_k)$, that is a function of x only, which is denoted by $f_k(x)$. These are the line solutions. Along any line, partial derivatives of $f(x, y)$ with respect to x will take the form of complete differentials of $f_k(x)$ with respect to x. For any value of x, partial derivatives with respect to y can be replaced by an appropriate finite difference expression and thus for all values of x can be expressed as appropriate finite difference expressions are substituted back to the given line (e.g. line y_n), then a set of simultaneous fourth order ordinary differential equations is obtained. These can be most readily solved by the matrix progression method. Details of this method are shown in the listed reference.

(III) Finite Element Method

In the Finite Element Method, structures are treated as an assembly of a number of elements. The actual continuum is replaced by the assembly of finite elements interconnected at nodal points. The behavior of a continuum is approximated by stiffness matrices which are developed for the finite elements based on assumed displacement or stress patterns. With the help of the direct stiffness method [11], the nodal displacements are determined and hence the internal stresses in the finite elements. The accuracy of the solution depends on the assumptions used in the derivation of the stiffness matrices and on the fineness of mesh sizes used in the subdivision of the structure. The results often satisfy compatibility, but not necessarily equilibrium in the continuum until a sufficiently fine mesh is used.

For bridge analysis, three main family of elements can be considered: one-dimensional elements, two-dimensional elements and three-dimensional elements. Among them, three-dimensional elements are rarely needed because most bridge structures can be well modelled by one-dimensional elements or two-dimensional

elements or combinations of these elements. The common types of one-dimensional elements are the bar element and the beam element. The bar element has one degree of freedom at each node because it can take only axial compression or tension; while the beam element has six-degree of freedom at each node because it can carry both bending strength with respect to principal axes of bending and axial strength. On the other hand, two-dimensional elements are, for the most part, triangular or rectangular in shape. The degrees of freedom at the nodes of the elements are dependent on the physical restriction. If a two-dimensional element has displacements only in its own plane, then the element will have two-degrees of freedom at each node. This type of elements is termed as an extensional or membrane element. Alternatively, the element may be used to simulate plate-bending (flexural) action by specifying three-degrees of freedom (one translation, two rotations) at each node. Furthermore, the element may combine both the membrane action and the flexural action to form a plate element of five-degrees of freedom at each node point. It should be noted that for such element it is usually assumed that the in-plane deformation and the bending deformation are uncoupled. These two-dimensional elements are not limited to the above degrees of freedom. Additional degrees of freedom per node (e.g. curvature, twist, etc.) or additional nodes within the element or along its edges may be introduced to improve accuracy or for different specialized applications. Nevertheless, the Finite Element Method usually requires large number of equations and matrix with comparatively large band width. These can be very expensive due to long computation time and at times even impossible to work out solution because of limitation in computing facilities.

In order to have a suitable choice of element type for a particular model, the

attention must be paid to the factors such as element accuracy, reliability, simplicity and computational cost.

(IV) Finite Strip Method

The Finite Strip Method, first published by Cheung [7], is acknowledged as a powerful and versatile tool for solving simply supported bridge deck structures in terms of accuracy and efficiency. Same method for rectangular slab-type bridge decks is also studied independently by Powell and Ogden [38]. The method retains advantages of both the orthotropic-plate theory and finite element concept.

This method can be considered as a special form of the finite element procedure using the displacement approach in which the minimum total potential energy theorem is employed to develop the relationship between the unknown nodal displacement parameters and the applied loading. However, the assumed displacement functions are different from the conventional Finite Element Method. In the Finite Element Method, the assumed displacement may take the form of two-way polynomial functions; while the Finite Strip Method calls for combinations of a one-way polynomial function in the transverse direction and a continuously differentiable smooth series (e.g. a harmonic function) in the longitudinal direction, with stipulation that the harmonic function should satisfy the boundary conditions at the two ends of the strips. In other words, the displacement function of the Finite Strip Method can generally be written as a product of polynomials and series. Thus it is possible to regard a two-dimensional strip as a one-dimensional problem using the displacement function below

$$w(x,y) = \sum_{m=1}^{r} f_m(x) Y_m(y)$$

where $f_m(x)$ = polynomials in transverse direction

$Y_m(y)$ = harmonic series in longitudinal direction

Besides the reduction in dimensions, the Finite Strip Method is also much easier to program and requires less effort to prepare the input data, less core storage, less computation time and thus more economical. Moreover, the finite strip analysis can even be programmed on micro-computers. These factors result in the superiority of the Finite Strip Method in the linear analysis of straight simply supported, continuous plate-girder bridges.

The philosophy of the Finite Strip Method is similar to that of the Kantorovich Method [32] which modifies the partial differential equations to ordinary differential equation by a unique separation of the variable function of x and y. The general procedure of the Finite Strip Method is outlined as follows:

(1) The continuum is first divided into strips by imaginary lines.

(2) The strips are assumed to be interconnected along a discrete number of nodal lines.

(3) A displacement function (usually a combination of a polynomial and a series) is chosen to represent the unknown nodal displacement parameters.

(4) By applying either virtual work or minimum potential energy principles to the chosen displacement function, a stiffness matrix and load matrix can be obtained in terms of a set of local coordinate system.

(5) An overall system stiffness and load matrix may be formed by assembling the local stiffness matrix and load matrix of all strips under a common coordinate system. A transformation matrix may be needed.

CHAPTER 3

FORMULATION OF LONGITUDINAL SHAPE FUNCTION Y_m

3.1 INTRODUCTION

For an accurate finite strip analysis, the choice of a suitable displacement function for a strip is the most crucial part. Thus, great care must be taken in choosing the displacement function. In general, the displacement function consists of two parts: (i) a series (or harmonic function) in the longitudinal direction, and (ii) a polynomial in the transverse direction. The series part Y_m of the displacement function is chosen to satisfy all the boundary conditions and to be continuously differentiable in the longitudinal direction. Also, Y_m should be converged to an exact solution when the number of terms is successively increased and have the valuable properties of orthogonality.

$$\left.\begin{array}{l} \int_L Y_m Y_n dy = 0 \\ \int_L Y_m'' Y_n'' dy = 0 \end{array}\right\} \; for \;\; m \neq n \qquad (3.1.1)$$

On the other hand, the polynomial part $f_m(x)$ of the displacement function must be able to represent a state of constant strain in the transverse direction.

In this chapter, only the series part Y_m will be discussed. The appropriate selection of the polynomial $f_m(x)$ will be discussed in chapter 4. Because of the similarity of behavior between a simply supported, continuous bridge and a simply supported, continuous beam, the derivation of the longitudinal series Y_m is based on the governing beam differential equation obtained from the free vibration analysis of

beams. A review of the free vibration analysis of beams will be given in section 3.2. Moreover, sections 3.3 and 3.4 will show the detail of the derivation and the eigen solution of the series part Y_m of the displacement function respectively.

3.2 FREE VIBRATION ANALYSIS OF BEAM

Up until the present, the free vibration analysis of beams [20,25] has been well known. The following is a brief review of the derivation of the governing differential equation for the free vibration of a continuous beam [47]. In deriving the beam differential equation (or equation of motion [45]) under free vibration, it is assumed that vibration occurs in one of the principal planes of the beam. Consider a small beam element of length dx as shown in figure 3.1. Bending moments M and shear forces V_s are acting on the ends of the element. The displacement at any section x at time t is denoted by Y (or $Y(x,t)$). The gravity forces will be neglected by measuring the displacement from the position of static equilibrium of the beam. The inertia force F on the element is given by

$$F = \rho A dx \frac{\partial^2 Y}{\partial t^2} \tag{3.2.1}$$

Taking moments about the center line of the element (neglecting products of small quantities), and resolving for forces in the y-direction, yields

$$V_s dx + M - (M + \frac{\partial M}{\partial x} dx) = 0 \tag{3.2.2}$$

or simplify

$$V_s = \frac{\partial M}{\partial x} \tag{3.2.3}$$

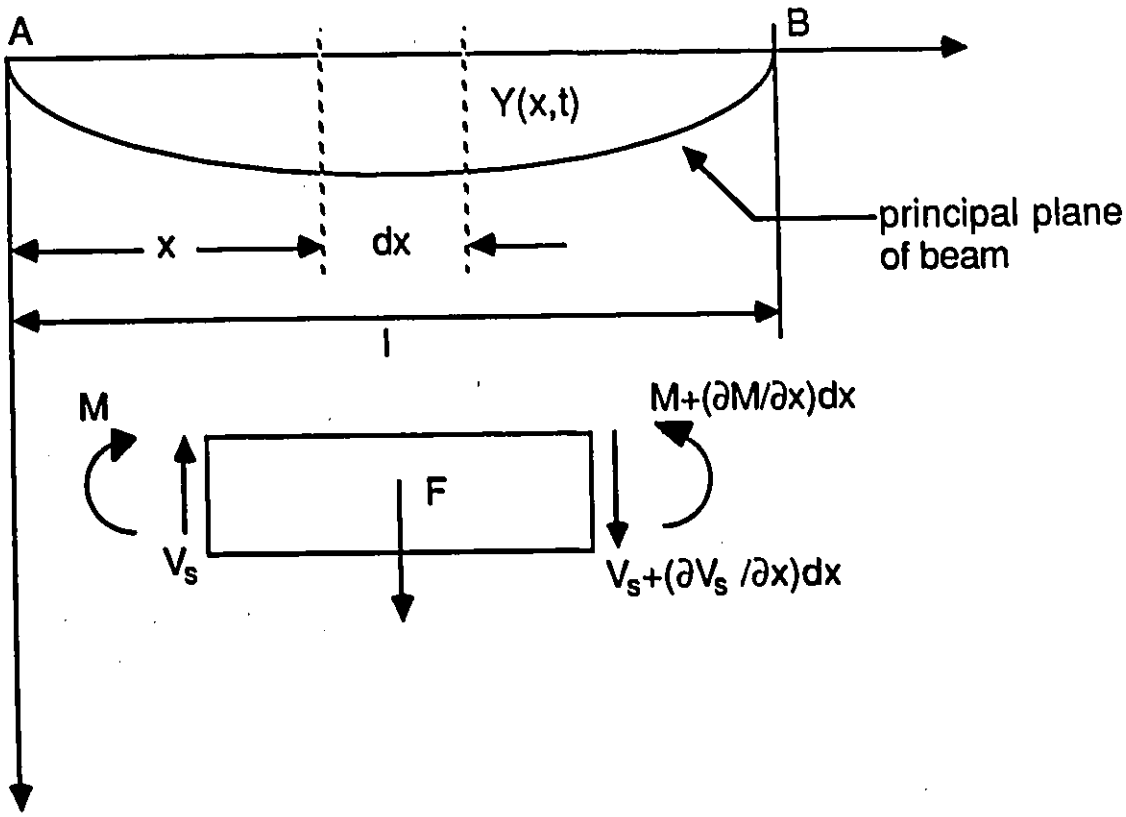

Figure 3.1: BEAM ELEMENT

Also, by the summation of forces in the y-direction, the relation between the shear force V_s and the inertia force F can be expressed by

$$\frac{\partial V_s}{\partial x} = \rho A \frac{\partial^2 Y}{\partial t^2} \tag{3.2.4}$$

From the statics [15], the relationship among the bending moment, the curvature and the displacement is given by

$$M = -EI \frac{\partial^2 Y}{\partial x^2} \tag{3.2.5}$$

Combining equations 3.2.3, 3.2.4 and 3.2.5, gives

$$\frac{\partial^2}{\partial x^2}(-EI \frac{\partial^2 Y}{\partial x^2}) = \rho A \frac{\partial^2 Y}{\partial t^2} \tag{3.2.6}$$

For a beam with uniform cross-section and constant EI, equation 3.2.6 becomes

$$EI \frac{\partial^4 Y}{\partial x^4} + \rho A \frac{\partial^2 Y}{\partial t^2} = 0 \tag{3.2.7}$$

It should be noted that the effects of the transverse shear deformation and of the rotatory inertia are neglected in equation 3.2.7. For equation 3.2.7 to be valid the distance between nodal points (in the longitudinal direction) must be large in comparison to beam transverse dimensions, so that the effects of the shear strain may be neglected. Equation 3.2.7 can be solved by means of the separation of variables [43]. The displacement $Y(x,t)$ can then be written as

$$Y(x,t) = f(t)g(x) \tag{3.2.8}$$

where f and g are function of t and x respectively.

Substituting equation 3.2.8 into equation 3.2.7 and solves

$$\frac{d^4 Y}{dx^4} - \frac{\rho A \omega^2}{EI} Y = 0 \tag{3.2.9}$$

or

$$\frac{d^4Y}{dx^4} = \mu^4 Y \tag{3.2.10}$$

where $\mu^4 = \frac{\rho A \omega^2}{EI}$

ω is the frequency of beam

As a result, the free vibration of beams can be analyzed by applying different boundary conditions to the governing beam differential equation. (i.e. equation 3.2.10)

3.3 DERIVATION OF FUNCTION Y_m

The harmonic function Y_m, for a simply supported, continuous beam as shown in figure 3.2, is obtained by solving the governing differential equation of a beam under free vibration and can be written as:

$$Y(y) = E\sin\mu y + F\cos\mu y + G\sinh\mu y + H\cosh\mu y \tag{3.3.1}$$

where E, F, G and H are coefficients determined by the boundary conditions of each span

μ as described in equation 3.2.10

The first and the second derivative of the solution Y with respect to y are given as follow

$$Y'(y) = E\mu\cos\mu y - F\mu\sin\mu y + G\mu\cosh\mu y + H\mu\sinh\mu y \tag{3.3.2}$$

and

$$Y''(y) = -E\mu^2\sin\mu y - F\mu^2\cos\mu y + G\mu^2\sinh\mu y + H\mu^2\cosh\mu y \tag{3.3.3}$$

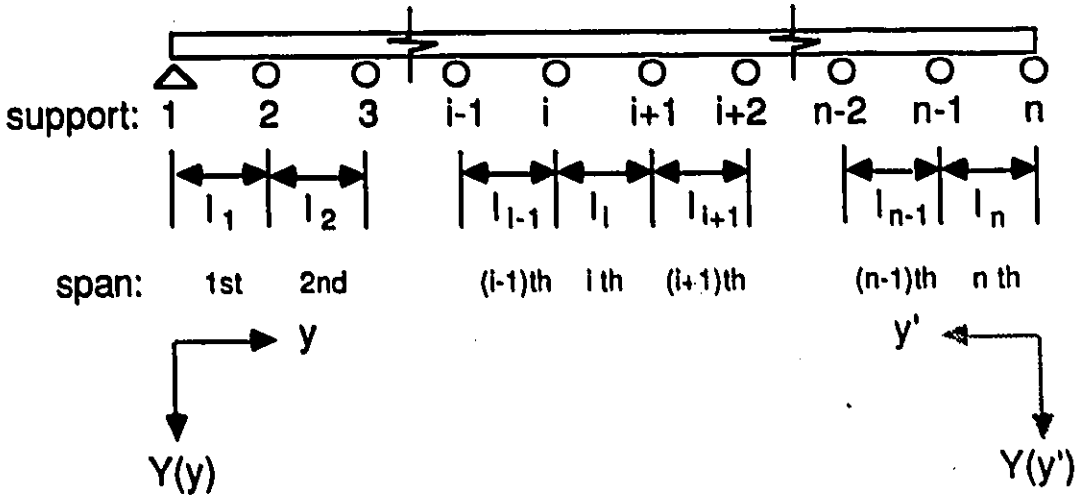

Figure 3.2: A CONTINUOUS SIMPLY SUPPORTED BEAM WITH n SPANS

The coefficients E, F, G and H are solved, in this case, under the boundary conditions of a simply supported, continuous beam with n spans. In order to have a complete solution, the boundary conditions for the first span, the interior spans and the last span should be satisfied. First of all, consider the first and the last span of the continuous beam in figure 3.3. For the first span, the boundary conditions are $Y_1(0) = Y_1''(0) = 0$ and $Y_1(l_1) = 0$. Substituting $Y_1(0) = Y_1''(0) = 0$ into equations 3.3.1 and 3.3.3, yields

$$Y_1(0) = F + H = 0 \tag{3.3.4}$$

and

$$Y_1''(0) = -F\mu^2 + H\mu^2 = 0 \tag{3.3.5}$$

Solving equations 3.3.4 and 3.3.5, gives

$$F = H = 0 \tag{3.3.6}$$

Thus, equation 3.3.1 becomes

$$Y(y) = E\sin\mu y + G\sinh\mu y \tag{3.3.7}$$

In order to have a non-trivial solution for equation 3.3.7, the value of the coefficients E and G cannot be zero. Substituting $Y_1(l_1) = 0$ into equation 3.3.7, yields

$$Y_1(l_1) = E\sin\mu l_1 + G\sinh\mu l_1 = 0 \tag{3.3.8}$$

or

$$\alpha_1 = -\frac{G}{E} = \frac{\sin\mu l_1}{\sinh\mu l_1} \tag{3.3.9}$$

The solution for the first span which is obtained by combining equations 3.3.7 and 3.3.9 has the following form:

$$Y_1(y) = A_1(\sin\mu y_1 - \alpha_1\sinh\mu y_1) \tag{3.3.10}$$

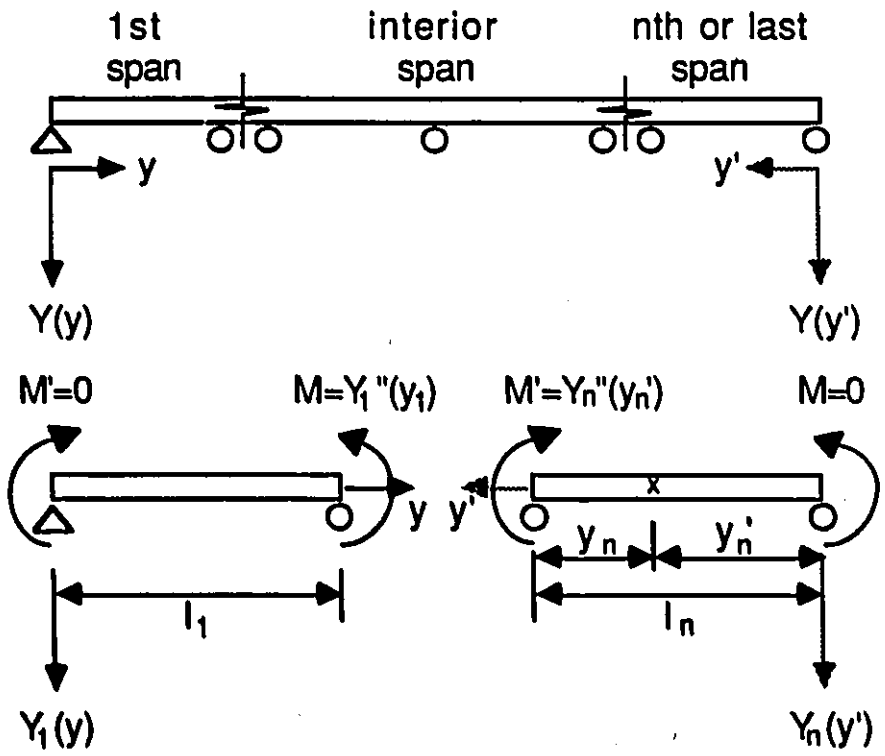

Figure 3.3: THE FIRST AND LAST SPAN OF A CONTINUOUS SIMPLY SUPPORTED BEAM

where A_1 is a coefficient for the first span

α_1 is defined as in equation 3.3.9

For the last span (or the n th span), the coordinate y is replaced by y' (see figure 3.3). It is convenient to use y' because the solution of equation 3.3.1 can easily be found by satisfying the boundary conditions based on the coordinate y': $Y_n(0) = Y_n''(0) = 0$ and $Y_n(l_n) = 0$. On the other hand, if the same coordinate y as used in the first span is employed, the boundary conditions will become $Y_n(0) = 0$ and $Y_n(l_n) = Y_n''(l_n) = 0$. It is noticed that when $Y_n(0) = 0$ and $Y_n(l_n) = Y_n''(l_n) = 0$ are substituted into equations 3.3.1 and 3.3.3, the following equations are found

$$Y_n(0) = F + H = 0 \tag{3.3.11}$$

$$Y_n(l_n) = E\sin\mu l_n + F\cos\mu l_n + G\sinh\mu l_n + H\cosh\mu l_n = 0 \tag{3.3.12}$$

and

$$Y_n''(l_n) = \mu^2(-E\sin\mu l_n - F\cos\mu l_n + G\sinh\mu l_n + H\cosh\mu l_n) = 0 \tag{3.3.13}$$

It is obvious that the coefficients E, F, G and H cannot be determined by solving above three equations. On the contrary, if the boundary conditions $Y_n(0) = Y_n''(0) = 0$ and $Y_n(l_n) = 0$ of the coordinate y' are used, then the following three equations will be obtained under the same procedure for the first span.

$$Y_n(0) = F + H = 0 \tag{3.3.14}$$

$$Y_n''(0) = -F\mu^2 + H\mu^2 = 0 \tag{3.3.15}$$

and

$$Y_n(l_n) = E\sin\mu l_n + G\sinh\mu l_n = 0 \tag{3.3.16}$$

Solving equations 3.3.14, 3.3.15 and 3.3.16, the solution for the last span with the coordinate y' is given by

$$Y_n(y') = A_n(\sin \mu y'_n - \alpha_n \sinh \mu y'_n) \tag{3.3.17}$$

where A_n is the coefficient for the last span (n th span)

$\alpha_n = \frac{\sin \mu l_n}{\sinh \mu l_n}$

$y'_n = l_n - y_n$

Finally, for the intermediate spans (figure 3.4), both coordinates y and y' are needed because there are moments M and M' at both ends of an intermediate span. Hence, the solution for an intermediate span (e.g. the i th span) can be obtained by simply combining the solutions of the first and the last span. Combining equations 3.3.10 and 3.3.17 for the solution of the i th span, gives

$$Y_i = A_{i,1}(\sin \mu y_i - \alpha_i \sinh \mu y_i) + A_{i,2}(\sin \mu y'_i - \alpha_i \sinh \mu y'_i) \tag{3.3.18}$$

where $A_{i,1}$ and $A_{i,2}$ are coefficients for i th span and the subscript 1 and 2 represent the direction in the y and y' coordinates respectively.

A comparison among equations 3.3.10, 3.3.17 and 3.3.18 shows that equations 3.3.10 and 3.3.17 are the special cases of equation 3.3.18. In other words, equation 3.3.18 becomes equations 3.3.10 and 3.3.17 by setting $A_{i,2} = 0$ and $A_{i,1} = 0$ respectively. Thus, equation 3.3.18 represents the general solution of the beam differential equation for every individual span of a simply supported, continuous beam.

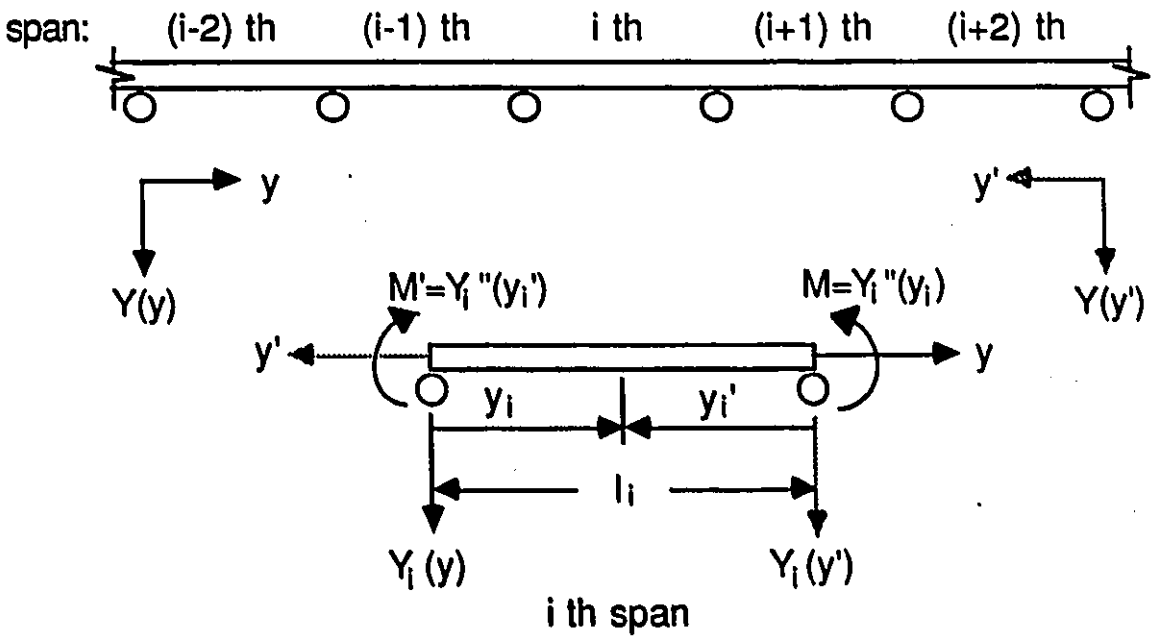

Figure 3.4: INTERMEDIATE SPANS OF A CONTINUOUS SIMPLY SUPPORTED BEAM

3.4 EIGEN SOLUTION OF FUNCTION Y_m

In order to obtain the eigen solution of equation 3.3.18 for the entire simply supported, continuous beam the following two conditions must be satisfied.

(i) Bending moments at both ends of the continuous beam must be zero. This can be done by setting

$$A_{1,2} = 0 \tag{3.4.1}$$

and

$$A_{n,1} = 0 \tag{3.4.2}$$

(ii) The slope and the curvature of adjacent intermediate spans must be equal and continuous respectively. The slope, the first derivative of equation 3.3.18, is given by

$$\frac{dY_i}{dy_i} = \mu A_{i,1}(\cos \mu y_i - \alpha_i \cosh \mu y_i) - \mu A_{i,2}(\cos \mu y_i' - \alpha_i \cosh \mu y_i') \tag{3.4.3}$$

and the curvature, the second derivative of equation 3.3.18, is defined by

$$\frac{d^2Y_i}{dy_i^2} = -\mu^2 A_{i,1}(\sin \mu y_i + \alpha_i \sinh \mu y_i) - \mu^2 A_{i,2}(\sin \mu y_i' + \alpha_i \sinh \mu y_i') \tag{3.4.4}$$

Consider the i th span and its adjacent span, the $(i-1)$ th span, at support i (i.e. $y_{i-1} = l_{i-1}$, $y_{i-1}' = 0$ and $y_i = 0$, $y_i' = l_i$, see figure 3.5), the slope of $(i-1)$ th and i th span can be written by

$$\frac{dY_{i-1}}{dy_{i-1}} = \mu A_{i-1,1}(\cos \mu l_{i-1} - \alpha_{i-1} \cosh \mu l_{i-1}) - \mu A_{i-1,2}(1 - \alpha_{i-1}) \tag{3.4.5}$$

and

$$\frac{dY_i}{dy_i} = \mu A_{i,1}(1 - \alpha_i) - \mu A_{i,2}(\cos \mu l_i - \alpha_i \cosh \mu l_i) \tag{3.4.6}$$

respectively. Equating equations 3.4.5 and 3.4.6, gives

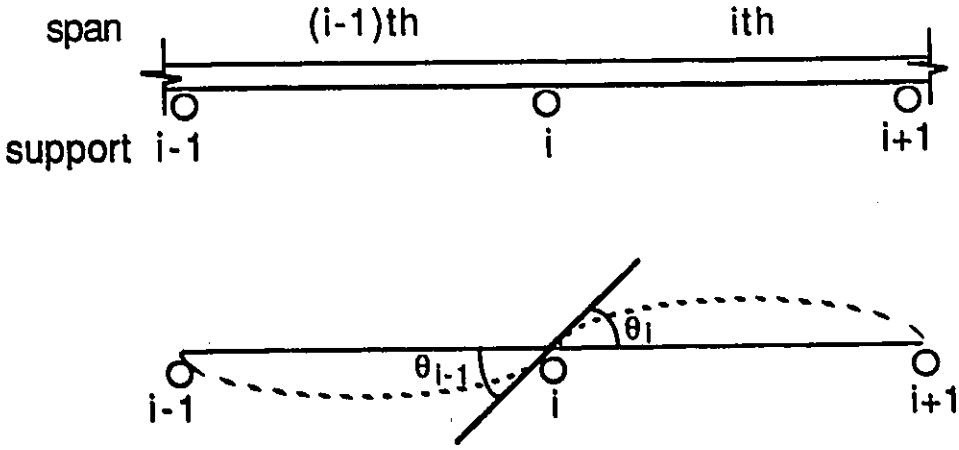

$$\theta_{i-1} = \frac{dY_{i-1}}{dy_{i-1}}$$

$$\theta_i = \frac{dY_i}{dy_i}$$

Figure 3.5: THE SLOPE AND CURVATURE OF AN INTERMEDIATE SPAN

$$A_{i-1,1}(\cos\mu l_{i-1} - \alpha_i \cosh\mu l_{i-1}) - A_{i-1,2}(1-\alpha_{i-1}) =$$
$$A_{i,1}(1-\alpha_i) - A_{i,2}(\cos\mu l_i - \alpha_i \cosh\mu l_i) \qquad (3.4.7)$$

Similarly, the continuous condition of the curvature for the adjacent spans can be satisfied by

$$A_{i-1,1}\sin\mu l_{i-1} = A_{i,2}\sin\mu l_i \qquad (3.4.8)$$

Thus, the eigen solution μ of Y_m can now be determined by satisfying all the required conditions (i.e. equations 3.4.1, 3.4.2, 3.4.7 and 3.4.8) as described above.

The eigen solution μ can be solved by using the following procedures. From equations 3.4.7 and 3.4.8, it is noticed that for a given value of μ, the values of $A_{i,1}$ and $A_{i,2}$ can be obtained by the previous known values of $A_{i-1,1}$ and $A_{i-1,2}$. In this way, every $A_{i,j}$ value (where $i = 2 \cdots n$ and $j = 1, 2$) can be obtained and written in terms of μ (e.g. $A_{i,j}(\mu)$). This procedure is started with satisfying the condition $A_{1,2} = 0$ (i.e. equation 3.4.1) and ended by satisfying the condition $A_{n,1} = 0$ (i.e. equation 3.4.2).

Since $A_{i,j}$ describes only the mode shape but not the actual amplitude, so it is possible to start with the assumptions

$$A_{1,1} = 1 \quad \textit{and} \quad A_{1,2} = 0 \qquad (3.4.9)$$

It is obvious that if the value $A_{i,2}$ in equation 3.4.8 is determined, then the $A_{i,1}$ value in equation 3.4.7 will also be found by substituting the known value of $A_{i-1,1}$ and $A_{i,2}$. The value $A_{i,2}$ in equation 3.4.8 can be solved by the following two possible cases: (i) $\sin\mu l_i \neq 0$ and (ii) $\sin\mu l_i = 0$

(i) $\sin\mu l_i \neq 0$

Equation 3.4.8 becomes

$$A_{i,2} = A_{i-1,1}\frac{\sin \mu l_{i-1}}{\sin \mu l_i} \tag{3.4.10}$$

and equation 3.4.7 becomes

$$A_{i,1} = \frac{[A_{i-1,1}(\cos \mu l_{i-1} - \alpha_i \cosh \mu l_{i-1}) - A_{i-1,2}(1-\alpha_{i-1}) + A_{i,2}(\cos \mu l_i - \alpha_i \cosh \mu l_i)]}{(1-\alpha_i)} \tag{3.4.11}$$

By putting the appropriate value into equations 3.4.10 and 3.4.11, both values $A_{i,2}$ and $A_{i,1}$ are solved.

(ii) $\sin \mu l_i = 0$ (i.e. $\mu l_i = n\pi$, $n = 1, 2 \cdots$ and $\alpha_i = \frac{\sin \mu l_i}{\sinh \mu l_i} = 0$)

From equation 3.3.18 and $y_i' = l_i - y_i$

$$\begin{aligned} Y_i &= A_{i,1} \sin \mu y_i + A_{i,2} \sin \mu y_i' \\ &= A_{i,1} \sin \mu y_i + A_{i,2} \sin(n\pi - \mu y_i) \\ &= (A_{i,1} \pm A_{i,2}) \sin \mu y_i \end{aligned} \tag{3.4.12}$$

Equation 3.4.12 shows that $A_{i,1}$ and $A_{i,2}$ are dependent of each other; therefore, it is possible to assume that $A_{i,2} = 0$. Equation 3.4.12 becomes

$$Y_i = A_{i,1} \sin \mu y_i \tag{3.4.13}$$

It should be noted that if $\sin \mu l_n = 0$ is substituted into equation 3.4.13, then $Y_n = A_{n,1} \sin \mu l_n = 0$ which means that the curvature at the end support of the last span of the beam is equal to zero and thus despite the equation 3.4.2 is not satisfied, it is still a valid solution.

Substituting $\sin \mu l_i = 0$ into equation 3.4.8, gives

$$A_{i-1,1} \sin \mu l_{i-1} = 0 \tag{3.4.14}$$

Equation 3.4.14 can be solved by two possible ways: (a) $\sin \mu l_{i-1} = 0$ and (b) $\sin \mu l_{i-1} \neq 0$.

(a) $\sin \mu l_{i-1} = 0$ (i.e. $\alpha_{i-1} = \frac{\sin \mu l_{i-1}}{\sinh \mu l_{i-1}} = 0$)

In equation 3.4.14, the condition $\sin \mu l_{i-1} = 0$ implies that the value $A_{i-1,1}$ cannot be zero, or a trivial solution will be produced. As a result, the value $A_{i,1}$ is solved by substituting $\sin \mu l_i = 0$, $\sin \mu l_{i-1} = 0$ and $A_{i,2} = 0$ into equation 3.4.7. After the substitution, the value $A_{i,1}$ is simply given by

$$A_{i,1} = A_{i-1,1} \cos \mu l_{i-1} \tag{3.4.15}$$

(b) $\sin \mu l_{i-1} \neq 0$ (i.e. $A_{i-1,1} = 0$, $A_{i,2} = 0$)

Similar to case (a), equation 3.4.7 becomes

$$A_{i,1} = -A_{i-1,2}(1 - \alpha_{i-1}) \tag{3.4.16}$$

In case (b) (i.e. $\sin \mu l_i = 0$, $A_{i,2} = 0$ and $\sin \mu l_{i-1} \neq 0$, $A_{i-1,1} = 0$), it is important to note that if $\sin \mu l_i = \sin \mu l_2 = 0$, then $\sin \mu l_{i-1} = \sin \mu l_1 \neq 0$ and it will result in $A_{i-1,1} = A_{1,1} = 0$ which contradicts the assumption $A_{1,1} = 1$ in equation 3.4.9. Also, when $A_{1,2} = 0$ is put into equation 3.4.16, $A_{2,1} = 0$ is obtained. In this way, the value of $A_{i,j}$ (where $i = 2 \cdots n$ and $j = 1, 2$) will be found to be equal to zero. Hence, under this situation, although the required condition $A_{n,1} = 0$ is satisfied, the eigen value μ is not the correct solution. In other words, the eigen solution μ is said to be the correct answer of the shape function Y_m if and only if all the conditions (i.e. equations 3.4.1, 3.4.2, 3.4.3 and 3.4.4) are satisfied by μ and all the $A_{i,j}$ values are not equal to zero at the same time.

With the help of equations 3.4.10, 3.4.11, 3.4.15 and 3.4.16, every $A_{i,j}$ value can be solved. The eigen value μ can finally be determined by satisfying the following

conditions.

$$\begin{aligned} A_{1,1} &= 1 \\ A_{1,2} &= 0 \\ A_{n,1}(\mu) &= 0 \quad for \quad \sin \mu l_n \neq 0 \end{aligned} \tag{3.4.17}$$

Equation 3.4.17 is solved by the first order reguli-falsi iteration [33]. Figure 3.6 shows the scheme of the reguli-falsi iteration pattern. This iteration is started with an initial value μ_0 and an increment $\Delta\mu$ which are defined by

$$\begin{aligned} \Delta\mu &= \frac{\pi}{30 l_{max}} \\ \mu_0 &= 29.5 \times \Delta\mu \end{aligned} \tag{3.4.18}$$

where l_{max} is the maximum of the span length

Both values are related to each other by

$$\Delta\mu = \mu_{m+1} - \mu_m \tag{3.4.19}$$

where $m = 0, 1, 2, \cdots$

For each μ_m and its increment μ_{m+1}, the value of $A_{n,1}(\mu)$ is checked against the signs (i.e. either +ve or -ve). If $A_{n,1}(\mu)$ value changes its sign in certain interval denoted by μ_m and μ_{m+1}, there will be an eigen solution μ within the interval. The actual eigen solution μ is approximated by the following scheme. A straight line is drawn from the point $A_{n,1}(\mu_m)$ to the point $A_{n,1}(\mu_{m+1})$. The intersection point of the straight line and the μ-axis will be denoted by μ_{m+2} which will be one step closer to the actual μ value. In the same way, a straight line is drawn from $A_{n,1}(\mu_m)$ to $A_{n,1}(\mu_{m+2})$ and the intersection point gives another value μ_{m+3} which is further

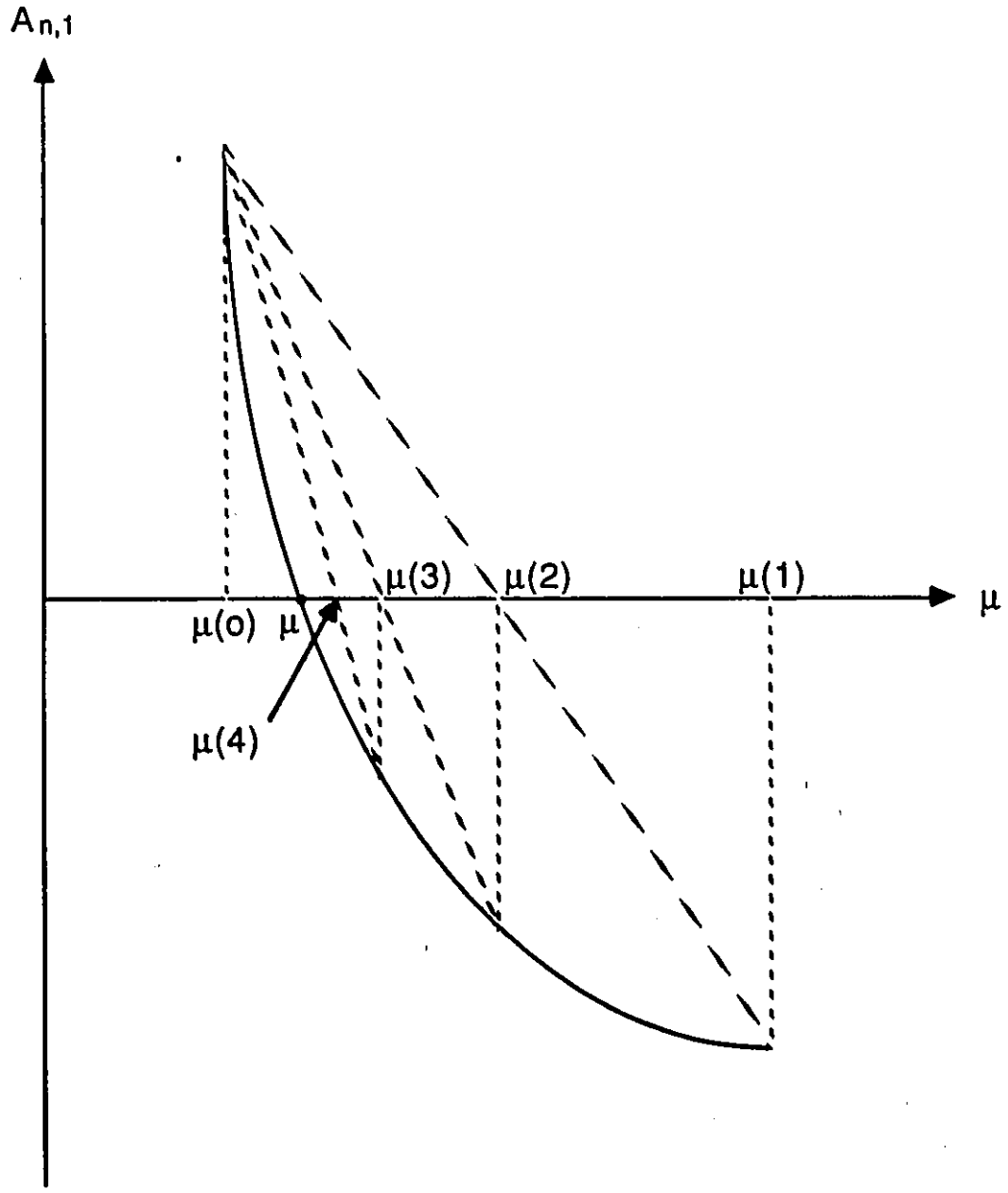

Figure 3.6: REGULI-FALSI ITERATION PATTERN

closer to the correct value μ. Finally, the actual eigen value μ can be found by setting the required accuracy

$$| A_{n,1}(\mu_M) | < \varepsilon_1 \tag{3.4.20}$$

where $M = 0, 1, 2, \cdots$

In this case, the accuracy is set to be

$$\varepsilon_1 = 1 \times 10^{-10} \tag{3.4.21}$$

The above iteration procedure can be summarized in terms of a equation as follows

$$\mu_{r+1} = \mu_r - \frac{\{A_{n,1}(\mu_r)[\mu_r - \mu_0]\}}{[A_{n,1}(\mu_r) - A_{n,1}(\mu_0)]} \tag{3.4.22}$$

where μ_0 and μ_r represent each interval (as shown in figure 3.6)

that contains an eigen solution μ

$r = 1, 2, \cdots$

This method can solve as many eigen solution μ_m and modes $(A_{i,j})_m$ as required.

It is necessary to ensure that no eigen solution μ is missed because any missing root will affect the convergency of the function Y_m. From equation 3.4.10, it should be noted that $A_{i,2}$ is obtained by dividing both sides by a value of $\sin \mu l_i$, which may result in missing the root $\sin \mu l_i = 0$ (i.e. $\mu l_i = m\pi$, $m = 1, 2, \cdots$). Therefore, during the increment of μ, the sign of $\sin \mu l_i (i = 2 \cdots n)$ is checked. If there is a change of sign, the value $\mu = \frac{m\pi}{l_i}$ will be used as the trial point to calculate $A_{i,j}$ value and verified whether $\mu = \frac{m\pi}{l_i}$ is one of the eigen solution or not. However, the value $\mu = \frac{m\pi}{l_i}$ cannot be used in any other cases because it may create the ill situation as described in case (b). Moreover, it is noticed that if the length of all spans are not

the same, but a little different from each other (e.g. $0 < \frac{(l_{max}-l_{min})}{l_{max}} < 0.05$, where l_{max} and l_{min} are the maximum and minimum of the span length respectively), a smaller increment $\Delta\mu'$ is needed to avoid missing some eigen solutions. It is because when $\mu = \frac{m\pi}{l_i}$ is not the solution, the value $A_{n,1}(\mu)$ changes its sign rapidly near $\mu = \frac{m\pi}{l_i}$. In order to prevent from missing the root at $\mu = \frac{m\pi}{l_{max}}$, the condition $\frac{m\pi}{l_{max}} - \mu < \Delta\mu$ is checked during the increment of μ. Whenever the condition is true, a smaller increment, $\Delta\mu'$ must be used

$$\Delta\mu' = \frac{m\pi}{4}(\frac{1}{l_{min}} - \frac{1}{l_{max}}) \tag{3.4.23}$$

and the next trial value will be

$$\mu = \frac{m\pi}{l_{max}} + \frac{1}{2}\Delta\mu' \tag{3.4.24}$$

Equations 3.4.23 and 3.4.24 are used until the eigen solution near $\frac{m\pi}{l_{max}}$ is found. The increment will then be resumed as $\Delta\mu$ in equation 3.4.18.

Following the above iteration processes, it can easily obtain as many eigen solutions as required. Then, the solutions are put into equation 3.3.18 to complete the series part Y_m of the shape function. The final Y_m function is given by

$$Y_m = \sum_{m=1}^{n} A_{m,i,1}(\sin\mu_m y_i - \alpha_i \sinh\mu_m y_i) + A_{m,i,2}(\sin\mu_m y_i' - \alpha_i \sinh\mu_m y_i') \tag{3.4.25}$$

where $m = 1, 2, \cdots, n$ represents the total number of terms required

$i = 1, 2, \cdots, n$ represents the number of spans

CHAPTER 4

FINITE STRIP FORMULATION FOR PLATE-GIRDER BRIDGES

4.1 INTRODUCTION

The Finite Strip Method has been recognized as a very effective and convenient way to analyse folded plate structures. This kind of analysis was first introduced by Cheung [9]. The same method is employed for the analysis of straight simply supported, continuous plate-girder bridges because their structural response can be easily solved by folded plate strips.

A folded plate structure may be considered an assembly of rectangular plates which are capable of undergoing both the bending and the in-plane deformation. However, in a linear elastic analysis, it is assumed that no interaction takes place between those two actions. Consequently, a rectangular folded plate strip can be formed through a simple combination of a bending strip (section 4.2) and a plane stress strip (section 4.3). The combination of the bending strip and the in-plane stress strip is shown in section 4.4. Moreover, the formulation for those strips are discussed.

4.2 BENDING OF A PLATE STRIP

Before an appropriate displacement field can be assumed for a finite strip, the characteristics of the actual deformed shape should be examined. Figure 4.1 shows a typical strip from a simply supported bridge. Because of the conditions of the simple

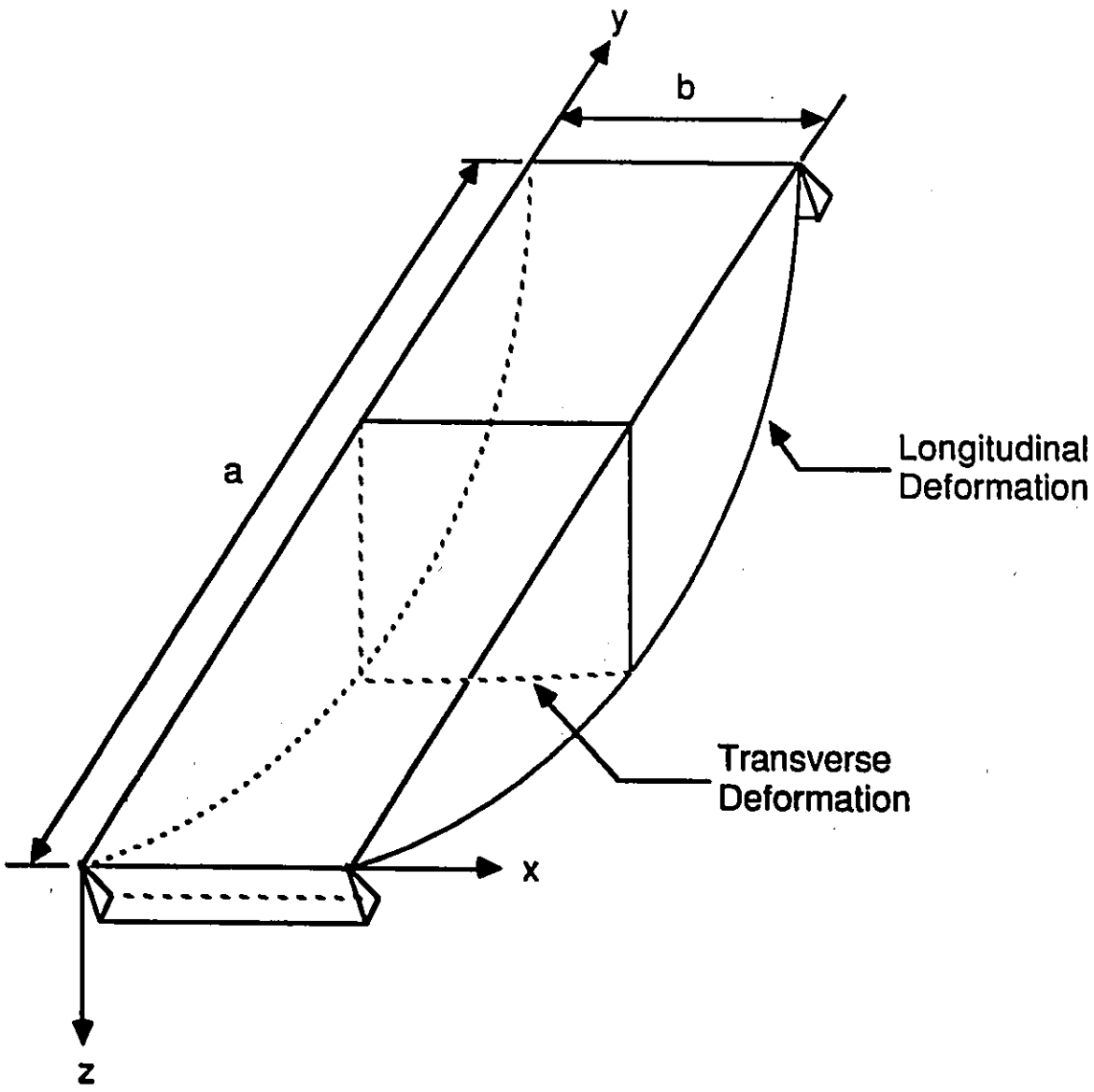

Figure 4.1: A TYPICAL RECTANGULAR STRIP

support, the displacement function must produce zero deflection at the supported sections. In addition, the bending moments in the longitudinal (spanwise) direction must also vanish at the two end supports. The longitudinal deformation of the strip can be well defined by a harmonic function as described in chapter 3. In the transverse direction, the deformation of the strip is given by the amount of the lateral displacement which can be expressed by a polynomial function. In order to establish a solution, the compatibility conditions between strips must be achieved. The simplest one is that the lateral displacement and its first partial derivative (i.e. rotation) are continuous over the interface between adjacent strips. Furthermore, a 'high order' strip which extends to include the compatibility of curvature (i.e. the second partial derivative of the lateral displacement) will theoretically improve the accuracy of the solution. However, for practical applications, a lower order strip (i.e. the simplest one) is usually used because of its simplicity and sufficiency in terms of the accuracy. Thus, this thesis will only be concentrated on the lower order finite strip.

For a strip in bending, the displacement function will be completely defined by a combination of a series Y_m and a polynomial function $f_m(x)$ as shown.

$$\begin{aligned} w(x,y) &= \sum_{m=1}^{r} f_m(x) Y_m \\ &= \sum_{m=1}^{r} (A + Bx + Cx^2 + Dx^3 + \cdots) Y_m \end{aligned} \qquad (4.2.1)$$

where A, B, C and D are coefficients of the polynomial.

m represents the m th term.

r is the total number of terms used.

On the other hand, the series function of the simple beam in bending [17] (see

figure 4.2) is given as follows.

$$w(y) = \sum_{m=1}^{r} \delta_m \sin \frac{m\pi y}{a} \tag{4.2.2}$$

where $w(y)$ is the displacement function with respect to y

δ_m is the displacement coefficient for the m th term

r is the total number of terms to be used

A comparison between equations 4.2.1 and 4.2.2 shows that $f_m(x)$ can be written in terms of the displacement parameters. If the deflection amplitudes w_{im} and w_{jm} (figure 4.3) at the two nodal lines i and j (i.e. $x = 0$ and $x = b$) for a continuous finite strip are chosen as the displacement parameters, then the displacement functions should be written as

$$\left\{ \begin{array}{c} w_i \\ w_j \end{array} \right\} = \sum_{m=1}^{r} \left\{ \begin{array}{c} w_{im} \\ w_{jm} \end{array} \right\} Y_m \tag{4.2.3}$$

For a complete solution, equation 4.2.3 is not enough because it only shows that the two adjacent strips possess the same deflection amplitude w_{im} for the common nodal line i and does not ensure the continuity of the slope across the strip boundaries. To guarantee the continuity of the slope, an additional unknown parameters for the transverse slope amplitude θ_{im} and θ_{jm} at nodal lines i and j are needed and shown in figure 4.3. The transverse slope function for the strip at $x = 0$ and $x = b$ are

$$\left\{ \begin{array}{c} \theta_i \\ \theta_j \end{array} \right\} = \left\{ \begin{array}{c} (\frac{\partial w}{\partial x})_i \\ (\frac{\partial w}{\partial x})_j \end{array} \right\} = \sum_{m=1}^{r} \left\{ \begin{array}{c} \theta_{im} \\ \theta_{jm} \end{array} \right\} Y_m \tag{4.2.4}$$

In order to solve the four unknown displacement parameters $w_{im}, \theta_{im}, w_{jm}$ and θ_{jm}, a third order polynomial is required.

$$f_m(x) = A + Bx + Cx^2 + Dx^3 \tag{4.2.5}$$

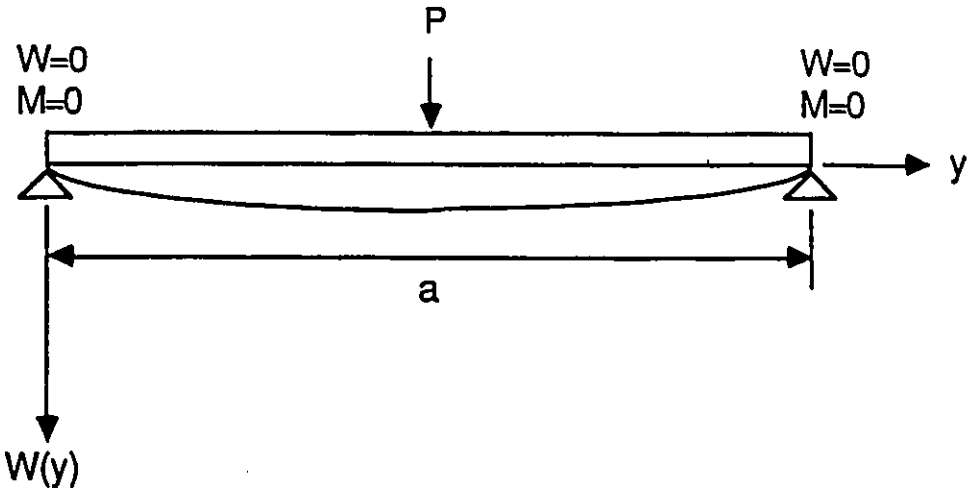

Figure 4.2: SIMPLE BEAM IN BENDING

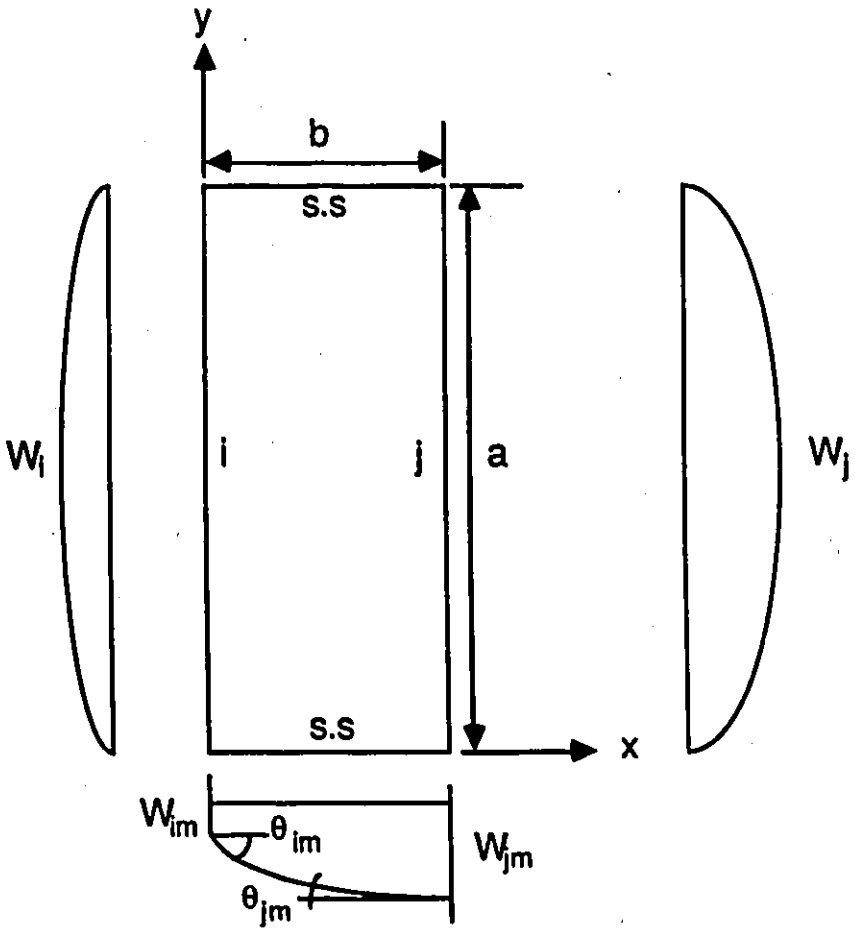

Figure 4.3: DISPLACEMENT FIELD OF A CONTINUOUS STRIP

By applying the compatibility conditions, the arbitrary constants A, B, C and D can be written in terms of the unknown parameters.

At $x = 0$: $\quad f_m(0) = w_{im}$ and $\frac{\partial fm(0)}{\partial x} = \theta_{im}$

At $x = b$: $\quad f_m(b) = w_{jm}$ and $\frac{\partial fm(b)}{\partial x} = \theta_{jm}$

The unknown coefficients of equation 4.2.5 becomes

$$\begin{aligned} A &= w_{im} \\ B &= \theta_{im} \\ A + Bb + Cb^2 + Db^3 &= w_{jm} \\ B + 2Cb + 3Db^2 &= \theta_{jm} \end{aligned} \tag{4.2.6}$$

or in matrix form,

$$\begin{bmatrix} 1 & 0 & 0 & 0 \\ 0 & 1 & 0 & 0 \\ 1 & b & b^2 & b^3 \\ 0 & b & 2b & 3b^2 \end{bmatrix} \begin{bmatrix} A \\ B \\ C \\ D \end{bmatrix} = \begin{bmatrix} w_{im} \\ \theta_{im} \\ w_{jm} \\ \theta_{jm} \end{bmatrix} \tag{4.2.7}$$

Solving equation 4.2.6 for A, B, C and D, yields

$$\begin{aligned} A &= w_{im} \\ B &= \theta_{im} \\ C &= -\frac{3w_{im}}{b^2} - \frac{2\theta_{im}}{b} + \frac{3w_{jm}}{b^2} - \frac{\theta_{jm}}{b} \\ D &= \frac{2w_{im}}{b^3} + \frac{\theta_{im}}{b^2} - \frac{2w_{jm}}{b^3} + \frac{\theta_{jm}}{b^2} \end{aligned} \tag{4.2.8}$$

Substituting equation 4.2.8 into equation 4.2.1, gives

$$\begin{aligned} w(x,y) = \sum_{m=1}^{r} \{ & (1 - \frac{3x^2}{b^2} + \frac{2x^3}{b^3}) w_{im} + (x - \frac{2x^2}{b} + \frac{x^3}{b^2}) \theta_{im} \\ & + (\frac{3x^2}{b^2} - \frac{2x^3}{b^3}) w_{jm} + (\frac{x^3}{b^2} - \frac{x^2}{b}) \theta_{jm} \} Y_m \end{aligned} \tag{4.2.9}$$

Equation 4.2.9 can be written in matrix form,

$$w(x,y) = \sum_{m=1}^{r} [C_1\, C_2\, C_3\, C_4] \begin{Bmatrix} w_{im} \\ \theta_{im} \\ w_{jm} \\ \theta_{jm} \end{Bmatrix} Y_m \tag{4.2.10}$$

or simply,

$$w_b(x,y) = \sum_{m=1}^{r} [C_b]\{\delta_{bm}\} Y_m \tag{4.2.11}$$

where subscript b represents a bending strip

$[C_b]$ represents the coefficient matrix for the displacement function

$\{\delta_{bm}\}$ represents the displacement amplitude

Based on the developed displacement function (equation 4.2.11), the strains (i.e. curvature) of the bending strip can be easily obtained through the appropriate differentiation. The strains for a plate in bending are given by the second partial derivatives of the displacement function and defined in the following.

$$\begin{aligned} \{\varepsilon_b\} &= \begin{Bmatrix} \psi_x \\ \psi_y \\ 2\psi_{xy} \end{Bmatrix} = \begin{Bmatrix} -\frac{\partial^2 w}{\partial x^2} \\ -\frac{\partial^2 w}{\partial y^2} \\ 2\frac{\partial^2 w}{\partial x \partial y} \end{Bmatrix} \\ &= \sum_{m=1}^{r} [B_{bm}]\{\delta_{bm}\} \end{aligned} \tag{4.2.12}$$

where $\{\varepsilon_b\}$ is the strain vector

$\{\delta_{bm}\} = [w_{im}\, \theta_{im}\, w_{jm}\, \theta_{jm}]^T$

ψ represents the curvature in the corresponding direction

and the $[B_{bm}]$ matrix is

$$\begin{bmatrix} (\frac{6}{b^2} - \frac{12x}{b^3})Y_m & (\frac{4}{b} - \frac{6x}{b^2})Y_m & (-\frac{6}{b^2} + \frac{12x}{b^3})Y_m & (-\frac{6x}{b^2} + \frac{2}{b})Y_m \\ (-1 + \frac{3x^2}{b^2} - \frac{2x^3}{b^3})Y_m'' & (-x + \frac{2x^2}{b} - \frac{x^3}{b^2})Y_m'' & (-\frac{3x^2}{b^2} + \frac{2x^3}{b^3})Y_m'' & (-\frac{x^3}{b^3} + \frac{x^2}{b^2})Y_m'' \\ (-\frac{12x}{b^2} + \frac{12x^2}{b^3})Y_m' & (2 - \frac{8x}{b} + \frac{6x^2}{b^2})Y_m' & (\frac{12x}{b^2} - \frac{12x^2}{b^3})Y_m' & (\frac{6x^2}{b^2} - \frac{4x}{b})Y_m' \end{bmatrix}$$

In addition, the stresses (or the moments) for a plate in bending are related to the strains through the material properties of the strip (i.e. the $[D_b]$ matrix). For the orthotropic material, the general formulation of the stresses are given by

$$\begin{aligned}
\{\sigma_b\} &= \left\{ \begin{array}{c} M_x \\ M_y \\ M_{xy} \end{array} \right\} = [D_b]\{\varepsilon_b\} \\
&= \left[\begin{array}{ccc} \frac{E_x t^3}{12(1-\nu_x\nu_y)} & \frac{\nu_y E_x t^3}{12(1-\nu_x\nu_y)} & 0 \\ \frac{\nu_x E_y t^3}{12(1-\nu_x\nu_y)} & \frac{E_y t^3}{12(1-\nu_x\nu_y)} & 0 \\ 0 & 0 & \frac{G_{xy} t^3}{12} \end{array} \right] \left\{ \begin{array}{c} \frac{-\partial^2 w}{\partial x^2} \\ \frac{-\partial^2 w}{\partial y^2} \\ 2\frac{\partial^2 w}{\partial x \partial y} \end{array} \right\} \\
&= [D_b] \sum_{m=1}^{r} [B_{bm}]\{\delta_{bm}\} \qquad (4.2.13)
\end{aligned}$$

Equation 4.2.13 can also be used for the isotropic material if $E_x = E_y = E$, $\nu_x = \nu_y = \nu$ and $G_{xy} = \frac{E}{2(1+\nu)}$ in the $[D_b]$ matrix are set.

Finally, the stiffness matrix $[S_b]$ and the load matrix $\{F_b\}$ can be derived by minimizing the total potential energy. The total potential energy for a strip in bending is given by

$$\begin{aligned}
U_t &= U_s + U_p \\
&= \frac{1}{2}\int_V (-M_x \frac{\partial^2 w}{\partial x^2} - M_y \frac{\partial^2 w}{\partial y^2} + 2M_{xy}\frac{\partial^2 w}{\partial x \partial y})dV - \int_A \{w_b\} q_b(x,y) dA \\
&= \frac{1}{2}\int_V \{\delta_b^T\}\{\varepsilon_b\} dV - \int_A \{w_b\}^T \{q_b\} dA \qquad (4.2.14)
\end{aligned}$$

where U_s and U_p are the strain and the potential energy of a strip

$\{q\}$ is the loading matrix

Substituting equation 4.2.11, 4.2.12 and 4.2.13 into equation 4.2.14, yields

$$U_t = \frac{1}{2}\int_A \{\delta_b\}^T [B_b]^T [D_b][B_b]\{\delta_b\} dA - \int_A \{\delta_b\}^T [C_b]^T Y_m \{q_b\} dA \qquad (4.2.15)$$

The first integral of equation 4.2.15 is changed to dA from dV because the thickness of the strip has been considered in the $[D]$ matrix. The minimization of equation 4.2.15 is achieved by setting $\frac{\partial U_t}{\partial \delta} = 0$, that is

$$\frac{\partial U_t}{\partial \delta} = \int_A [B_{bm}]^T [D_b][B_{bn}] dA\{\delta_b\} - \int_A [C_b]^T \{q_b\} Y_m dA = 0 \tag{4.2.16}$$

By comparing with

$$[S]\{\delta\} - \{F\} = \{0\} \tag{4.2.17}$$

it is noticed that the stiffness matrix and the load matrix can be expressed by

$$[S_b] = \int_A [B_{bm}]^T [D_b][B_{bn}] dA \tag{4.2.18}$$

and

$$\{F_b\} = \int_A [C_b]^T \{q_b\} Y_m dA \tag{4.2.19}$$

respectively.

4.3 IN-PLANE STRESS OF A PLATE STRIP

In this section, the displacement function for a plane stress strip is discussed. Under the in-plane forces, any point in a rectangular plate undergoes displacements in plane of the plate which can be resolved into components parallel to the x and y axes (see figure 4.4). This is so called the lower order finite strip which was first introduced by Cheung [5,6]. A higher order strip which includes an additional internal nodal line was developed by Loo and Cusens [35]. This higher order strip is found, as expected, to be more accurate. However, the assembly procedure is quite complicated. In order to reduce the bandwidth of the overall matrix and to facilitate computation, the parameters associated with the internal nodal line are usually eliminated through the static condensation before the assembly stage.

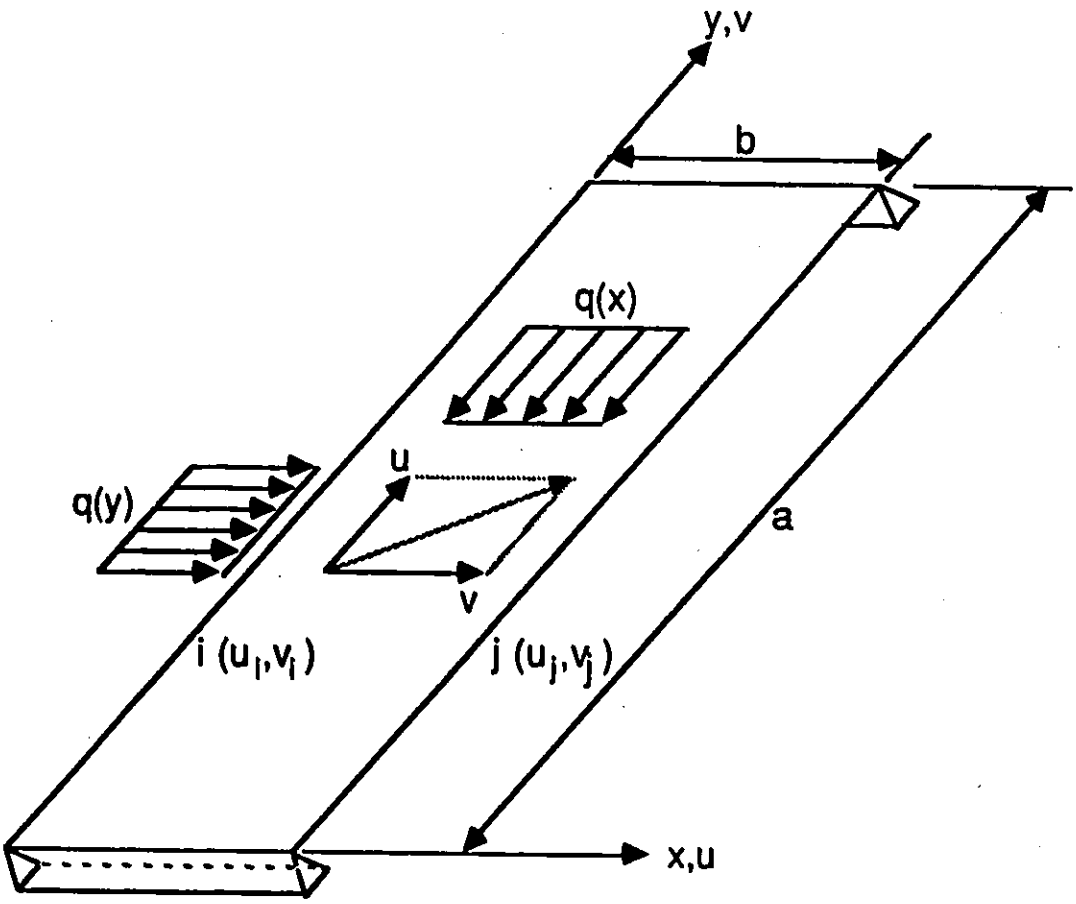

Figure 4.4: SIMPLY SUPPORTED PLATE UNDER IN-PLANE FORCE

In addition, several plane stress strips using (u, $\frac{\partial u}{\partial x}$, v), (u, v, $\frac{\partial v}{\partial x}$) and ($u$, $\frac{\partial u}{\partial x}$, v, $\frac{\partial v}{\partial x}$) as the nodal parameters were studied by Yoshida and Oka [49]. They found that the displacement functions with (u, $\frac{\partial u}{\partial x}$, v, $\frac{\partial v}{\partial x}$) as a nodal parameter was the best in terms of accuracy. But, such a strip cannot be used directly for problems having sudden change in property or plate thickness because of the discontinuous of strains at these locations. As a result, a lower order displacement function is chosen because of its simplicity and ease of assemblage.

Similar to the bending strip analysis, the displacement function for the plane stress strip consists of two parts: a series Y_m and a polynomial $f_m(x)$. From the small deflection theory of beam, the relationship between the transverse deflection u and the longitudinal displacement v is observed as

$$v = A\frac{du}{dy} \tag{4.3.1}$$

If Y_m and Y'_m are assumed to be the series part of the displacement functions u and v respectively, then the general form for the displacements is given by

$$\begin{aligned} u &= \sum_{m=1}^{r} f_{m_u}(x) Y_m \\ &= \sum_{m=1}^{r} (A + Bx + \cdots) Y_m \end{aligned} \tag{4.3.2}$$

and

$$\begin{aligned} v &= \sum_{m=1}^{r} f_{m_v}(x) \frac{Y'_m}{\mu_m} \\ &= \sum_{m=1}^{r} (C + Dx + \cdots) \frac{Y'_m}{\mu_m} \end{aligned} \tag{4.3.3}$$

where A, B, C and D are unknown coefficients of the polynomial

The polynomials in equations 4.3.2 and 4.3.3 can be in terms of the displacement

parameters (u_{im}, v_{im} and u_{jm}, v_{jm} as shown in figure 4.4) at nodal lines i and j in the transverse and the longitudinal directions. The polynomial represents the u and v displacement function at nodal lines i and j are

$$\begin{aligned} u_i &= \sum_{m=1}^{r} u_{im} Y_m \\ u_j &= \sum_{m=1}^{r} u_{jm} Y_m \end{aligned} \tag{4.3.4}$$

and

$$\begin{aligned} v_i &= \sum_{m=1}^{r} v_{im} \frac{Y'_m}{\mu_m} \\ v_j &= \sum_{m=1}^{r} v_{jm} \frac{Y'_m}{\mu_m} \end{aligned} \tag{4.3.5}$$

For the unknown displacement parameters (u_{im}, v_{im} and u_{jm}, v_{jm}), the first order polynomial is sufficient for obtaining a solution. Using the same procedure as before, the unknown coefficients A, B, C and D are found to be

$$\begin{aligned} A &= u_{im} \\ B &= \frac{u_{jm}}{b} - \frac{u_{im}}{b} \\ C &= v_{im} \\ D &= \frac{v_{jm}}{b} - \frac{v_{im}}{b} \end{aligned} \tag{4.3.6}$$

Substituting equation 4.3.6 into equations 4.3.4 and 4.3.5, yields

$$u = \sum_{m=1}^{r} [(1 - \frac{x}{b}) u_{im} + \frac{x}{b} u_{jm}] Y_m \tag{4.3.7}$$

and

$$v = \sum_{m=1}^{r} [(1 - \frac{x}{b}) v_{im} + \frac{x}{b} v_{jm}] \frac{Y'_m}{\mu_m} \tag{4.3.8}$$

Equations 4.3.7 and 4.3.8 can be combined to form a matrix

$$\begin{bmatrix} u \\ v \end{bmatrix} = \sum_{m=1}^{r} \begin{bmatrix} (1-\frac{x}{b})Y_m & 0 & \frac{x}{b}Y_m & 0 \\ 0 & (1-\frac{x}{b})\frac{Y'_m}{\mu_m} & 0 & \frac{x}{b}\frac{Y'_m}{\mu_m} \end{bmatrix} \begin{Bmatrix} u_{im} \\ v_{im} \\ u_{jm} \\ v_{jm} \end{Bmatrix} \tag{4.3.9}$$

or simply

$$\begin{Bmatrix} u \\ v \end{Bmatrix} = \sum_{m=1}^{r} [C_{pm}]\{\delta_{pm}\} \tag{4.3.10}$$

where subscript p represents a plane stress strip

$[C_{pm}]$ represents the coefficient matrix for the displacement function of an in-plane stress strip

$\{\delta_{pm}\}$ represents the displacement parameters

In the plane stress analysis, there are three strain components which are the transverse strain ε_x, the longitudinal strain ε_y and the shear strain γ_{xy}. Those strains are related to the displacements by

$$\begin{aligned} \{\varepsilon_p\} &= \begin{Bmatrix} \varepsilon_x \\ \varepsilon_y \\ \gamma_{xy} \end{Bmatrix} = \begin{Bmatrix} \frac{\partial u}{\partial x} \\ \frac{\partial v}{\partial y} \\ \frac{\partial u}{\partial y} + \frac{\partial v}{\partial x} \end{Bmatrix} \\ &= \begin{bmatrix} -\frac{1}{b}Y_m & 0 & \frac{1}{b}Y_m & 0 \\ 0 & (1-\frac{x}{b})\frac{Y''_m}{\mu_m} & 0 & \frac{x}{b}\frac{Y''_m}{\mu_m} \\ (1-\frac{x}{b})Y'_m & -\frac{1}{b}\frac{Y'_m}{\mu_m} & \frac{x}{b}Y'_m & \frac{1}{b}\frac{Y'_m}{\mu_m} \end{bmatrix} \begin{Bmatrix} u_{im} \\ v_{im} \\ u_{jm} \\ v_{jm} \end{Bmatrix} \\ &= \sum_{m=1}^{r} [B_{pm}]\{\delta_{pm}\} \end{aligned} \tag{4.3.11}$$

where $[B_{pm}]$ represents the strain matrix.

In addition, the in-plane stresses and the displacements have the following relationship

$$\{\sigma_p\} = \begin{Bmatrix} \sigma_x \\ \sigma_y \\ \tau_{xy} \end{Bmatrix} = [D_p]\{\varepsilon_p\}$$

$$= \begin{bmatrix} \frac{E_x}{(1-\nu_x\nu_y)} & \frac{\nu_x E_x}{(1-\nu_x\nu_y)} & 0 \\ \frac{\nu_y E_y}{(1-\nu_x\nu_y)} & \frac{E_y}{(1-\nu_x\nu_y)} & 0 \\ 0 & 0 & G_{xy} \end{bmatrix} \begin{Bmatrix} \varepsilon_x \\ \varepsilon_y \\ \gamma_{xy} \end{Bmatrix}$$

$$= [D_p] \sum_{m=1}^{r} [B_{pm}]\{\delta_{pm}\} \tag{4.3.12}$$

The above $[D_p]$ matrix is used for the orthotropic material only. If the isotropic material is used, the same requirements for matrix $[D_b]$ as shown in section 4.2 should be satisfied.

According to the same minimization procedure as given in section 4.2, the formation of the stiffness matrix and the load matrix can be achieved. For a plate strip with constant thickness (t), the stiffness matrix $[S_p]$ and the load matrix $\{F_p\}$ of a plane stress strip are expressed by

$$[S_p] = t \int_A [B_{pm}]^T [D_p][B_{pm}] dA \tag{4.3.13}$$

and

$$\{F_p\} = \int_A [C_{pm}]\{q_p\} dA \tag{4.3.14}$$

where $\{q_p\}$ is the loading function consists of $q(x)$ and $q(y)$ (see figure 4.4) at nodal lines i and j

4.4 FOLDED PLATE STRIP AND ITS FORMULATION

For every folded plate strip, both the bending forces and the in-plane stresses play a very important role. Because of the assumption that no interaction takes place between the bending forces and the in-plane stress, folded plate strips can easily be formed through a simple combination of a bending strip and a plane stress strip. In this thesis, only a lower order strip is interested. As a result, the

formulation of the folded plate strip is based on the bending strip in section 4.2 and the plane stress strip in section 4.3.

In this section, the formulation of a folded plate strip will be focused on the following two categories:

(i) with constant width (i.e. a rectangular folded plate strip) which is used for analyzing the flange, slab and web of a plate-girder bridge, and

(ii) with variable width which can describe the haunched web of a haunched plate-girder bridge.

4.4.1 FORMULATION OF A STRIP WITH CONSTANT WIDTH

Consider a typical folded plate strip as shown in figure 4.5. If both the bending and the in-plane nodal displacements occur simultaneously, then there will be four displacement components (u, v, w and θ) at each of the two nodal lines (e.g. u_i, v_i, w_i and θ_i at nodal line i and u_j, v_j, w_j and θ_j at nodal line j).

From section 4.2, it is noticed that the displacement parameters (w and θ) are related to each other through equation 4.2.9. Therefore, for a lower order strip with nodal lines i and j, the relationship between the displacement parameters w_i, θ_i and w_j, θ_j can be written as

$$w = \sum_{m=1}^{\infty} \{(1-\frac{3x^2}{b^2}+\frac{2x^3}{b^3})w_{im}+(x-\frac{2x^2}{b}+\frac{x^3}{b^2})\theta_{im}+(\frac{3x^2}{b^2}-\frac{2x^3}{b^3})w_{jm}+(\frac{x^3}{b^2}-\frac{x^2}{b})\theta_{jm}\}Y_m(y) \tag{4.4.1}$$

Similarly, from equations 4.3.7 and 4.3.8, the displacement components u_i, v_i, u_j and v_j are related by

$$u = \sum_{m=1}^{\infty} [(1-\frac{x}{b})u_{im} + \frac{x}{b}u_{jm}]Y_m(y) \tag{4.4.2}$$

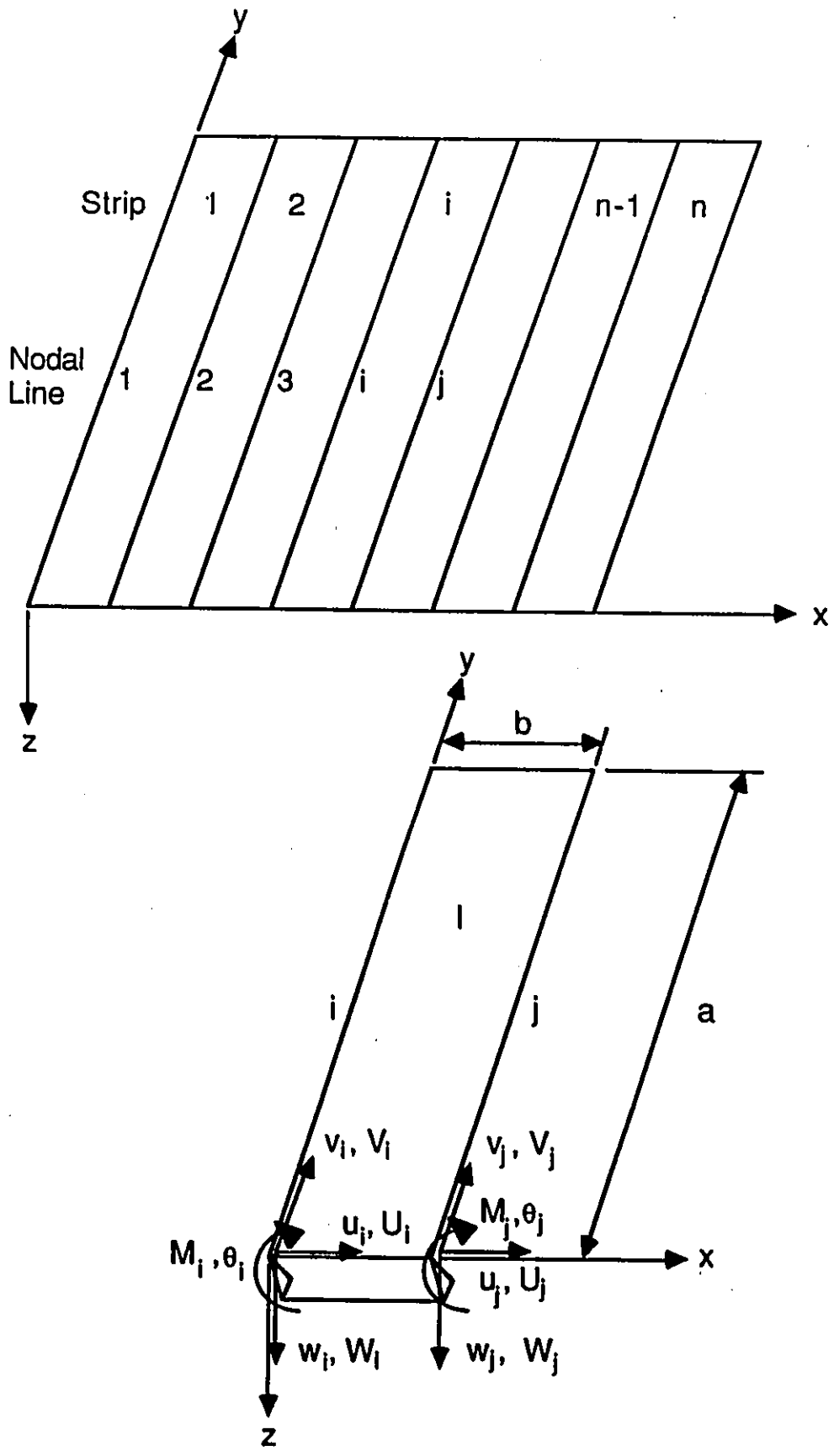

Figure 4.5: A TYPICAL FOLDED PLATE STRIP

and

$$v = \sum_{m=1}^{\infty}[(1-\frac{x}{b})v_{im} + \frac{x}{b}v_{jm}]\frac{Y'_m(y)}{\mu_m} \tag{4.4.3}$$

According to the assumption that there is no interaction between the bending and the in-plane actions, the relationship between the strain and the displacement for a rectangular folded plate strip is defined by combining the strain-displacement equations of the bending strip (equation 4.2.12) and the plane stress strip (equation 4.3.11). Such strain-displacement relation is shown by

$$\{\varepsilon\} = \begin{Bmatrix} \{\varepsilon_p\} \\ \{\varepsilon_b\} \end{Bmatrix} = \begin{Bmatrix} \varepsilon_x \\ \varepsilon_y \\ \gamma_{xy} \\ \psi_x \\ \psi_y \\ 2\psi_{xy} \end{Bmatrix} = \begin{Bmatrix} \frac{\partial u}{\partial x} \\ \frac{\partial v}{\partial y} \\ \frac{\partial u}{\partial y} + \frac{\partial v}{\partial x} \\ -\frac{\partial^2 w}{\partial x^2} \\ -\frac{\partial^2 w}{\partial y^2} \\ 2\frac{\partial^2 w}{\partial x \partial y} \end{Bmatrix} \tag{4.4.4}$$

or

$$\{\varepsilon\} = \sum_{m=1}^{\infty}[B_m]\{\delta_m\} \tag{4.4.5}$$

where $\{\delta_m\} = [u_i\ v_i\ w_i\ \theta_i\ u_j\ v_j\ w_j\ \theta_j]^T_m$

The above $[B_m]$ matrix, which is composed of $[B_{pm}]$ and $[B_{bm}]$ as described in equation 4.3.11 and 4.2.12 respectively, has the following form

$$[B_m] = \begin{bmatrix} -\frac{1}{b}Y_m & 0 & 0 & 0 & \frac{1}{b}Y_m & 0 & 0 & 0 \\ 0 & \bar{b}\frac{Y''_m}{\mu_m} & 0 & 0 & 0 & \frac{x}{b}\frac{Y''_m}{\mu_m} & 0 & 0 \\ \bar{b}Y'_m & -\frac{1}{b}\frac{Y'_m}{\mu_m} & 0 & 0 & \frac{x}{b}Y'_m & \frac{1}{b}\frac{Y'_m}{\mu_m} & 0 & 0 \\ 0 & 0 & K_1Y_m & K_4Y_m & 0 & 0 & -K_1Y_m & K_8Y_m \\ 0 & 0 & K_2Y''_m & K_5Y''_m & 0 & 0 & K_7Y''_m & K_9Y''_m \\ 0 & 0 & K_3Y'_m & K_6Y'_m & 0 & 0 & -K_3Y'_m & K_{10}Y'_m \end{bmatrix} \tag{4.4.6}$$

where

$$\begin{aligned} \bar{b} &= (1-\tfrac{x}{b}) \\ K_1 &= \tfrac{6}{b^2} - \tfrac{12x}{b^3} & K_2 &= -1 + \tfrac{3x^2}{b^2} - \tfrac{2x^3}{b^3} \\ K_3 &= -\tfrac{12x}{b^2} + \tfrac{12x^2}{b^3} & K_4 &= \tfrac{4}{b} - \tfrac{6x}{b^2} \\ K_5 &= -x + \tfrac{2x^2}{b} + \tfrac{x^3}{b^2} & K_6 &= 2 - \tfrac{8x}{b} + \tfrac{6x^2}{b^2} \\ K_7 &= -\tfrac{3x^2}{b^2} + \tfrac{2x^3}{b^3} & K_8 &= -\tfrac{6x}{b^2} + \tfrac{2}{b} \\ K_9 &= \tfrac{x^2}{b^2} - \tfrac{x^3}{b^3} & K_{10} &= \tfrac{6x^2}{b^2} - \tfrac{4x}{b} \end{aligned}$$

The transpose of the matrix $[B_m]$ is found to be

$$[B_m]^T = \begin{bmatrix} -\frac{1}{b}Y_m & 0 & \bar{b}Y'_m & 0 & 0 & 0 \\ 0 & \bar{b}\frac{Y''_m}{\mu_m} & -\frac{1}{b}\frac{Y'_m}{\mu_m} & 0 & 0 & 0 \\ 0 & 0 & 0 & K_1Y_m & K_2Y''_m & K_3Y'_m \\ 0 & 0 & 0 & K_4Y_m & K_5Y''_m & K_6Y'_m \\ \frac{1}{b}Y_m & 0 & \frac{x}{b}Y'_m & 0 & 0 & 0 \\ 0 & \frac{x}{b}\frac{Y''_m}{\mu_m} & \frac{1}{b}\frac{Y'_m}{\mu_m} & 0 & 0 & 0 \\ 0 & 0 & 0 & -K_1Y_m & K_7Y''_m & -K_3Y'_m \\ 0 & 0 & 0 & K_8Y_m & K_9Y''_m & K_{10}Y'_m \end{bmatrix} \tag{4.4.7}$$

On the other hand, the stresses and the strains have the following relationship

$$\{\sigma\} = \begin{Bmatrix} \{\sigma_p\} \\ \{\sigma_b\} \end{Bmatrix} = \begin{Bmatrix} \sigma_x \\ \sigma_y \\ \tau_{xy} \\ M_x \\ M_y \\ M_{xy} \end{Bmatrix} = [D]\{\varepsilon\} \tag{4.4.8}$$

where $\{\sigma_p\} = [D_p]\{\varepsilon_p\}$ (equation 4.3.12)

$\{\sigma_b\} = [D_b]\{\varepsilon_b\}$ (equation 4.2.13)

The matrix $[D]$ in equation 4.4.8 is the combination of $[D_p]$ and $[D_b]$ and defined by

$$[D] = \begin{bmatrix} t[D_p] & 0 \\ 0 & [D_b] \end{bmatrix} \tag{4.4.9}$$

or

$$[D] = \begin{bmatrix} D_x t & \nu_x D_x t & 0 & 0 & 0 & 0 \\ \nu_y D_y t & D_y t & 0 & 0 & 0 & 0 \\ 0 & 0 & G_{xy}t & 0 & 0 & 0 \\ 0 & 0 & 0 & \frac{t^3}{12}D_x & \frac{t^3}{12}\nu_y D_x & 0 \\ 0 & 0 & 0 & \frac{t^3}{12}\nu_x D_y & \frac{t^3}{12}D_y & 0 \\ 0 & 0 & 0 & 0 & 0 & \frac{t^3}{12}G_{xy} \end{bmatrix} \tag{4.4.10}$$

where $D_x = \frac{E_x}{1-\nu_x\nu_y}$

$D_y = \frac{E_y}{1-\nu_x\nu_y}$

t is the thickness of the strip

It should be careful that the above $[D]$ matrix is used for the orthotropic material only. If the isotropic material is concerned, then it is necessary to set $E_x = E_y = E$, $\nu_x = \nu_y = \nu$ and $G_{xy} = \frac{E}{2(1+\nu)}$.

Following the same procedure for the minimization of the total potential energy as described in section 4.2, the stiffness matrix of a folded plate strip corresponding to the m th and n th series terms is

$$[S_{mn}] = \int_L \int_b [B_m]^T [D][B_n]\, dx\, dy \tag{4.4.11}$$

where L is the length of the strip

b is the width of the strip

$[B_m]$ and $[B_n]$ are the same and defined in equation 4.4.6

The product of $[B_m]^T[D][B_n]$ is expanded in a matrix form as below

$$[B_m]^T[D][B_n] = [B^T D B]$$
$$= \begin{bmatrix} T_{11} & T_{12} & 0 & 0 & T_{15} & T_{16} & 0 & 0 \\ T_{21} & T_{22} & 0 & 0 & T_{25} & T_{26} & 0 & 0 \\ 0 & 0 & T_{33} & T_{34} & 0 & 0 & T_{37} & T_{38} \\ 0 & 0 & T_{43} & T_{44} & 0 & 0 & T_{47} & T_{48} \\ T_{51} & T_{52} & 0 & 0 & T_{55} & T_{56} & 0 & 0 \\ T_{61} & T_{62} & 0 & 0 & T_{65} & T_{66} & 0 & 0 \\ 0 & 0 & T_{73} & T_{74} & 0 & 0 & T_{77} & T_{78} \\ 0 & 0 & T_{83} & T_{84} & 0 & 0 & T_{87} & T_{88} \end{bmatrix} \tag{4.4.12}$$

where

$$
\begin{aligned}
T_{11} &= t(\tfrac{D_x}{b^2}Y_{00} + \bar{b}^2 G) & T_{12} &= -\tfrac{t\bar{b}}{b\mu_n}(\nu_x D_x Y_{02} + G)\\
T_{15} &= \tfrac{t}{b}(-\tfrac{D_x}{b}Y_{00} + x\bar{b}G) & T_{16} &= -\tfrac{t\bar{b}}{b\mu_n}(\nu_x D_x Y_{02} + G)\\
T_{21} &= -\tfrac{t\bar{b}}{b\mu_m}(\nu_y D_y Y_{20} + G) & T_{22} &= \tfrac{t}{\mu_m\mu_n}(\bar{b}^2 D_y Y_{22} + \tfrac{G}{b^2})\\
T_{25} &= \tfrac{t}{b\mu_m}(\bar{b}\nu_y D_y Y_{20} - \tfrac{x}{b}G) & T_{26} &= \tfrac{t}{b\mu_m\mu_n}(x\bar{b}D_y Y_{22} - \tfrac{G}{b})\\
T_{33} &= \tfrac{t^3}{12}(K_1M_1 + K_2M_2 + K_3^2 G) & T_{34} &= \tfrac{t^3}{12}(K_1M_3 + K_2M_4 + K_3K_6 G)\\
T_{37} &= \tfrac{t^3}{12}(K_1M_5 + K_2M_6 - K_3^2 G) & T_{38} &= \tfrac{t^3}{12}(K_1M_7 + K_2M_8 + K_3K_{10} G)\\
T_{43} &= \tfrac{t^3}{12}(K_4M_1 + K_5M_2 + K_3K_6 G) & T_{44} &= \tfrac{t^3}{12}(K_4M_3 + K_5M_4 + K_6^2 G)\\
T_{47} &= \tfrac{t^3}{12}(K_4M_5 + K_5M_6 - K_3K_6 G) & T_{48} &= \tfrac{t^3}{12}(K_4M_7 + K_5M_8 + K_6K_{10} G)\\
T_{51} &= -\tfrac{t}{b}(\tfrac{D_x}{b}Y_{00} - x\bar{b}G) & T_{52} &= \tfrac{t}{b\mu_n}(\bar{b}\nu_x D_x Y_{02} - \tfrac{xG}{b})\\
T_{55} &= \tfrac{t}{b^2}(D_x Y_{00} + x^2 G) & T_{56} &= \tfrac{xt}{b^2\mu_n}(\nu_x D_x Y_{02} + G)\\
T_{61} &= -\tfrac{t}{b\mu_m}(\tfrac{x}{b}\nu_x D_y Y_{20} - \bar{b}G) & T_{62} &= \tfrac{t}{b\mu_m\mu_n}(x\bar{b}D_y Y_{22} - \tfrac{G}{b})\\
T_{65} &= \tfrac{xt}{b^2\mu_m}(\nu_x D_y Y_{20} + G) & T_{66} &= \tfrac{t}{b^2\mu_m\mu_n}(x^2 D_y Y_{22} + G)\\
T_{73} &= \tfrac{t^3}{12}(-K_1M_1 + K_7M_2 - K_3^2 G) & T_{74} &= \tfrac{t^3}{12}(-K_1M_3 + K_7M_4 - K_3K_6 G)\\
T_{77} &= \tfrac{t^3}{12}(-K_1M_5 + K_7M_6 - K_3^2 G) & T_{78} &= \tfrac{t^3}{12}(-K_1M_7 + K_7M_8 + K_3K_{10} G)\\
T_{83} &= \tfrac{t^3}{12}(K_8M_1 + K_9M_2 + K_3K_{10} G) & T_{84} &= \tfrac{t^3}{12}(K_8M_3 + K_9M_4 + K_6K_{10} G)\\
T_{87} &= \tfrac{t^3}{12}(K_8M_5 + K_9M_6 - K_3K_{10} G) & T_{88} &= \tfrac{t^3}{12}(K_8M_7 + K_9M_8 + K_{10}^2 G)\\
\bar{b} &= (1 - \tfrac{x}{b}) & & \\
K_1 &= \tfrac{6}{b^2} - \tfrac{12x}{b^3} & K_2 &= -1 + \tfrac{3x^2}{b^2} - \tfrac{2x^3}{b^3}\\
K_3 &= -\tfrac{12x}{b^2} + \tfrac{12x^2}{b^3} & K_4 &= \tfrac{4}{b} - \tfrac{6x}{b^2}\\
K_5 &= -x + \tfrac{2x^2}{b} + \tfrac{x^3}{b^2} & K_6 &= 2 - \tfrac{8x}{b} + \tfrac{6x^2}{b^2}\\
K_7 &= -\tfrac{3x^2}{b^2} + \tfrac{2x^3}{b^3} & K_8 &= -\tfrac{6x}{b^2} + \tfrac{2}{b}\\
K_9 &= \tfrac{x^2}{b^2} - \tfrac{x^3}{b^3} & K_{10} &= \tfrac{6x^2}{b^2} - \tfrac{4x}{b}\\
G &= G_{xy}Y_{11} & Y_{00} &= Y_m Y_n\\
Y_{02} &= Y_m Y_n'' & Y_{11} &= Y_m' Y_n'\\
Y_{20} &= Y_m'' Y_n & Y_{22} &= Y_m'' Y_n''\\
M_1 &= D_x(K_1 Y_{00} + K_2\nu_y Y_{02}) & M_2 &= D_y(K_1\nu_x Y_{20} + K_2 Y_{22})\\
M_3 &= D_x(K_4 Y_{00} + K_5\nu_y Y_{02}) & M_4 &= D_y(K_4\nu_x Y_{20} + K_5 Y_{22})\\
M_5 &= D_x(-K_1 Y_{00} + K_7\nu_y Y_{02}) & M_6 &= D_y(-K_1\nu_x Y_{20} + K_7 Y_{22})\\
M_7 &= D_x(K_8 Y_{00} + K_9\nu_y Y_{02}) & M_8 &= D_y(K_8\nu_x Y_{20} + K_9 Y_{22})
\end{aligned}
$$

Substituting equation 4.4.12 into equation 4.4.11, gives

$$[S_{mn}] = \int_L \int_b [B^T D B]\, dx\, dy \tag{4.4.13}$$

The stiffness matrix can now be determined by taking the appropriate integration. The integral $\int_b dx$, represents the integration in the transverse direction of a strip, is

calculated according to the usual method of integration, while the integration in the y direction (i.e. the longitudinal direction) is obtained by the numerical method. In this case, Gaussian Integration [50] is employed because of its simplicity and accuracy. This numerical integration consists of the following Gaussian Quadrature Formula

$$I = \int_{-1}^{1} f(\xi)d\xi = \sum_{i=1}^{n} \mathcal{W}_i f(\xi_i) \tag{4.4.14}$$

where $f(\xi)$ represents a function or polynomial of any degree

n is the total number of Gaussian Integration points used

and a table (table 4.1) which summaries the abscissae (ξ_i) and weight coefficients ($\mathcal{W}_i$) of equation 4.4.14. The number of Gaussian Integration point (i.e. n in table 4.1) used for a N th degree polynomial is found to be

$$N = 2n - 1 \tag{4.4.15}$$

For illustration, the following polynomial is solved.

$$y = \int_{-1}^{1} (x^3 + x^2)dx \tag{4.4.16}$$

If Gaussian Integration is used, equation 4.4.16 would be written in terms of equation 4.4.14, that is

$$\begin{aligned} y &= \int_{-1}^{1} (x^3 + x^2)dx \\ &= \int_{-1}^{1} f(\xi)d\xi \\ &= \sum_{1}^{n} W_i f(\xi) \end{aligned} \tag{4.4.17}$$

From equation 4.4.15, the Gaussian Integration point is found to be equal to 2

n	$\pm\xi$	W
1	0	2.00000 00000 00000
2	0.57735 02691 89626	1.00000 00000 00000
3	0.77459 66692 41483	0.55555 55555 55556
	0.00000 00000 00000	0.88888 88888 88889
4	0.86113 63115 94053	0.34785 48451 37454
	0.33998 10435 84856	0.65214 51548 62546
5	0.90617 98459 38664	0.23692 68850 56189
	0.53846 93101 05683	0.47862 86704 99366
	0.00000 00000 00000	0.56888 88888 88889
6	0.93246 95142 03152	0.17132 44923 79170
	0.66120 93864 66265	0.36076 15730 48139
	0.23861 91860 83197	0.46791 39345 72691
7	0.94910 79123 42759	0.12948 49661 68870
	0.79666 64774 13627	0.22238 10344 53374
	0.52553 24099 16329	0.31370 66458 77887
	0.18343 46424 95650	0.36268 37833 78362
8	0.96028 98564 97536	0.10122 85362 90376
	0.79666 64774 13627	0.22238 10344 53374
	0.52553 24099 16329	0.31370 66458 77887.
	0.18343 46424 95650	0.36268 37833 78362
9	0.96816 02395 07626	0.08127 43883 61574
	0.83603 11073 26636	0.18064 81606 94857
	0.61337 14327 00590	0.26061 06964 02935
	0.32425 34234 03809	0.31234 70770 40003
	0.00000 00000 00000	0.33023 93550 01260
10	0.97390 65285 17172	0.06667 13443 08688
	0.86506 33666 88985	0.14945 13491 50581
	0.67940 95682 99024	0.21908 63625 15982
	0.43339 53941 29247	0.26926 67193 09996
	0.14887 43389 81631	0.29552 42247 14753

Table 4.1: ABSCISSAE AND WEIGHT COEFFICIENT FOR GAUSSIAN INTEGRATION

for this 3rd degree polynomial. With the help of table 4.1, the solution of equation 4.4.17 is obtained as

$$\begin{aligned} y &= \int_{-1}^{1}(x^3+x^2)dx \\ &= 1\times[(0.57735)^3+(0.57735)^2]+1\times[(-0.57735)^3+(-0.57735)^2] \\ &= 0.66667 \end{aligned} \tag{4.4.18}$$

The result is checked by the direct integration of equation 4.4.16, which is

$$\begin{aligned} y &= \int_{-1}^{1}(x^3+x^2)dx \\ &= [\frac{x^4}{4}+\frac{x^3}{3}]_{-1}^{1} \\ &= \frac{2}{3} \end{aligned} \tag{4.4.19}$$

From both results, it is verified that Gaussian Integration is a very simple but accurate numerical method if the Gaussian Integration points are correctly chosen.

By using Gaussian Integration method, the integral $\int_L dy$ is solved as follows. Since the accuracy of the result is affected by the number of Gaussian Integration points, so it is important to have adequate number of Gaussian points in the calculation. In addition, the accuracy might be improved if the span length of each span is divided into smaller segments. The number of segments is determined by the value n_{μ_m} which is expressed by

$$n_{\mu_m} = \frac{\mu_m l_i}{\pi} \tag{4.4.20}$$

where μ_m is the m th term of the eigen solution obtained from chapter 3

l_i represents the length of the i th span

By trial and error, the value n_{μ_m} of each segment should not be bigger than 5. For example, if $n_{\mu_m} = 15$ is found in the 2nd span, then the 2nd span should be

$n_{\mu m}$	Segments	Gaussian Points
$1 \sim 3$	1	8
$4 \sim 5$	1	10
$6 \sim 7$	2	8
$8 \sim 10$	2	10
$11 \sim 12$	3	8
$13 \sim 15$	3	10
$16 \sim 19$	4	10
> 19	5	10
> 25	6	10

Table 4.2: NUMBER OF SEGMENTS AND GAUSSIAN POINTS

divided into 3 segments to satisfy the condition ($n_{\mu m} \not> 5$). Moreover, the number of Gaussian Integration points is chosen within the range of 8 to 10 for each segment. Table 4.2 gives a summary of the proper number of segments and Gaussian points in solving the integral $\int_L dy$.

According to the four displacement components shown in figure 4.5, there should be four corresponding force components which are U, V, W and M. These force parameters may be written in a matrix form called the load matrix. This load matrix is formed by using the same procedure as described for the stiffness matrix.

Combining the load matrix of the bending strip and the plane stress strip, yields

$$\{F\} = \begin{Bmatrix} \{F_p\} \\ \{F_b\} \end{Bmatrix} \tag{4.4.21}$$

where $\{F_p\} = \int_A [C_{pm}]\{q_p\}dA$ (equation 4.3.14)

$\{F_b\} = \int_A [C_b]^T \{q_b\} Y_m dA$ (equation 4.2.19)

or in the form

$$\{F\} = \int_A [C_m]\{q\}dA \tag{4.4.22}$$

The matrices $[C_m]$ and $\{q\}$ in equation 4.4.22 are composed of matrices $[C_{pm}]$, $[C_b]^T Y_m$ and matrices $\{q_p\}$, $\{q_b\}$ respectively. Also, the integral $\int_A dA$ can be replaced by the integral $\int_L \int_b dxdy$. Corresponding to the stiffness matrix, matrices $\{C_m\}$ and $\{q\}$ have the following form.

$$\{C_m\} = \begin{Bmatrix} (1-\frac{x}{b})Y_m \\ (1-\frac{x}{b})\frac{Y'_m}{\mu_m} \\ (1-\frac{3x^2}{b^2}+\frac{2x^3}{b^3})Y_m \\ (x-\frac{2x^2}{b}+\frac{x^3}{b^2})Y_m \\ \frac{x}{b}Y_m \\ \frac{x}{b}\frac{Y'_m}{\mu_m} \\ (\frac{3x^2}{b^2}-\frac{2x^3}{b^3})Y_m \\ (\frac{x^3}{b^2}-\frac{x^2}{b})Y_m \end{Bmatrix} \tag{4.4.23}$$

and

$$\{q\} = \begin{Bmatrix} U_i \\ V_i \\ W_i \\ M_i \\ U_j \\ V_j \\ W_j \\ M_j \end{Bmatrix} \tag{4.4.24}$$

Putting equations 4.4.23 and 4.4.24 into equation 4.4.22, yields

$$\{F\} = \int_L \int_b \begin{Bmatrix} (1-\frac{x}{b})Y_m \\ (1-\frac{x}{b})\frac{Y'_m}{\mu_m} \\ (1-\frac{3x^2}{b^2}+\frac{2x^3}{b^3})Y_m \\ (x-\frac{2x^2}{b}+\frac{x^3}{b^2})Y_m \\ \frac{x}{b}Y_m \\ \frac{x}{b}\frac{Y'_m}{\mu_m} \\ (\frac{3x^2}{b^2}-\frac{2x^3}{b^3})Y_m \\ (\frac{x^3}{b^2}-\frac{x^2}{b})Y_m \end{Bmatrix} \begin{Bmatrix} U_i \\ V_i \\ W_i \\ M_i \\ U_j \\ V_j \\ W_j \\ M_j \end{Bmatrix} dxdy \tag{4.4.25}$$

The above integrals are calculated by the same method as used for evaluating the stiffness matrix. If a uniformly distributed load over a strip length L is applied,

then equation 4.4.25 will become

$$\{F\} = \frac{b}{2}\int_L \begin{Bmatrix} Y_m \\ \frac{Y'_m}{\mu_m} \\ Y_m \\ \frac{b}{6}Y_m \\ Y_m \\ \frac{Y'_m}{\mu_m} \\ Y_m \\ -\frac{b}{6}Y_m \end{Bmatrix} \begin{Bmatrix} U_i \\ V_i \\ W_i \\ M_i \\ U_j \\ V_j \\ W_j \\ M_j \end{Bmatrix} dy \qquad (4.4.26)$$

The matrix $\{F\}$ in equation 4.4.26 will finally be determined by using Gaussian Integration.

The stiffness matrix and the load matrix of a lower order folded plate strip have so far been derived in terms of a set of local axes. If a number of strips are considered, the derived formulation of each strip has to be assembled into an overall stiffness matrix and the corresponding load matrix of the whole structure. The system matrices can be directly constructed by joining the corresponding individual stiffness matrix and load matrix at the same nodal line if all strips are coplanar. However, in folded plate structures, any two strips, in general, may meet at an angle which results in some non-coplanar strips. Hence, the assembly of the system matrices cannot be done until all the strip stiffness are transformed to a common coordinates [10], say the global coordinates system. This conversion is completed by means of the transformation matrix $[T_r]$.

$$[T_r] = \begin{bmatrix} [t_r] & 0 \\ 0 & [t_r] \end{bmatrix} \qquad (4.4.27)$$

The matrix $[t_r]$ has the following form

$$[t_r] = \begin{bmatrix} \cos\alpha & 0 & \sin\alpha & 0 \\ 0 & 1 & 0 & 0 \\ -\sin\alpha & 0 & \cos\alpha & 0 \\ 0 & 0 & 0 & 1 \end{bmatrix}$$

where α is the angle between axes x and x' as shown in figure 4.6

Figure 4.6 shows the local axes x', y' and z' of a strip and the global coordinate system x, y and z of the whole structure. It is noted that axes y and y' are coincident with each other and also with the intersection line of two adjoining strips. Moreover, the angle α between axes x and x' is considered positive in the anti-clockwise direction. The transformation of the displacements and the forces between these two sets of coordinate system is given by

$$\{\delta'_m\} = [T_r]\{\delta_m\} \tag{4.4.28}$$

and

$$\{F_m\} = [T_r]^T\{F'_m\} \tag{4.4.29}$$

Rewriting equation 4.4.29, gives

$$\begin{aligned} \{F_m\} &= [T_r]^T\{F'_m\} \\ &= [T_r]^T[S'_{mn}]\{\delta'_m\} \\ &= [T_r]^T[S'_{mn}][T_r]\{\delta_m\} \end{aligned} \tag{4.4.30}$$

Comparing equations 4.2.17 and 4.4.30, it is observed that the stiffness matrix in global coordinate can be written as

$$[S_{mn}] = [T_r]^T[S'_{mn}][T_r] \tag{4.4.31}$$

Once the stiffness matrix and the load matrix have been transformed into the global coordinate system, it is ready to be assembled into the overall stiffness matrix and the load matrix of the structure in the conventional manner. In conclusion, the formulation of a rectangular strip are completely derived.

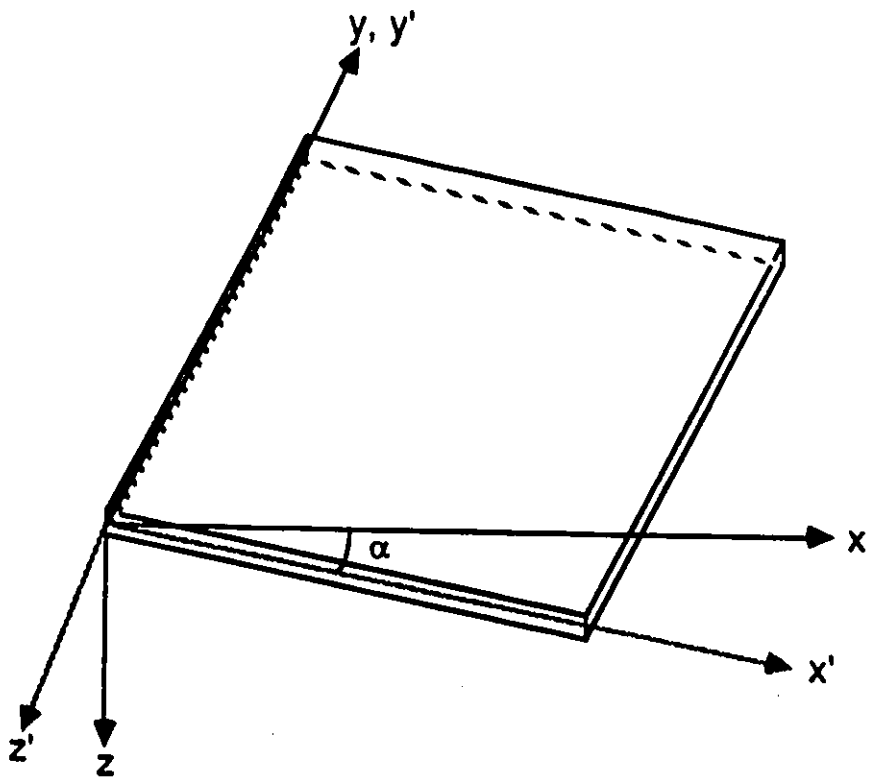

Figure 4.6: LOCAL AXES $x'\,y'\,z'$ AND GLOBAL COORDINATES $x,\ y,\ z$

4.4.2 FORMULATION OF A STRIP WITH VARIABLE WIDTH

In order to analyse the haunched web of a plate-girder bridge, a folded plate strip with variable width is developed. Such development has been done by Li [3]. Although the formulation of this type of strips follows the same idea described for the rectangular strip, these formulations are derived in terms of a new set of coordinates called the curvilinear coordinate system $(\zeta - \eta)$ [44]. Only the formulation of the stiffness matrix is discussed because the curvilinear coordinates have no effect on the formulation of the load matrix and the transformation matrix.

The web shown in figure 4.7 can be divided into a number of strips. The width of each strip which may be equal or unequal to each other is given in terms of a fraction of the actual width of the haunched web.

$$b_h = cb_l \tag{4.4.32}$$

where b_h is the width of a variable width strip for the haunched section

c is the coefficient that is $0 < c \leq 1$

b_l is the actual width of the variable width strip

and is defined in figure 4.7

This divided web is mainly subjected to the in-plane bending, although the out of plane action may have some contributions. Both actions can be described by a matrix similar to those $[B]$ matrices of a rectangular strip.

In the curvilinear coordinates, the out of plane bending matrix $[B_{op}]$ is obtained

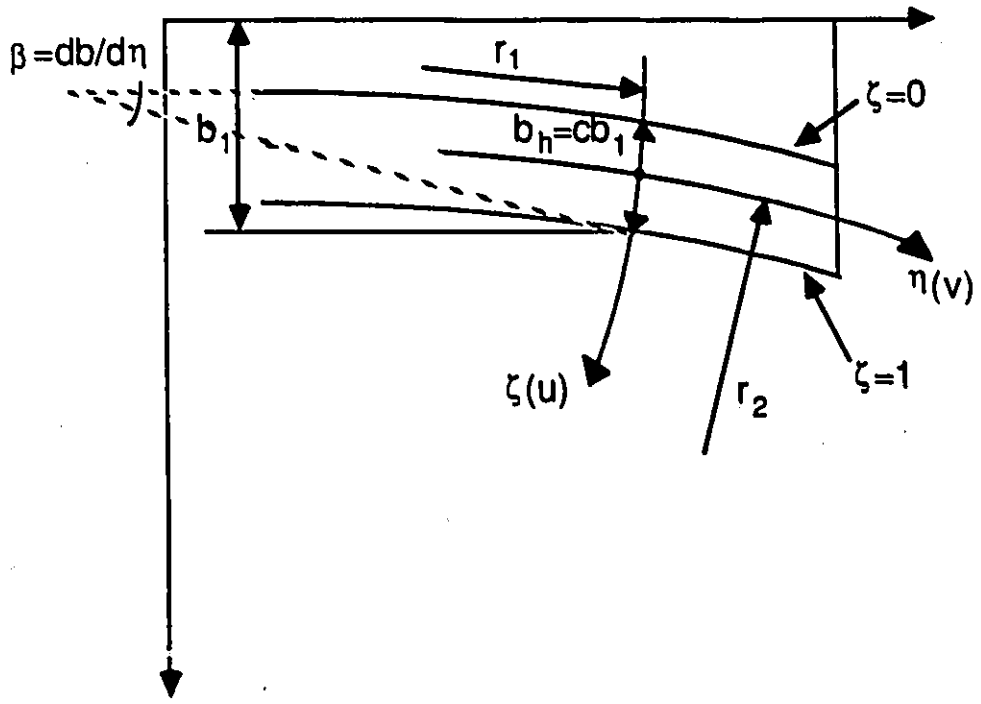

Figure 4.7: CURVILINEAR COORDINATE SYSTEM FOR A VARIABLE WIDTH STRIP

by using the parameters ζ and cb_1 instead of x and b in the $[B_{bm}]$ matrix in equation 4.2.12. The detail of $[B_{op}]$ matrix is given by

$$[B_{op}] = \begin{bmatrix} (\frac{6}{b_h^2} - \frac{12\zeta}{b_h^3})Y_m & (\frac{4}{b_h} - \frac{6\zeta}{b_h^2})Y_m & (-\frac{6}{b_h^2} + \frac{12\zeta}{b_h^3})Y_m & (-\frac{6\zeta}{b_h^2} + \frac{2}{b_h})Y_m \\ (-1 + \frac{3\zeta^2}{b_h^2} - \frac{2\zeta^3}{b_h^3})Y''_m & (-\zeta + \frac{2\zeta^2}{b_h} - \frac{\zeta^3}{b_h^2})Y''_m & (-\frac{3\zeta^2}{b_h^2} + \frac{2\zeta^3}{b_h^3})Y''_m & (-\frac{\zeta^3}{b_h^2} + \frac{\zeta^2}{b_h^2})Y''_m \\ (-\frac{12\zeta}{b_h^2} + \frac{12\zeta^2}{b_h^3})Y'_m & (2 - \frac{8\zeta}{b_h} + \frac{6\zeta^2}{b_h^2})Y'_m & (\frac{12\zeta}{b_h^2} - \frac{12\zeta^2}{b_h^3})Y'_m & (\frac{6\zeta^2}{b_h^2} - \frac{4\zeta}{b_h})Y'_m \end{bmatrix} \tag{4.4.33}$$

The series Y_m, Y'_m and Y''_m in the curvilinear coordinates is a function of η instead of y.

On the other hand, the formation of the in-plane bending matrix $[B_{ip}]$ is more complicated. For the same web shown in figure 4.7, the displacements and the strains (i.e. ε_ζ strain in ζ direction, ε_η strain in η direction and $\gamma_{\zeta\eta}$ the shear strain) are related to each other by the following equations.

$$\varepsilon_\zeta = \frac{1}{b_h}\frac{\partial u}{\partial \zeta} + \frac{v}{r_1} \tag{4.4.34}$$

$$\varepsilon_\eta = -\frac{u}{r_2} + \frac{\partial v}{\partial \eta} \tag{4.4.35}$$

and

$$\gamma_{\zeta\eta} = \frac{\partial u}{\partial \eta} + \frac{1}{b_h}\frac{\partial v}{\partial \zeta} - \frac{u}{r_1} + \frac{v}{r_2} \tag{4.4.36}$$

In general, it is possible to assume that $r_1 \gg b_h$, $u \gg v$ and $r_2 \gg r_1$. With these assumptions, the value of $\frac{v}{r_1}$ and $\frac{v}{r_2}$ in equation 4.4.34 and 4.4.36 respectively can be neglected. Moreover, the term $\frac{u}{r_2}$ in equation 4.4.35 is related to the axial stress at the cross-section and it can be ignored without losing too much accuracy. This axial stress resultant in any cross-section of the girder web becomes insignificant because the deformation of the web is mainly due to shear forces. Also, in bridge structures, usually only one support is designed against the longitudinal movement; therefore, the induced axial stress resultant is so small that it can be safely neglected.

Eliminating the above unimportant terms, equations 4.4.34, 4.4.35 and 4.4.36 are rewritten as

$$\varepsilon_\zeta = \frac{1}{b_h}\frac{\partial u}{\partial \zeta} \tag{4.4.37}$$

$$\varepsilon_\eta = \frac{\partial v}{\partial \eta} \tag{4.4.38}$$

and

$$\gamma_{\zeta\eta} = \frac{\partial u}{\partial \eta} + \frac{1}{b_h}\frac{\partial v}{\partial \zeta} - \frac{u}{r_1} \tag{4.4.39}$$

The in-plane displacement is found by satisfying the condition that the shear strain, $\gamma_{\zeta\eta}$, should be equal to zero or at least very close to zero. If $r_1 = \frac{b_1}{\frac{db_1}{d\eta}}$ is assumed, the in-plane displacement function (u, v) could be obtained by

$$u = \sum_{m=1}^{\infty}[(1-\zeta)u_{im} + \zeta u_{jm}]Y_m(\eta) \tag{4.4.40}$$

and

$$v = \sum_{m=1}^{\infty}\frac{1}{\mu_m}[(1-\zeta)v_{im} + \zeta v_{jm}][\frac{b_1 dY_m(\eta)}{d\eta} - \frac{db_1}{d\eta}Y_m(\eta)] \tag{4.4.41}$$

Following the same procedure for the formation of $[B_{pm}]$ matrix in equation 4.3.11, the in-plane bending matrix $[B^w_{ip}]$ of a web strip is defined as

$$[B^w_{ip}] = \begin{bmatrix} -\frac{Y_m}{b_h} & 0 & \frac{Y_m}{b_h} & 0 \\ 0 & \frac{(1-\zeta)b_1}{\mu_m}Y''_m & 0 & \frac{\zeta b_1}{\mu_m}Y''_m \\ (1-\zeta)Y'_m & -\frac{Y'_m}{c\mu_m} & \zeta Y'_m & \frac{Y'_m}{c\mu_m} \end{bmatrix} \tag{4.4.42}$$

In order to meet the compatibility requirement (i.e. same function v in the η direction) at the connection between the flange and the web of the bridge structure, the following $[B^f_{ip}]$ matrix of a flange strip should be used.

$$[B^f_{ip}] = \begin{bmatrix} -\frac{Y_m}{b_f} & 0 & \frac{Y_m}{b_f} & 0 \\ 0 & (1-\frac{x}{b_f})\frac{b_1}{\mu_m}Y''_m & 0 & \frac{xb_1}{b_f\mu_m}Y''_m \\ (1-\frac{x}{b_f})Y'_m & -\frac{b_1}{b_f\mu_m}Y'_m & \frac{x}{b_f}Y'_m & \frac{b_1}{b_f\mu_m}Y'_m \end{bmatrix} \tag{4.4.43}$$

where b_f is the width of a flange strip

b_1 is the actual width of the haunched web

Both $[B_{op}]$ and $[B_{ip}]$ matrices can be put together to form a complete $[B_{fm}]$ matrix and $[B_{wm}]$ matrix for the flange strip and the web strip respectively. The final flange strip matrix $[B_{fm}]$ is formed by combining equations 4.4.43 and 4.4.33 while the final web strip matrix $[B_{wm}]$ is made by combining equations 4.4.42 and 4.4.33. The details of the matrices $[B_{fm}]$ and $[B_{wm}]$ are given as follows

$$[B_{fm}] \text{ or } [B_{wm}] = \begin{bmatrix} -\frac{1}{b}Y_m & 0 & 0 & 0 & \frac{1}{b}Y_m & 0 & 0 & 0 \\ 0 & (1-X)\frac{b_1}{\mu_m}Y_m'' & 0 & 0 & 0 & \frac{Xb_1}{\mu_m}Y_m'' & 0 & 0 \\ (1-X)Y_m' & -\frac{1}{c\mu_m}Y_m' & 0 & 0 & XY_m' & \frac{1}{c\mu_m}Y_m' & 0 & 0 \\ 0 & 0 & k_1Y_m & k_4Y_m & 0 & 0 & -k_1Y_m & k_8Y_m \\ 0 & 0 & k_2Y_m'' & k_5Y_m'' & 0 & 0 & k_7Y_m'' & k_9Y_m'' \\ 0 & 0 & k_3Y_m' & k_6Y_m' & 0 & 0 & -k_3Y_m' & k_{10}Y_m' \end{bmatrix} \quad (4.4.44)$$

where $b = b_f$, $c = \frac{b_f}{b_1}$ and $X = \frac{x}{b_f}$ for $[B_{fm}]$ matrix

$b = b_h$, $c = \frac{b_h}{b_1}$ and $X = \zeta$ for $[B_{wm}]$ matrix

$$k_1 = \frac{6}{b_h^2} - \frac{12\zeta}{b_h^3} \qquad k_2 = -1 + \frac{3\zeta^3}{b_h^2} - \frac{2\zeta^3}{b_h^3}$$

$$k_3 = -\frac{12\zeta}{b_h^2} + \frac{12x^2}{b_h^3} \qquad k_4 = \frac{4}{b_h} - \frac{6x}{b_h^2}$$

$$k_5 = -\zeta + \frac{2\zeta^2}{b_h^2} + \frac{\zeta_3}{b_h^2} \qquad k_6 = 2 - \frac{8\zeta}{b_h} + \frac{6\zeta^2}{b_h^2}$$

$$k_7 = -\frac{3\zeta^3}{b_h^2} + \frac{2\zeta^3}{b_h^3} \qquad k_8 = -\frac{6x}{b_h^2} + \frac{2}{b_h}$$

$$k_9 = \frac{\zeta}{b_h^2} - \frac{\zeta^3}{b_h^3} \qquad k_{10} = \frac{6\zeta^2}{b_h^2} - \frac{4\zeta}{b_h}$$

The stiffness matrix of a flange strip or a web strip can now be determined by putting equation 4.4.44 into equation 4.4.11. Since the transformation matrix will not be changed, so the overall stiffness matrix and the load matrix are obtained by the same way as described for the rectangular strip in the proceeding section. Finally, the formulation for a variable width strip have been developed.

When all the formulation (including both constant and variable width) of a folded plate strip have been done, the required displacements, stresses and moments

can be solved by using the finite strip analysis. A computer program of such analysis is written and verified by some examples described in the following chapter.

CHAPTER 5

NUMERICAL EXAMPLES AND DISCUSSION

5.1 INTRODUCTION

In the previous two chapters, the derivation of the shape function and the formulation of a continuous folded plate strip have been discussed. Based on these formulation, a computer program for the finite strip analysis is written. A number of examples are presented in order to verify the accuracy and efficiency of the computer program. The nature of the examples can be divided into two main categories: (i) structures with constant cross-section and (ii) structures with variable cross-section. All structures were assumed to have homogenous and isotropic material properties and the value of E, ν and G are set to be equal to 1.0, 0.0 and 0.5 respectively. Arbitrary E, ν and G values are used in the examples because they have no influence whatsoever in the accuracy of the final results. However, for a real bridge design, the actual material properties should be substituted. Moreover, simply supported, continuous structures are only considered here since bridges always have this kind of configuration. Finally, the structural response are checked either with the exact solutions obtained from the beam theory or with those obtained numerically by using the finite element program (ADINA).

5.2 STRUCTURES WITH CONSTANT CROSS-SECTION

In this section, a total of eight examples are examined. The first five (i.e. example 5.2.1 to example 5.2.5) are beam structures in which different types of

loading conditions (e.g. point load, uniformly distributed load or even a combination of both) and different number of spans (equal or unequal spans) are used. Only two to five spans are considered because plate-girder bridges, in general, seldom exceed five spans. The rest of the examples are compositions of a constant bridge web (or constant vertical plate, example 5.2.6), a thin plate (example 5.2.7) and a T-shaped beam (example 5.2.8) which may be regarded as a practical section for plate-girder bridges.

The results in terms of the bending moment of the first five examples obtained from the strip program were compared with the results solved by the beam theory. The details of the comparison are given in tables. On the other hand, examples 5.2.6, 5.2.7 and 5.2.8 were analyzed by both the Finite Element Method (ADINA) and the Finite Strip Method. A comparison of these solutions (displacement and stresses) is also made and presented in tabular forms. Each example is given as follows:

Example 5.2.1, [reference 36, page 402 example 19.1]

A two span, continuous beam with span length 20 feet and 25 feet is shown in figure 5.1. The beam carries a point load of 20 kips at mid-span of the first span and a uniformly distributed load of 3 k/f. The result is given in table 5.1.

Example 5.2.2, [reference 27, page 289 problem 13.7]

A three span, continuous beam with unequal span length of 12 feet, 16 feet and 12 feet (see figure 5.2). Point loads of 12 kips and 4 kips are located in the middle of the first and the last span respectively. Table 5.2 summaries the results.

Example 5.2.3, [reference 36, page 500 example 22.2]

This is also a three span, continuous beam, but with equal span length of 25

feet. the beam is loaded with both concentrated and uniformly distributed load. The uniformly distributed load is applied only over the first two spans while the point load is located 10 feet from the end support in the last span. Figure 5.3 shows the whole picture. The magnitude of the point load and the uniformly distributed load is 20 kips and 2 k/f respectively, again the final results are shown in table (see table 5.3).

Example 5.2.4, [reference 22, pages 33 – 36 example 2.3]

Figure 5.4 shows the four span, continuous beam. Each span is 20 feet long. A uniformly distributed load of 3 k/f is applied to the four spans. A comparison of the bending moments is given in table 5.4.

Example 5.2.5, [reference 27, page 280 problem 13.6]

A five equal span, continuous beam is loaded with a uniformly distributed load of 1.2 k/f. The loading is applied at the first, the third and the last span only. Each span is 24 feet in length. Same as previous examples, the results of the bending moments are tabulated in table 5.5.

Example 5.2.6

The two span, continuous vertical plate (or web) shown in figure 5.6 has two loading conditions: (i) a point load of 20 kips is applied at each midspan, (ii) a uniformly distributed load of 3 k/f is applied over all the spans. Each span has a length of 30 feet. The accuracy of the ADINA program (two different meshes are tried in order to confirm the convergency of the ADINA results) and the strip program is verified by comparing with the theoretical solutions solved by the beam formula [26] using the beam theory. Table 5.6 gives a comparison among three methods for the point loaded case while table 5.7 shows the results of the uniformly

distributed loaded case. Furthermore, the stress distribution diagram for the point loaded case and the uniformly distributed loaded case is given in figure 5.7 and figure 5.9 respectively.

Example 5.2.7

A thin plate (3 feet width, 48 feet long and 0.1 feet thick) is considered in this example. The plate is divided into two equal spans. In the middle of each span, a concentrated load of 100 kips is applied. The loading is divided into four components located along the transverse direction as shown in figure 5.10. Similar to the previous example, the beam theory, the ADINA program and the strip program are used to solve this plate problem. The results are compared and presented in table 5.8. The convergency of ADINA results is established by using two models having a fine and a corase mesh respectively (refer to appendix A).

Example 5.2.8

A two span, continuous T-shaped beam is loaded according to the OHBD truck load [37] (see figure 5.11 for the detail location of the truck load). Because of the symmetry of the section and the loadings, it is possible to analyse only half of the whole section with appropriate boundary conditions. If u, v, w and θ represent the translation in axes x, y, z and rotation about y axis respectively, then the required boundary conditions should be that both the displacement u and the rotation θ are fixed while the others are free to move. This example is analyzed by both the Finite Element Method and the Finite Strip Method (see table 5.9). The mesh for the Finite Element Method is plotted in Appendix A for reference. Also, the stress distribution along the cross-section is given in figure 5.12.

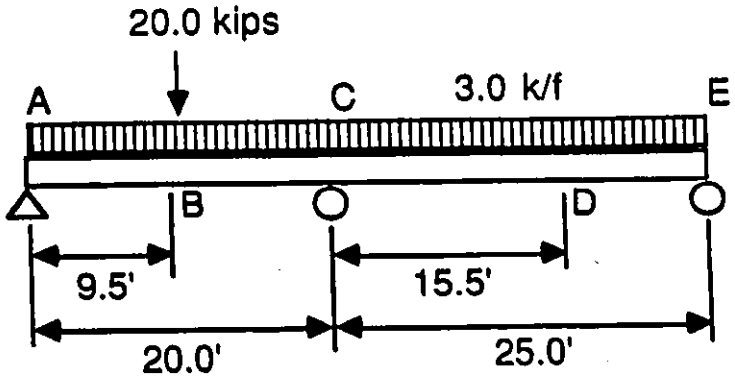

Figure 5.1: LOADS AND LAYOUT OF EXAMPLE 5.2.1

Bending Moment ($K-ft$) @	Beam Theory	Strip Results (No. of Terms)				
		10	20	30	40	45
A	0.0	0.00	0.00	0.00	0.00	0.00
B	136.0	129.7	135.1	135.9	136.0	136.0
C	-230.0	-224.5	-229.5	-230.0	-230.1	-230.0
D	134.0	134.2	133.6	133.4	133.4	133.4

Table 5.1: A COMPARISON OF BENDING MOMENT FOR EXAMPLE 5.2.1

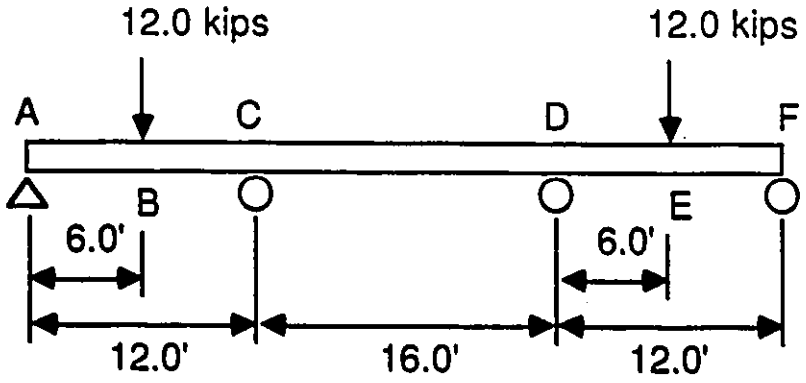

Figure 5.2: LOADS AND LAYOUT OF EXAMPLE 5.2.2

Bending Moment ($K - ft$) @	Beam Theory	Strip Results (No. of Terms)				
		10	20	30	40	45
A	0.00	0.00	0.00	0.00	0.00	0.00
B	30.30	26.74	27.98	28.95	29.25	29.46
C	-11.40	-11.30	-11.69	-11.44	-11.30	-11.44
D	-0.600	-0.6504	-0.6503	-0.5994	-0.5819	-0.6175
E	11.70	10.50	10.91	11.25	11.35	11.42

Table 5.2: A COMPARISON OF BENDING MOMENT FOR EXAMPLE 5.2.2

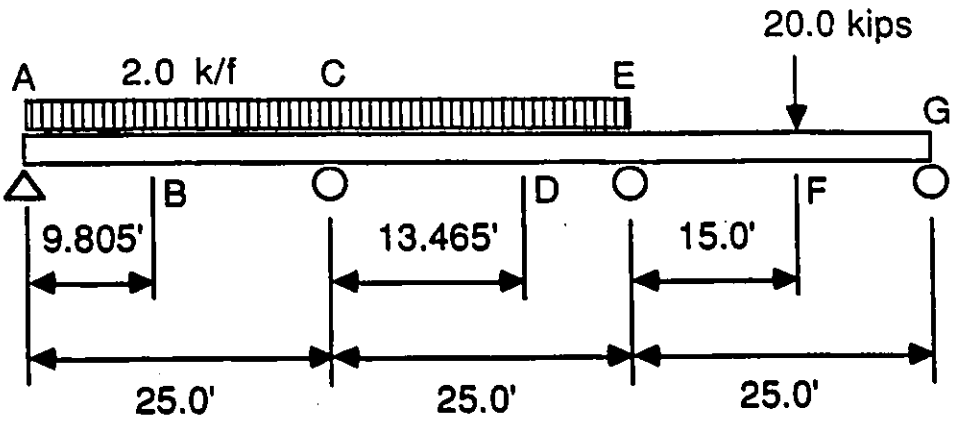

Figure 5.3: LOADS AND LAYOUT OF EXAMPLE 5.2.3

Bending Moment $(K-ft)$ @	Beam Theory	Strip Results (No. of Terms)				
		10	20	30	40	45
A	0.00	0.00	0.00	0.00	0.00	0.00
B	96.138	93.78	96.16	96.08	96.02	96.18
C	-134.75	-129.5	-132.7	-134.0	-134.2	-134.4
D	46.560	47.16	46.95	46.56	46.52	46.67
E	-86.50	-81.24	-84.94	-85.77	-86.03	-86.50
F	85.40	72.30	78.58	80.45	81.86	82.16

Table 5.3: A COMPARISON OF BENDING MOMENT FOR EXAMPLE 5.2.3

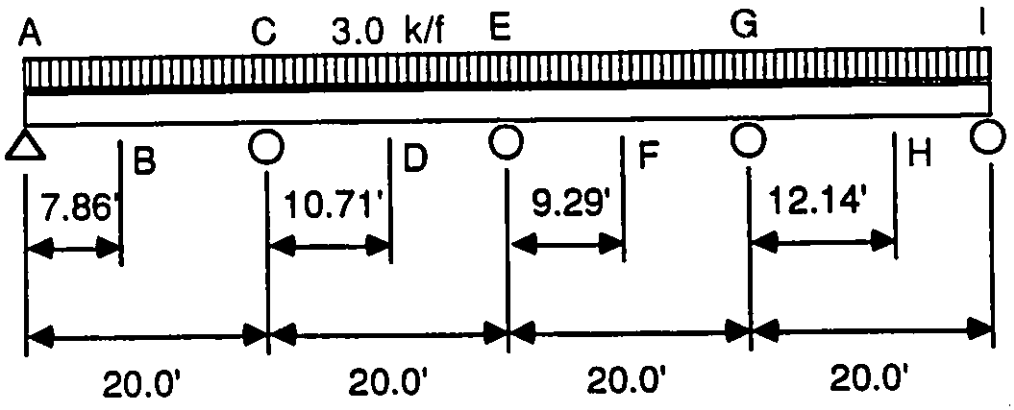

Figure 5.4: LOADS AND LAYOUT OF EXAMPLE 5.2.4

Bending Moment ($K - ft$) @	Beam Theory	Strip Results (No. of Terms)				
		10	20	30	40	45
A	0.00	0.00	0.00	0.00	0.00	0.00
B	92.63	94.45	92.67	92.74	92.52	92.66
C	-128.5	-118.4	-126.6	-127.5	-127.9	128.1
D	43.61	48.36	43.80	43.52	43.66	43.62
E	-85.80	-73.18	-83.82	-84.70	-85.06	-85.25
F	43.56	48.36	43.80	43.52	43.66	43.62
G	-128.6	-118.4	-126.6	-127.5	-127.9	-128.1
H	92.63	94.45	92.67	92.74	92.52	92.66
I	134.0	134.2	133.6	133.4	133.4	133.4

Table 5.4: A COMPARISON OF BENDING MOMENT FOR EXAMPLE 5.2.4

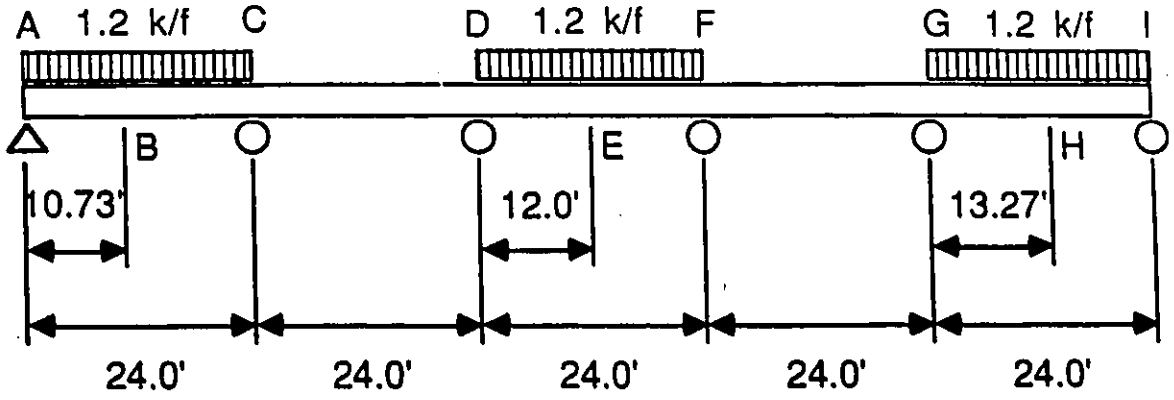

Figure 5.5: LOADS AND LAYOUT OF EXAMPLE 5.2.5

Bending Moment ($K-ft$) @	Beam Theory	Strip Results (No. of Terms)				
		10	20	30	40	45
A	0.00	0.00	0.00	0.00	0.00	0.00
B	69.10	71.71	68.73	69.28	69.14	69.18
C	-36.53	-33.05	-35.29	-35.85	-36.07	-36.17
D	-27.14	-24.19	-26.24	-26.77	-26.98	-27.08
E	58.99	61.72	58.57	59.31	59.03	59.16
F	-27.41	-24.19	-26.24	-26.77	-26.98	-27.08
G	-36.53	-33.05	-35.29	-35.85	-36.07	-36.17
H	69.10	71.71	68.73	69.28	69.14	69.18

Table 5.5: A COMPARISON OF BENDING MOMENT FOR EXAMPLE 5.2.5

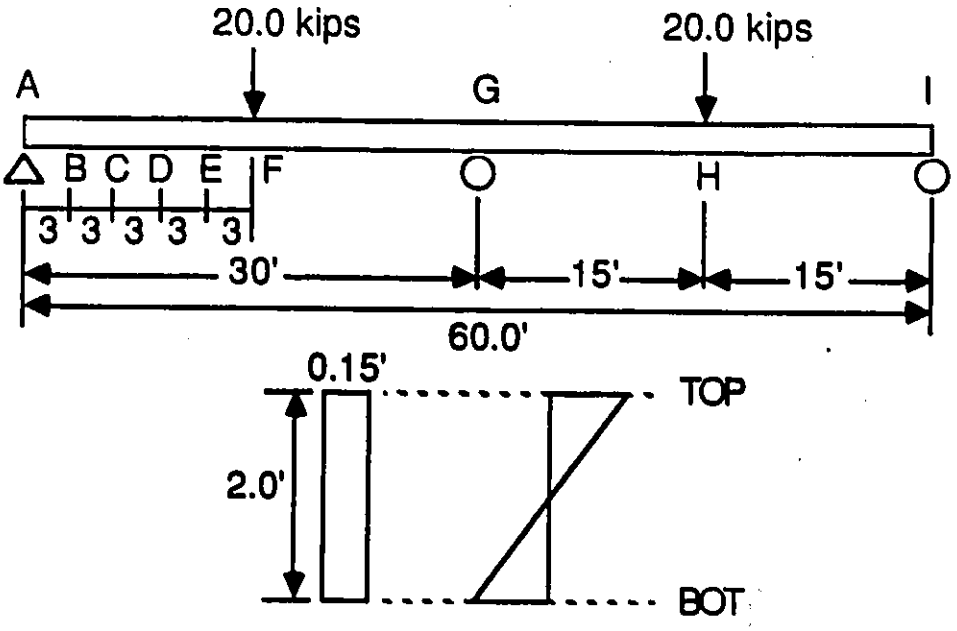

Figure 5.6: LOADS (POINT LOAD) AND LAYOUT OF EXAMPLE 5.2.6

Stresses (K/ft^2) @		Beams Theory	Strip Results (No. of Terms)			ADINA Results (No. of Elements)	
			10	20	30	20	80
B	TOP	-187.8	-187.6	-187.6	-187.5	-192.7	-187.9
	BOT	187.8	187.6	187.6	187.5	180.9	189.6
C	TOP	-375.6	-375.1	-375.1	-374.9	-376.0	-375.7
	BOT	375.6	375.1	375.1	374.9	376.5	375.7
D	TOP	-563.4	-561.6	-562.5	-562.6	-562.6	-563.5
	BOT	563.4	561.6	562.5	562.6	562.8	563.5
E	TOP	-751.2	-755.1	-749.2	-750.2	-769.1	-749.6
	BOT	751.2	755.1	749.2	750.2	747.6	751.5
F	TOP	-936.0	-879.2	-907.7	-917.5	-1020	-1165
	BOT	936.0	879.2	907.7	917.5	941.0	926.9
G	TOP	1128	1135	1122	1126	1124	1105
	BOT	-1128	-1135	-1122	-1126	-1233	-1432

Table 5.6: STRESSES DUE TO POINT LOAD FOR EXAMPLE 5.2.6

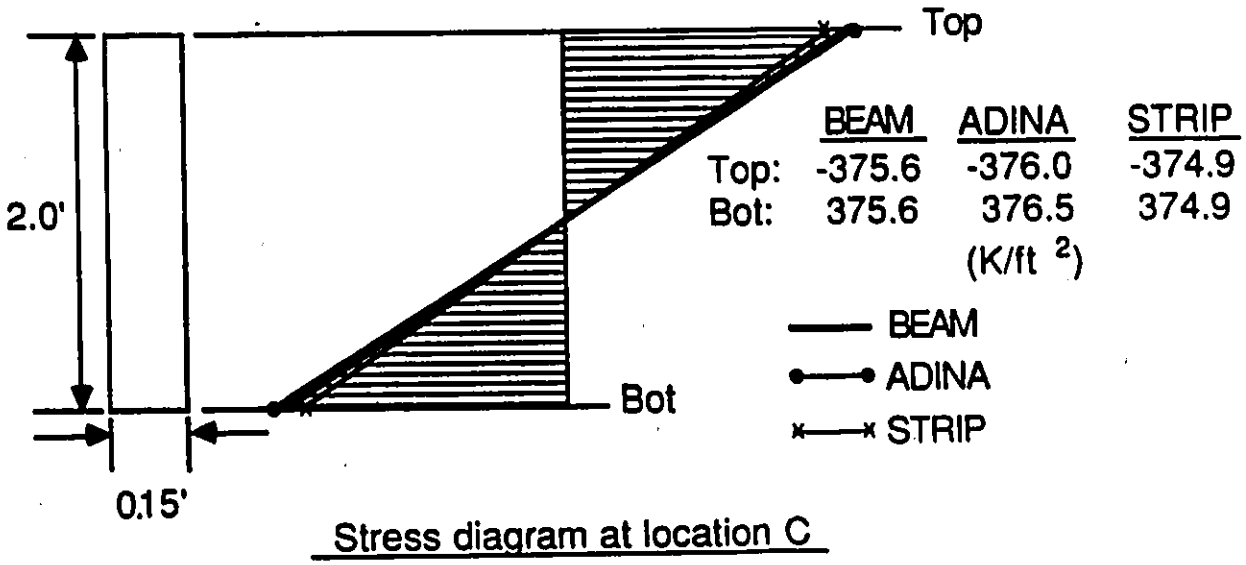

Figure 5.7: STRESS DISTRIBUTION (POINT LOAD) OF EXAMPLE 5.2.6

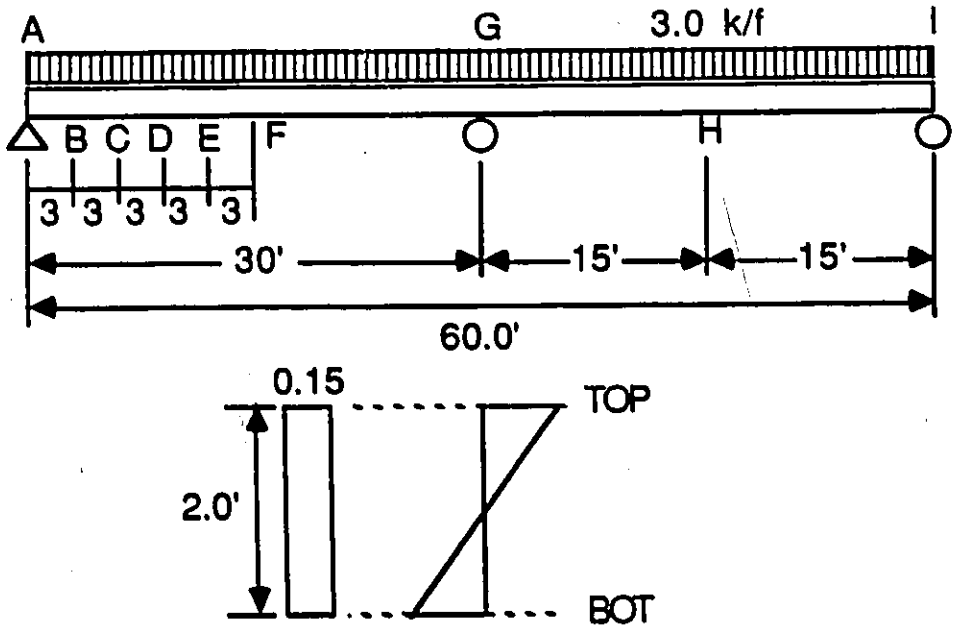

Figure 5.8: LOADS (UNIFORM LOAD) AND LAYOUT OF EXAMPLE 5.2.6

Stresses (K/ft^2) @		Beams Theory	Strip Results (No. of Terms)			ADINA Results (No. of Elements)	
			10	20	30	20	80
B	TOP	-877.5	-880.8	-876.9	-877.7	-916.9	-889.9
	BOT	877.5	880.8	876.9	877.7	847.1	891.9
C	TOP	-1485	-1482	-1485	-1485	-1502	-1498
	BOT	1485	1482	1485	1485	1498	1491
D	TOP	-1823	-1825	-1822	-1823	-1838	-1837
	BOT	1823	1825	1822	1823	1838	1829
E	TOP	-1890	-1888	-1890	-1890	-1907	-1905
	BOT	1890	1888	1890	1890	1907	1898
F	TOP	-1688	-1689	-1687	-1688	-1706	-1704
	BOT	1688	1689	1687	1688	1700	1696
G	TOP	3375	3359	3371	3373	3360	3285
	BOT	-3375	-3359	-3371	-3373	-3813	-4623

Table 5.7: STRESSES DUE TO DISTRIBUTED LOADS FOR EXAMPLE 5.2.6

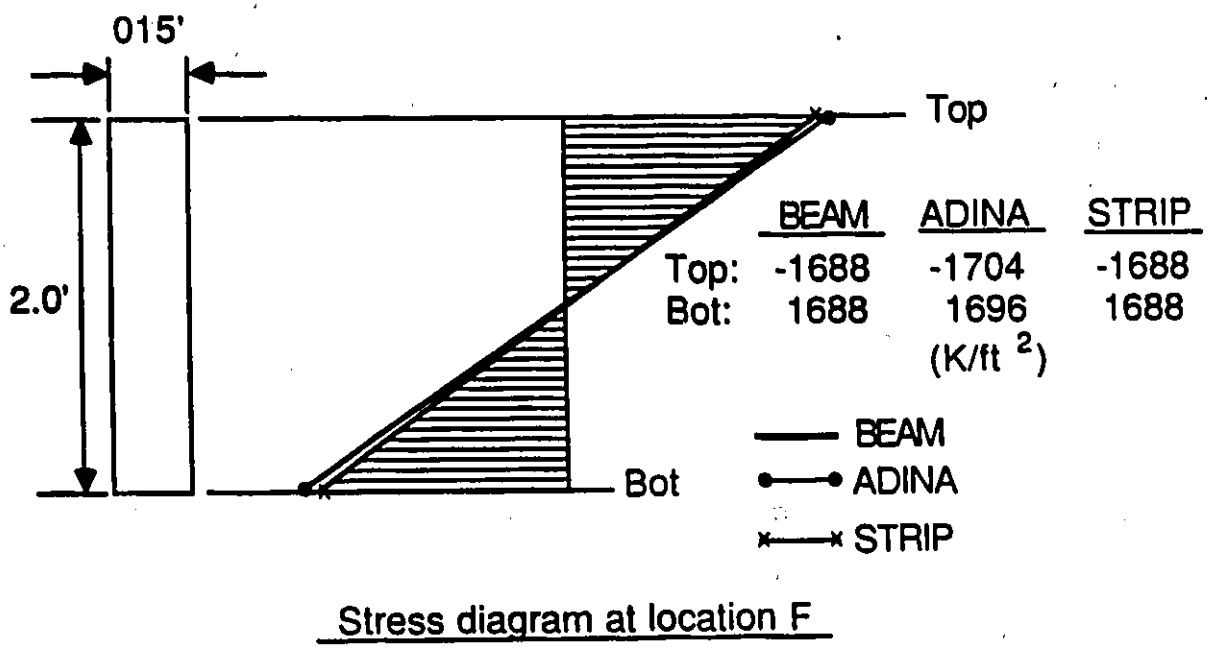

Figure 5.9: STRESS DISTRIBUTION (DISTRIBUTED LOAD) OF EXAMPLE 5.2.6

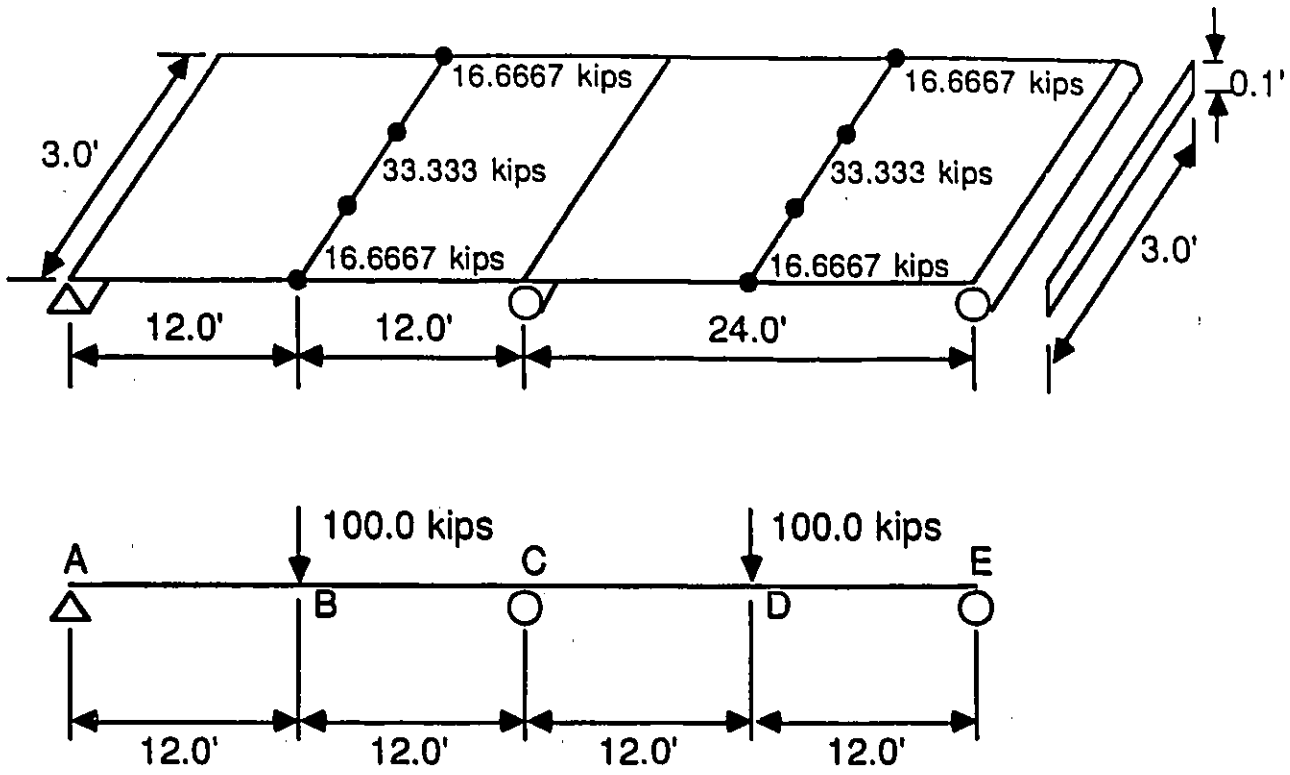

Figure 5.10: LOADS AND LAYOUT OF EXAMPLE 5.2.7

Average Displacement ($\times 10^8 ft$) @		Strip Results (No. of Terms)			ADINA Results (No. of Elements)	
		10	20	30	36	72
B		0.5038	0.5040	0.5040	0.5040	0.5040
Stresses ($\times 10^5 K/ft^2$) @		10	20	30	36	72
B	TOP	0.7032	0.7254	0.7332	0.7498	0.7503
	BOT	-0.7032	-0.7254	-0.7332	-0.7498	-0.7503
C	TOP	-0.9078	-0.8982	-0.9012	-0.9000	-0.9000
	BOT	0.9078	0.8982	0.9012	0.9000	0.9000

Table 5.8: DISPLACEMENT AND STRESSES OF EXAMPLE 5.2.7

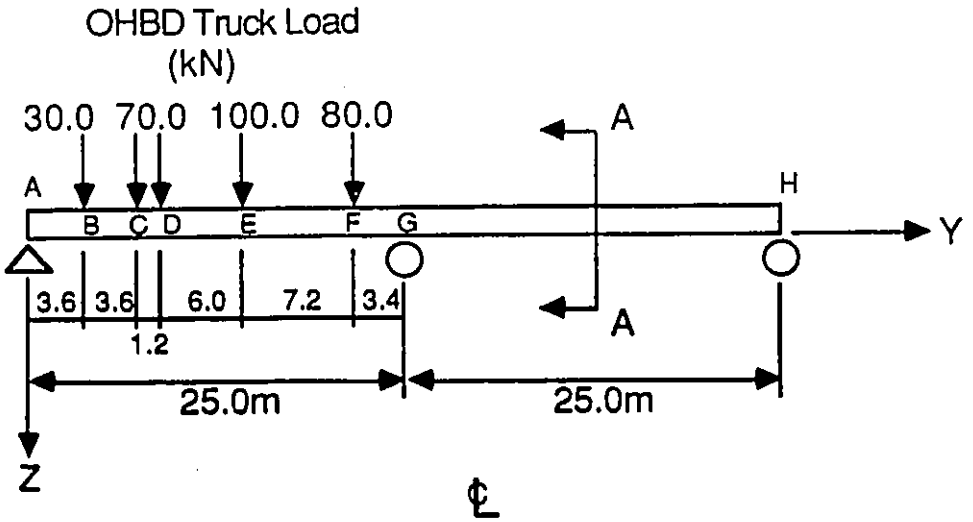

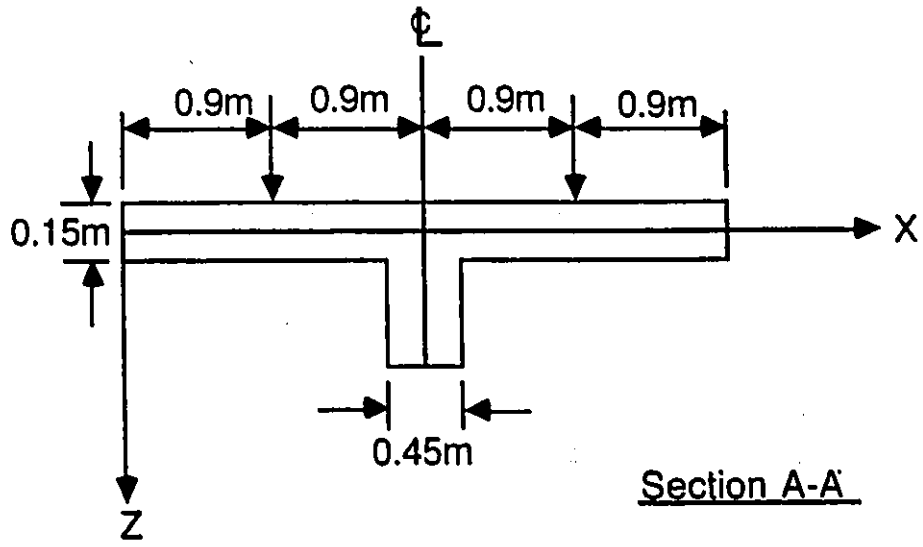

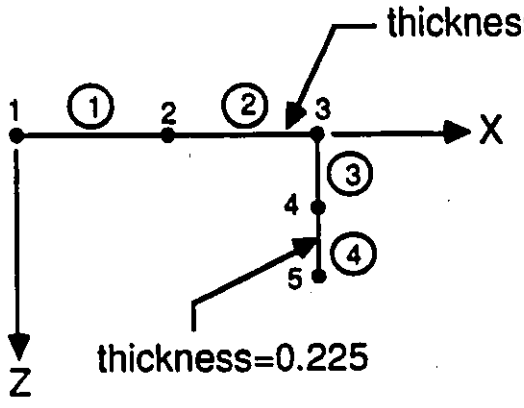

Node	X	Z
1	0.0	0.0
2	0.9	0.0
3	1.8	0.0
4	1.8	0.4
5	1.8	0.8

NOTE: Half of the Whole Section (due to symmetry)

Figure 5.11: LOADS AND LAYOUT OF EXAMPLE 5.2.8

Average Displacement ($\times 10^6 m$) @		ADINA Results 168 Elements	Strip Results (No. of Terms) 10	20	30	40	45
B		1.0500	1.0290	1.0283	1.0284	1.0284	1.0284
C		1.8440	1.8067	1.8083	1.8084	1.8084	1.8084
D		2.0145	1.9754	1.9763	1.9764	1.9764	1.9764
E		2.0645	2.0234	2.0259	2.0259	2.0260	2.0260
F		0.7479	0.7284	0.7302	0.7304	0.7304	0.7304
G		-0.8719	-0.8750	-0.8747	-0.8747	-0.8747	-0.8747
Stresses (MPa) @		168 Elements	10	20	30	40	45
B	TOP	-4.852	-4.665	-4.573	-4.642	-4.637	-4.639
	MID	-3.311	-3.178	-3.114	-3.164	-3.160	-3.161
	BOT	12.650	12.66	12.43	12.54	12.53	12.54
C	TOP	-9.307	-8.642	-8.889	-8.895	-8.909	-8.911
	MID	-6.518	-5.890	-6.068	-6.071	-6.082	-6.082
	BOT	24.210	23.42	23.92	23.94	23.96	23.95
D	TOP	-8.398	-7.325	-7.782	-7.827	-7.855	-7.864
	MID	-5.794	-4.988	-5.313	-5.345	-5.364	-5.370
	BOT	21.310	19.92	20.92	20.98	21.01	21.02
E	TOP	2.554	2.585	2.539	2.565	2.564	2.564
	MID	1.739	1.760	1.742	1.746	1.746	1.747
	BOT	-6.959	-7.041	-6.978	-6.981	-6.983	-6.984

Table 5.9: DISPLACEMENT AND STRESSES OF EXAMPLE 5.2.8

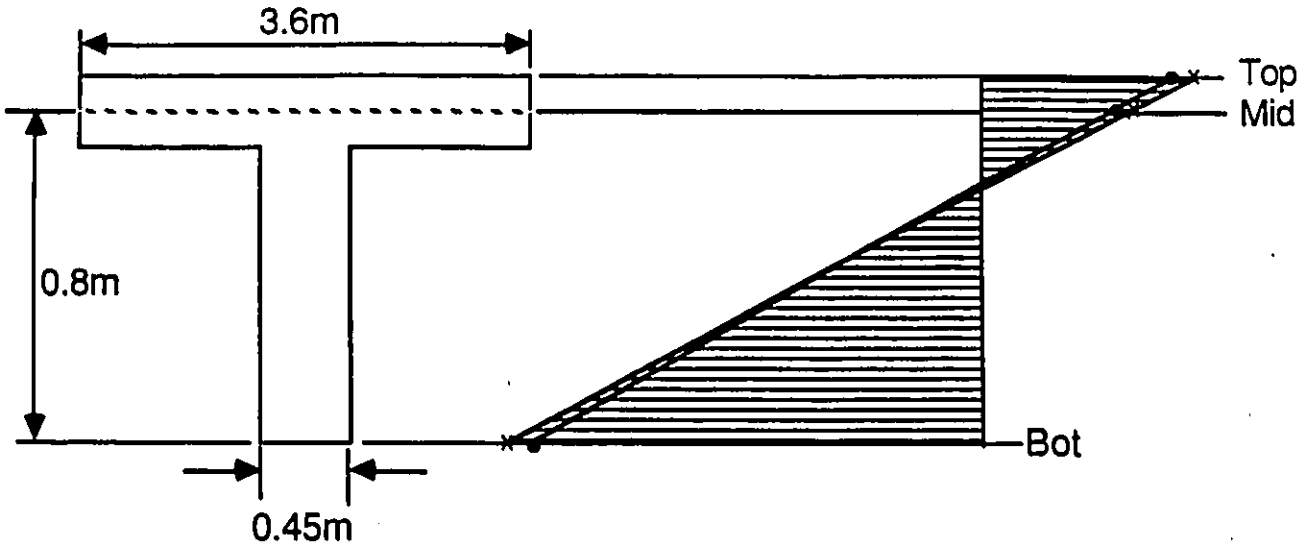

	ADINA	STRIP
Top:	2.554	2.564
Mid:	1.739	1.747
Bot:	-6.959	-6.984

(MPa)

ADINA

STRIP

Stress diagram at location E

Figure 5.12: STRESS DISTRIBUTION OF EXAMPLE 5.2.8

5.3 STRUCTURES WITH VARIABLE CROSS-SECTION

This type of structures has been suggested in section 4.4.2 to be analyzed by employing a folded plate strip with variable width. The accuracy and the efficiency of this folded plate strip are established by four examples which were solved by using both the Finite Element Method (all element meshes are drawn in Appendix A) and the Finite Strip Method. The first three are concerned mainly with the vertical plates (i.e. haunched web of a plate-girder bridge) while the last one is a study of a practical bridge model [39]. The web is described by either a straight or curved haunch. In this case, the curved haunch is approximated by a parabolic function. Despite the last example is concerned with a real bridge model, some assumptions such as parabolic haunch, material properties etc. have been made in order to simplify the comparison of the results. Again, the final results (the displacement and the stress distribution) are compared and illustrated in tables and figures. Following is the detail of each example:

Example 5.3.1

A two span, continuous web with straight haunch is given in figure 5.13. Each span is 40 feet long and 0.1 feet thick. The height of the web at the two end supports and the center support is 1 feet and 2 feet respectively. The displacement and the bending stress resulting from a 20 kips concentrated load at each mid-span are found and are given in table 5.10.

Example 5.3.2

Figure 5.14 shows a two span, continuous girder with parabolic haunch. The first span is 25 feet long with a parabolic function ($z = 1.76 \times 10^{-3}Y^2 + 1.3$) between supports while the second span is 30 feet long with a parabolic function

($z = 1.2222 \times 10^{-3}Y^2 + 1.3$) between two supports. The web with 0.45 feet in thickness has an initial depth of 1.3 feet at both end supports and a maximum depth of 2.4 feet at the interior support. A combination of a point load and a uniformly distributed load is considered here. A point load of 20 kips is applied at a distance of 10 feet from the end support in the first span while the uniformly distributed load of 1.2 k/f is applied over the entire second span. In table 5.11, the results obtained by both analyses are compared. Moreover, the stress distribution along the cross-section is plotted in figure 5.15.

Example 5.3.3

This example is a three span, continuous web of span length 30 feet, 90 feet and 30 feet respectively. The dimensions of the straight haunch with constant thickness of 0.45 feet (see figure 5.16) are 2.6 feet deep at both end supports and 4.4 feet deep between the interior supports. In this example, only the second span is loaded by a uniformly distributed load of 3 k/f. The displacement and the stress distribution are shown in table 5.12

Example 5.3.4 [39]

In figure 5.17, a continuous three span, haunched girder reinforced concrete bridge is displayed. The span lengths are 44 feet, 55 feet and 44 feet respectively. The cross-section consists of a 0.5208 feet deck with two girders (8 feet apart). The girder has a thickness of 1.3958 feet and a height of 2.526 feet and 4.3594 feet at end supports and interior supports respectively. An OHBD truck load shown in figure 5.17, is used to simulate the displacement and the stress distribution along the section. All haunched regions of the bridge are assumed to be a parabola ($z = 1.0849 \times 10^{-2}Y^2 + 2.526$) starting with a distance 13 feet away from the

interior supports. The material properties described in section 5.1 are used instead of the real one because they will not affect the accuracy of the solution. Since the cross-section of the bridge is symmetrical about its centerline, only half of the section is analyzed. In order to make such analysis possible, the same boundary conditions as in example 5.2.8 are used. The final displacements and stresses are given in table 5.13. The stress distribution diagram along the cross-section is shown in figure 5.18.

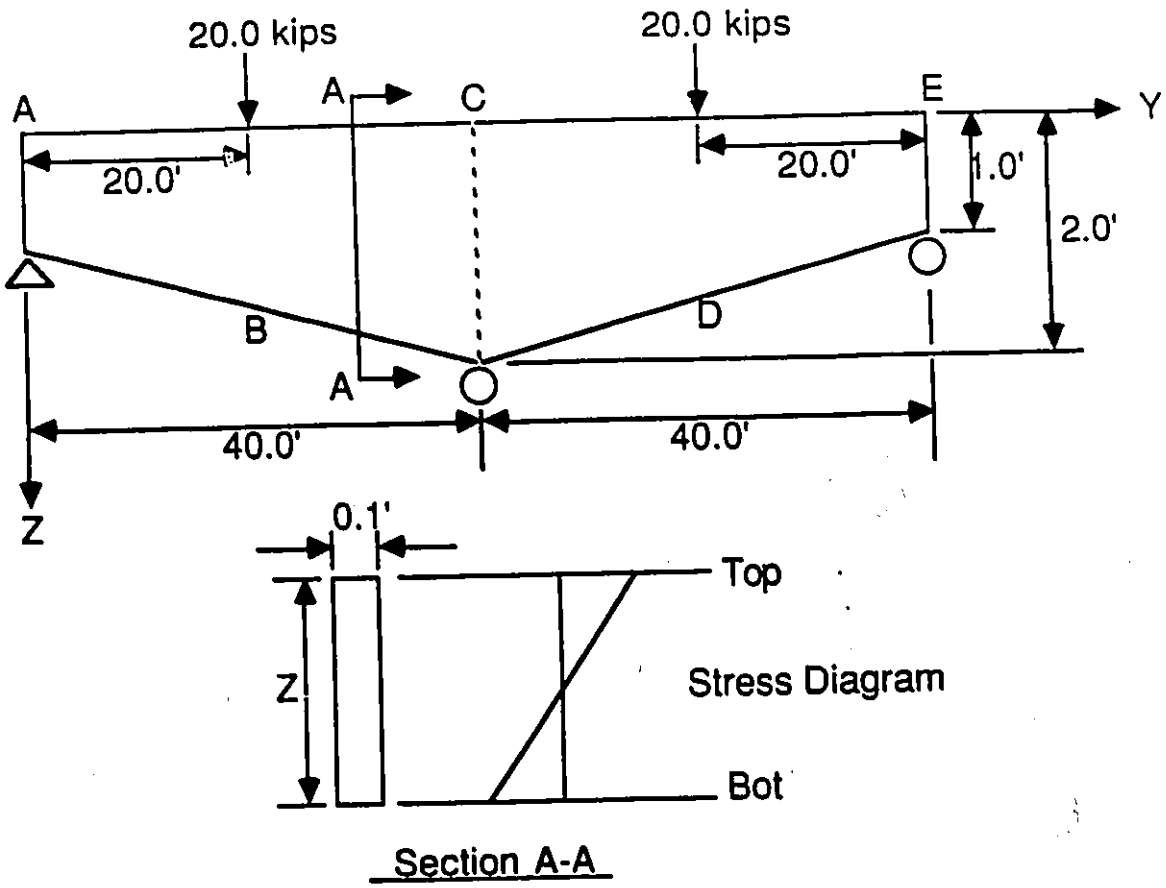

Figure 5.13: LOADS AND LAYOUT OF EXAMPLE 5.3.1

Average Displacement ($\times 10^6 ft$) @		Strip Results (No. of Terms)			ADINA Results (No. of Elements)	
		10	20	30	80	160
B		0.3483	0.3484	0.3484	0.3521	0.3522
Stresses ($\times 10^4 K/ft^2$) @		10	20	30	80	160
B	TOP	-0.2430	-0.2535	-0.2577	-0.2849	-0.3195
	BOT	0.2429	0.2526	0.2555	0.2624	0.2608
C	TOP	0.3065	0.3028	0.3039	0.3041	0.3030
	BOT	-0.3064	-0.3031	-0.3035	-0.3268	-0.3727

Table 5.10: DISPLACEMENT AND STRESSES OF EXAMPLE 5.3.1

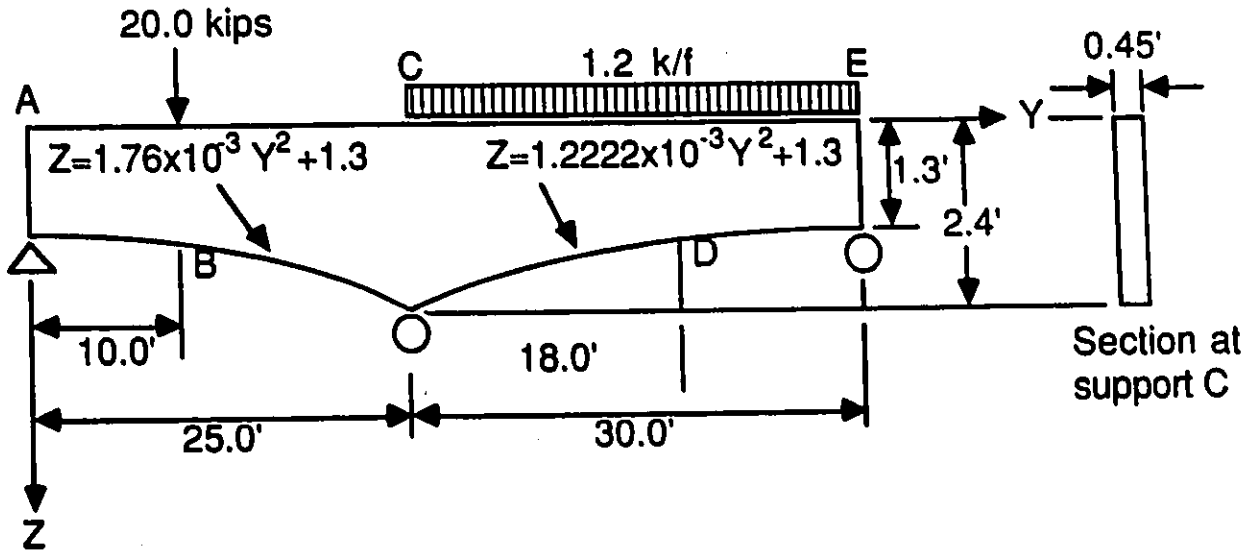

Figure 5.14: LOADS AND LAYOUT OF EXAMPLE 5.3.2

Average Displacement ($\times 10^5 ft$) @		ADINA Results 56 Elements	Strip Results (No. of Terms) 10	20	30	40	45
B		0.1089	0.1040	0.1047	0.1048	0.1048	0.1049
D		0.3796	0.3748	0.3750	0.3750	0.3750	0.3750
Stresses ($\times 10^3 K/ft^2$) @		56 Elements	10	20	30	40	45
B	TOP	-0.3895	-0.2789	-0.3094	-0.3201	-0.3256	-0.3283
	BOT	0.3377	0.2787	0.3083	0.3168	0.3198	0.3209
C	TOP	0.3776	0.3862	0.3733	0.3734	0.3750	0.3730
	BOT	-0.4274	-0.3861	-0.3731	-0.3731	-0.3732	-0.3730
D	TOP	-0.4013	-0.3938	-0.3978	-0.3979	-0.3986	-0.3986
	BOT	0.3999	0.3938	0.3978	0.3980	0.3986	0.3987

Table 5.11: DISPLACEMENT AND STRESSES OF EXAMPLE 5.3.2

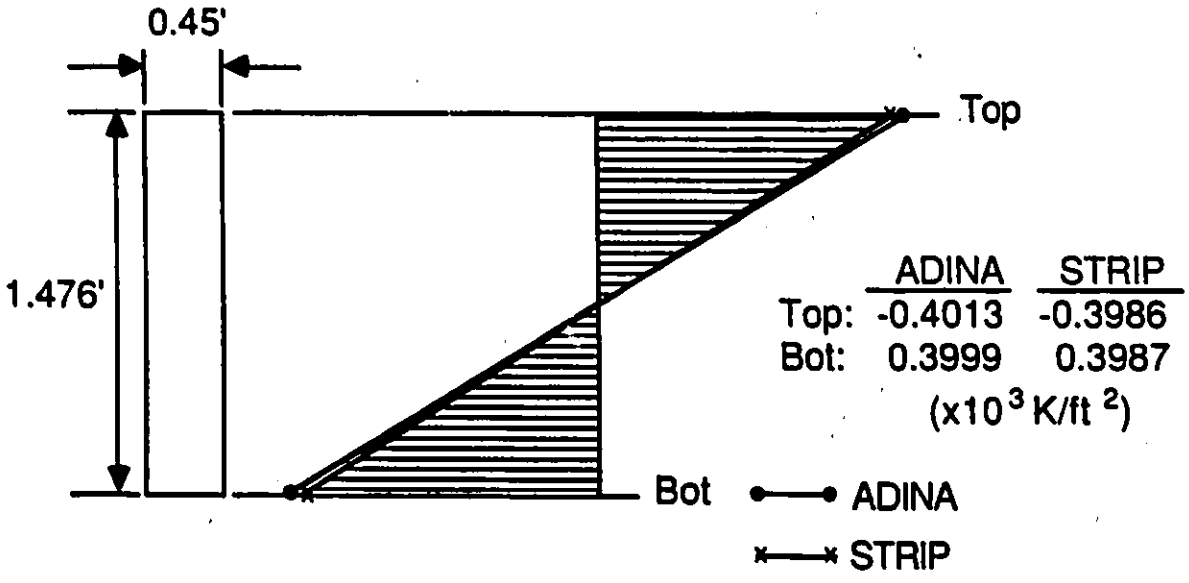

Figure 5.15: STRESS DISTRIBUTION OF EXAMPLE 5.3.2

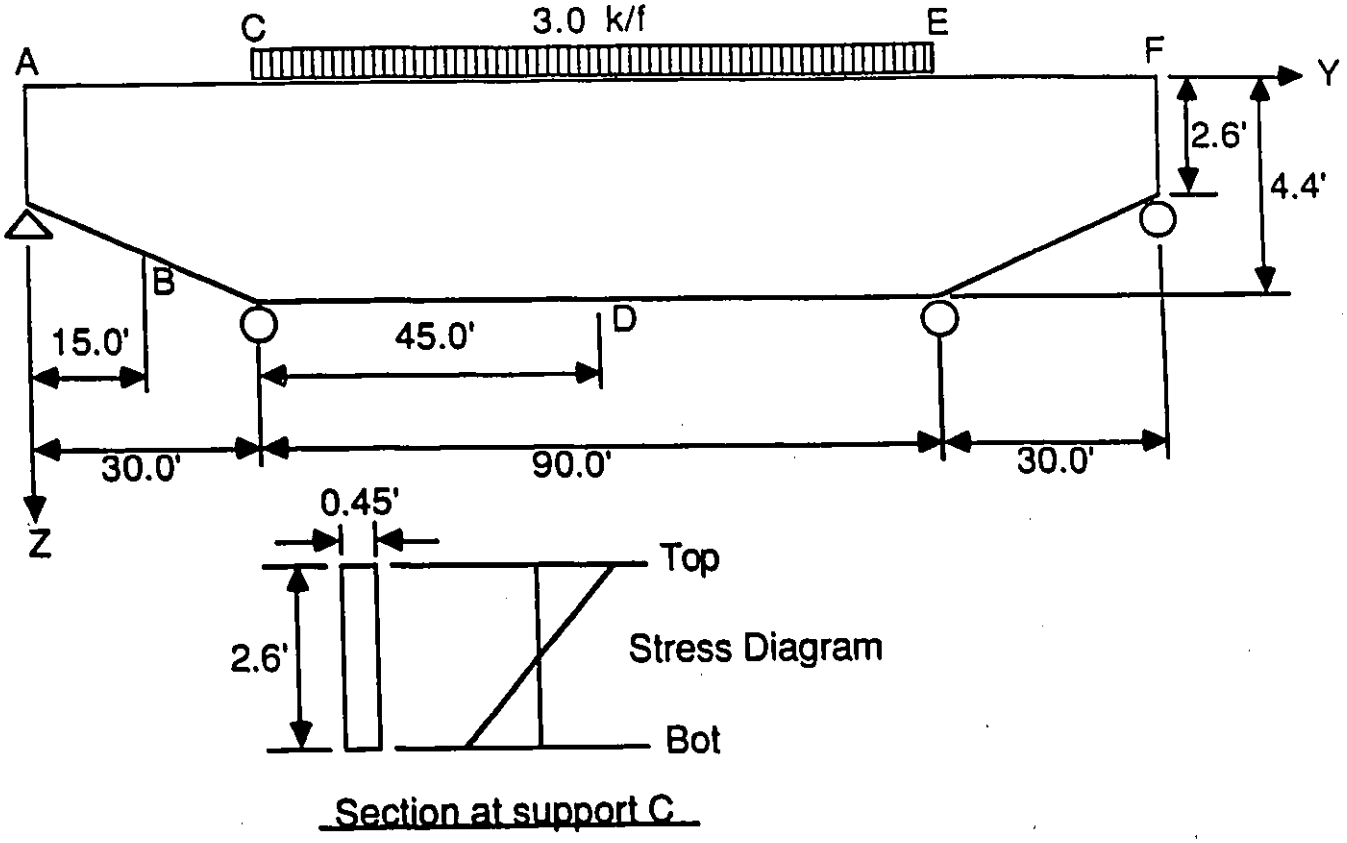

Figure 5.16: LOADS AND LAYOUT OF EXAMPLE 5.3.3

Average Displacement ($\times 10^6 ft$) @		ADINA Results 60 Elements	Strip Results (No. of Terms) 10	20	30	40	45
B		-0.0497	-0.0498	-0.0498	-0.0498	-0.0498	-0.0498
D		0.3237	0.3190	0.3190	0.3191	0.3191	0.3191
Stresses ($\times 10^4 K/ft^2$) @		60 Elements	10	20	30	40	45
B	TOP	0.0830	0.0858	0.0827	0.0834	-0.0831	0.0832
	BOT	-0.0832	-0.0858	-0.0827	-0.0834	-0.0831	-0.0832
C	TOP	0.1047	0.1036	0.1050	0.1052	0.1053	0.1053
	BOT	-0.1183	-0.1036	-0.1049	-0.1051	-0.1052	-0.1051
D	TOP	-0.1047	-0.1053	-0.1037	-0.1040	-0.1039	-0.1039
	BOT	0.1045	0.1053	0.1037	0.1040	0.1039	0.1039

Table 5.12: DISPLACEMENT AND STRESSES OF EXAMPLE 5.3.3

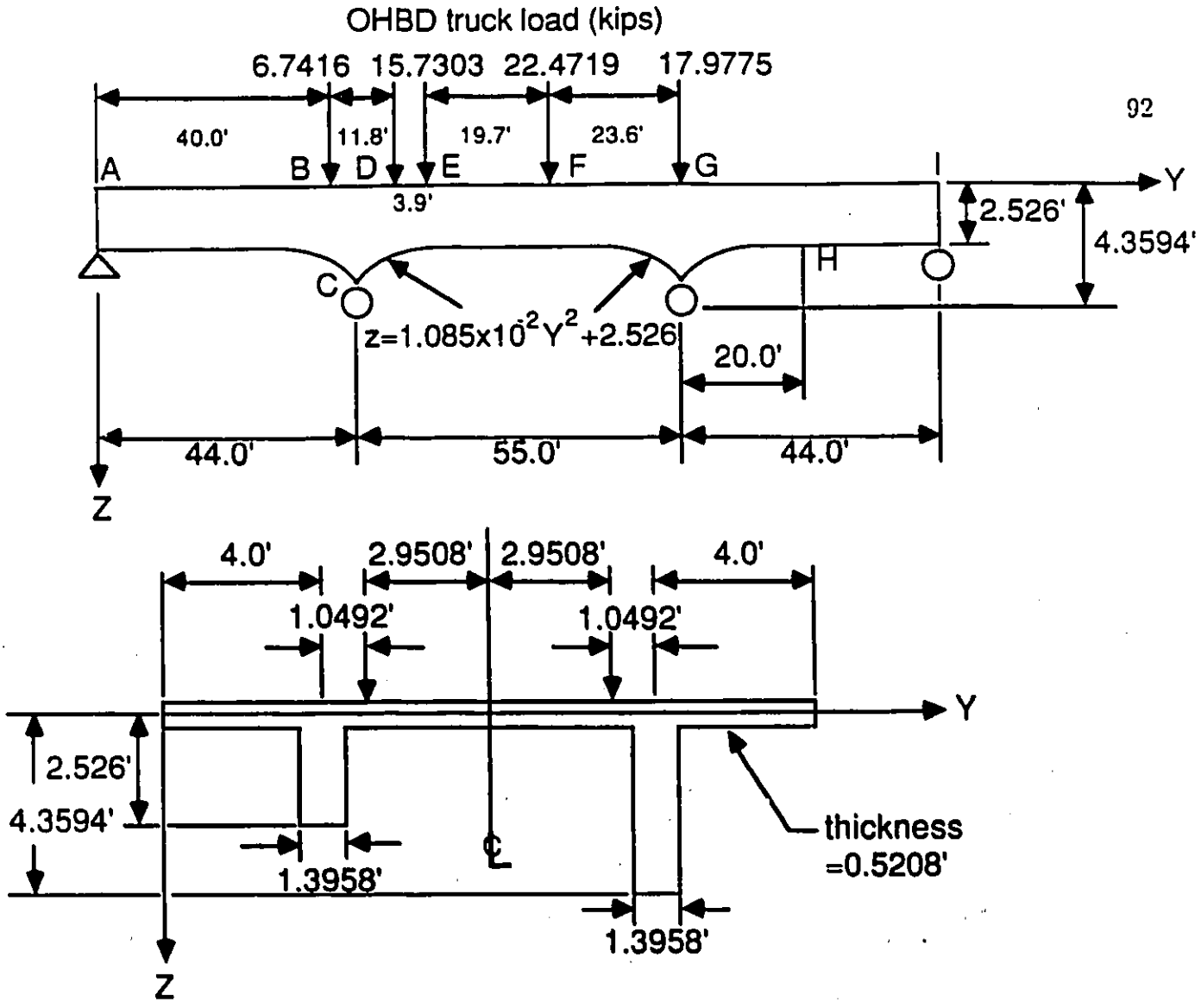

Section at the end and the interior supports

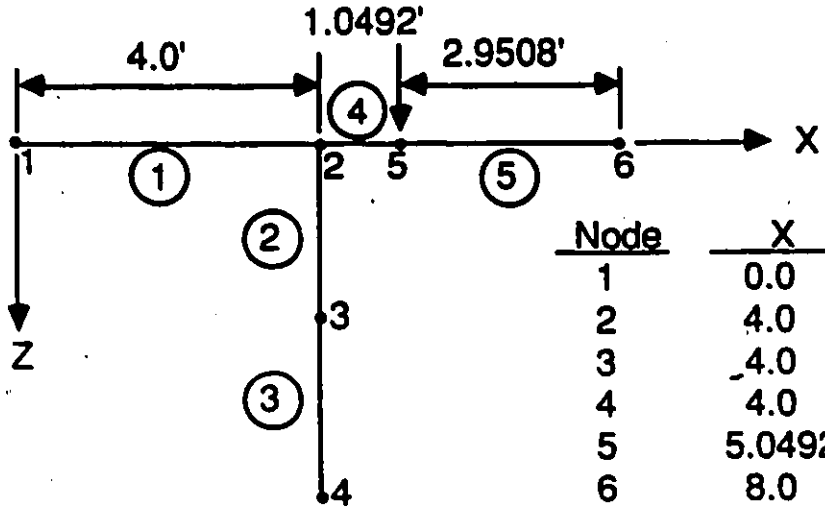

Node	X	Z
1	0.0	0.0
2	4.0	0.0
3	4.0	2.1797
4	4.0	4.3594
5	5.0492	0.0
6	8.0	0.0

Figure 5.17: LOADS AND LAYOUT OF EXAMPLE 5.3.4

Average Displacement ($\times 10^4 ft$) @		ADINA Results 180 Elements	Strip Results (No. of Terms) 10	20	30
B		-0.1790	-0.1846	-0.1835	-0.1826
D		0.4345	0.4195	0.4274	0.4276
E		0.6457	0.6211	0.6382	0.6380
F		1.0144	0.9972	1.0066	1.0067
H		-0.4203	-0.4294	-0.4284	-0.4283
Stresses ($\times 10^2 K/ft^2$) @		180 Elements	10	20	30
B	TOP	0.2029	0.2481	0.2135	0.2083
	MID	0.1643	0.1880	0.1647	0.1642
	BOT	-0.4950	-0.5364	-0.4677	-0.4637
C	TOP	0.2268	0.2428	0.2198	0.2196
	MID	0.1809	0.1942	0.1699	0.1654
	BOT	-0.4131	-0.4591	-0.3883	-0.3857
E	TOP	-0.2617	-0.1502	-0.2083	-0.2169
	MID	-0.1713	-0.1043	-0.1433	-0.1483
	BOT	0.4716	0.2983	0.4285	0.4409
F	TOP	-0.4605	-0.3560	-0.3728	-0.3936
	MID	-0.3035	-0.2456	-0.2559	-0.2682
	BOT	0.8776	0.7884	0.8107	0.8395
H	TOP	0.1664	0.1757	0.1671	0.1703
	MID	0.1148	0.1188	0.1134	0.1150
	BOT	-0.3857	-0.4180	-0.3978	-0.4057

Table 5.13: DISPLACEMENT AND STRESSES OF EXAMPLE 5.3.4

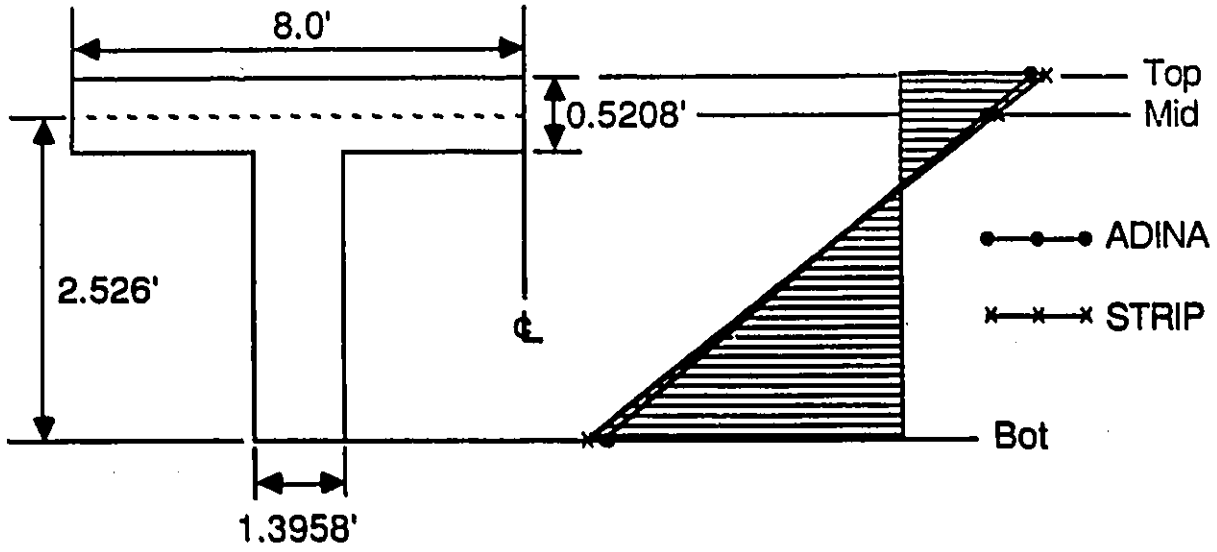

	ADINA	STRIP
Top:	0.1664	0.1703
Mid:	0.1148	0.1150
Bot:	-0.3857	-0.4057

($\times 10^2$ K/ft^2)

Stress diagram at location H

NOTE: Due to the symmetry of the cross-section , only half of the stress diagram is drawn.
The other half will have the same shape and magnitude.

Figure 5.18: STRESS DISTRIBUTION OF EXAMPLE 5.3.4

5.4 DISCUSSION

A total number of twelve examples which can be classified into three types of structures: (I) beams, (II) plates and (III) build up sections are chosen to verify and investigate the adaptability of the strip program in terms of both structural geometry and loading configurations. These examples are analyzed by the beam theory, the Finite Element Method (ADINA) and the Finite Strip Method (the strip program). The comparisons of the solutions obtained from these analyses dictates the accuracy and the efficiency of the strip program.

(I) Beams, examples 5.2.1 to 5.2.5

Five beam problems have been analyzed by both the beam theory, and the strip program in which a continuous strip and different numbers of the series terms (e.g. 10, 20, 30, 40 and 45 terms) are used. The bending moments found by the two methods are compared in tables 5.1 to 5.5 which correspond to examples 5.2.1 to 5.2.5 respectively. It is evident that twenty terms in the shape function series is sufficient to obtain an accurate stress. The maximum difference between the strip program results and the beam theory results was below three percent. Such agreement between these results clearly indicate the ability of the strip program in predicting the structural response of the beam problems.

From examples 5.2.2 to 5.2.5, for the same accuracy of the solutions, the rate of convergency of the results due to the uniformly distributed load is much faster (around twenty terms faster) than that due to the point load. This explains the fact that the steep deflection shape of the point load requires more terms to simulate than the smooth deflection curve of the uniformly distributed load. On the other hand, the results of examples 5.2.1 and 5.2.5 show that the increase in the number of spans

has no strong effect on the accuracy of the results, though the rate of convergency of the solutions may become slower for some cases. Moreover, it is observed that the loading pattern, especially the location of the point load, have contributed some effects on the accuracy and the rate of convergency of the results. From the results of examples 5.2.1 and 5.2.3, the rate of convergency has been greatly improved if the point load is applied in combination with uniformly distributed load. This phenomenon is important since every bridge, regardless of the type of the external loads, has its own weight distributed along the spans.

(II) Plates, examples 5.2.6, 5.2.7 and 5.3.1 to 5.3.3

So far, the strip program has been justified in the analysis of beam problems in terms of different loading types and different number of spans. Thus, the purpose here is to examine and discuss the reliability of the strip program in the analysis of plate problems. A total of five plate problems are studied. Two of them have constant cross-section (examples 5.2.6 and 5.2.7) while the others (examples 5.3.1 to 5.3.3) are with variable cross-section which may be regarded as the haunched web of a bridge. Both examples 5.2.6 and 5.2.7 are analyzed by the beam theory, the ADINA program and the strip program while the others are analyzed by the last two methods only.

In example 5.2.6, a constant web (or vertical plate) with two loading conditions: (a) concentrated load and (b) uniformly distributed load, is considered. This example is used to show the reliability of both the ADINA results and the strip results in the analysis of the plate problems. Two meshes (i.e. twenty and eighty elements) are used for the ADINA program while one strip mesh with three sets of number of terms (ten, twenty and thirty terms) is employed for the strip program. Since the

loading and the geometry of the plate are symmetrical about its interior support, only the symmetrical modes is taken as the shape function in the longitudinal direction for the finite strip analysis. The bending stresses at the top and the bottom of the cross-section obtained by the three methods are given in tables 5.6 and 5.7 for the point load and for the uniformly distributed load respectively. Both the ADINA results and the strip results are compared with the exact solutions obtained from the beam theory.

(a) The concentrated loaded case

From table 5.6, it is noted that the strip results with ten terms can converge to the theoretical value of the beam theory within one percent difference except at the locations of the concentrated loads. At these locations, an addition of twenty terms is required to maintain the same accuracy. On the other hand, the ADINA results need eighty elements to obtain the same accuracy. However, at the location of the point loads and the supports, the ADINA results have a remarkably high percentage difference from the solution of the beam theory. This is mainly due to the effect of the high stress concentration at these locations.

(b) The uniformly distributed loaded case

In this case (table 5.7), the effect of the high stress concentration is minimized in the finite strip analysis. Moreover, the rate of convergency and the accuracy of the strip results are even better than the previous case. On the contrary, the ADINA results still have the stress concentration problem at the supports. Although the ADINA results for both the point load and the uniformly distributed loaded cases may be theoretically improved by using finer mesh at these regions of high stress concentration, the limitation on the computer capacity has resulted in no further

effective improvement for the results. For the other locations, the ADINA program gives excellent solutions. Since the ADINA program is the only available finite element analysis package at the University of Ottawa and it gives reliable solutions, so the ADINA results are employed as reference values unless other theoretical solutions can be found.

The other constant plate problem (example 5.2.7) is a horizontally oriented thin plate with concentrated load. In table 5.8, the bending moments of the three methods (the ADINA, the strip program and the beam theory) are compared. The convergency of both the ADINA results and the strip results are confirmed by using two different meshes (thirty-six and seventy-two elements) and by employing three sets of number of terms (ten, twenty and thirty terms) respectively. With the same reason described in example 5.2.6, only the symmetrical modes are used as the shape function in longitudinal direction for the finite strip analysis. In this example, the effect of the stress concentration has not been observed. This phenomenon indicates the fact that the bending-action, instead of the in-plane action in the previous example, is the main factor to cause the deformation. Furthermore, the ADINA results and the strip results are in a very good agreement with the theoretical results obtained from the beam theory.

The vertical plates with variable depth are illustrated by the following examples. These examples (examples 5.3.1 to 5.3.3) with different geometries are examined in order to show the ability of strip program in analyzing different type of haunches (straight or curve). In the strip program, the actual shape of the haunch is approximated by a parabolic function. The accuracy and the rate of convergency of the results has been verified and is shown in tables 5.10 to 5.12. The strip results are

generally in a good agreement with the ADINA solutions except some differences between the two results are observed right at the locations of the loading points and over the supports. The disagreement between the two results is mainly due to the effect of the stress concentration on the ADINA solutions as discussed before. Although, the accuracy of the strip results at these locations cannot be assured by comparing with ADINA solutions, the good agreement of the two results at other locations can sufficiently prove the reliability of the strip results. On the other hand, the efficiency of the strip program is noticed – for these haunched sections, twenty terms are sufficient for the uniformly distributed load while thirty terms (or at most forty-five terms for certain locations) are generally required for the point load. As a result, the strip program is also good for the plate problems including different geometric shapes.

(III) Build-up sections, examples 5.2.8 and 5.3.4

Up to now, the finite strip analysis has been shown to be a very effective, reliable and powerful tool for the analysis of the beam and plate problems. Besides these, the strip program can also be used for more complicated structures such as plate-girder bridges which may be considered as a combination of the horizontal and vertical plates (constant or variable depth). For this reason, two examples consist of a T-shaped section (example 5.2.8) and a real bridge model section (example 5.3.3) are discussed here. Both examples are loaded with an OHBD truck load and analyzed by the ADINA program and the strip program. From the previous experience, the actual comparison between the ADINA results and the strip results at certain locations may be invalid because of the stress concentration effect on the ADINA results at those locations. Due to the symmetry of the cross-sections

and the loading configurations, each example can be solved by considering only half of the whole section with some appropriate boundary conditions. The required boundary conditions have been discussed and given in examples 5.2.8 and 5.3.4.

In example 5.2.8, the T-shaped section is constant throughout the whole structure. An ADINA mesh of 168 elements has been constructed and no further finer meshes can be created because of the limitation on the availablility of the computer facilities. On the other hand, a total of four strips is used for the strip analysis. From table 5.9, the good accuracy and the rapid convergency of the strip results are revealed. However, the stress concentration effect on the ADINA solutions right at the locations of the loading points and over the supports have again shown by the bending stress results. For example, the percentage difference between the ADINA results and the strip results at the top and the bottom of the web are 5.8 and 1.7 respectively. Except for this discrepancy the overall strip results are in a very good agreement with ADINA solutions.

In addition, the strip program has been employed for the analysis of a continuous haunched girder bridge model (example 5.3.4). With the same reason described in the previous problem, only an ADINA mesh of 180 elements can be assembled for the half of the bridge section. Also, five strips are found to suffice for an accurate strip analysis. Both the ADINA results and the strip results given in table 5.13 are generally agreed with each other. Although the percentage difference between two results was gone up to a maximum of three percent, the strip results are still an acceptable solutions. Such percentage difference may be attributed to the complexity of the structure, the approximation in the curvilinear coordinate system, and the cumulative computing error in the numerical integrations. Under these

circumstances, the strip results are considered an accurate and acceptable solution. In terms of efficiency, the strip results are rapidly converged (around thirty terms) to an acceptable answer. These results are attractive for such complex section.

In conclusion, with the help of the above discussed examples, the strip program is found to be not only good for the beam and plate problems, but also for build up sections such as the plate-girder bridges.

CHAPTER 6

CONCLUSION

The linear analysis of straight simply supported, continuous plate-girder bridges was successfully carried out by the Finite Strip Method. This method was programmed not only for analyzing sections with constant depth, but also for sections with variable depth.

In this analysis, a new formulated continuous strip was developed based on the shape function for a continuous beam under free vibration. And the curvilinear coordinate system was introduced for the analysis of haunched bridge structures. Through the accuracy and the rapid convergency of the results of the given examples, a number of important conclusions with respect to the applicability of this finite strip analysis can be made:

(1) This method can be used for analyzing not only continuous beams and thin plates, but also for complex section such as continuous plate-girder bridges having uniform or variable depth along the longitudinal axis of the structure.

(2) The convergency of the new formulated continuous strip is much better than that of the flexibility method. Regardless of the type of loading (point load or uniformly distributed load), the flexibility method required at least 50 terms to obtain an acceptable solution. In contrast, the new formulated continuous strip required only 30 terms for the point load and much less for the uniformly distributed load to obtain accurate results.

(3) The introduction of the curvilinear coordinate system in the analysis of the

haunched structures is very satisfactory in terms of the efficiency and accuracy.

As a result, the Finite Strip Method with the new formulated continuous strips can be concluded as a powerful and an effective tool for the linear analysis of the straight simply supported continuous plate-girder bridges.

References

[1] Cheung, M. S., "Finite Strip Method And Its Application to Slab And Girder Bridge", MSc. Thesis, University of Calgary, July 1969.

[2] Cheung, M. S. and Lau, Wilson W. S., "A Computer Program of the Finite Strip Analysis for the Straight Simply Supported, Continuous Plate-girder Bridges", Dept. of Civil Engineering, University of Ottawa, 1987. (To be published)

[3] Cheung, M. S. and Li, WenChang, "Analysis of Haunched, Continuous Bridges by The Finite Strip Method", Dept. of Civil Engineering, University of Ottawa, 1987. (To be published)

[4] Cheung, M. S. and Li, WenChang, "Finite Strip Analysis of Continuous Structures", Dept. of Civil Engineering, University of Ottawa, 1987. (To be published)

[5] Cheung, Y. K., "Analysis of Box Girder Bridge by Finite Strip Method", Second International Symposium on Concrete Bridge Design, Chicago, March 1979.

[6] Cheung, Y. K., "Concrete Bridge Design", ACI Publication SP-26, 1971, Pp. 357-378.

[7] Cheung, Y. K., "Finite Strip Method Analysis of Elastic Slabs", Proc. ASCE, Vol. 94, No. EM6, December 1968, Pp. 1365-1378.

[8] Cheung, Y. K., "Finite Strip Method in Structural Analysis", Pergamon Press, 1976.

[9] Cheung, Y. K., "Folded Plate Structures by Finite Strip Method", Am. Soc. Civ. Engers 95, No. ST12, Dec. 1969, Pp. 2963-2979.

[10] Cheung, Y. K., "The Finite Strip Method in The Analysis of Elastic Plates With Two Opposite Simply Supported Ends", Proc. Instit. Civil Engrs 40, 1-7, May 1968.

[11] Cook, Robert D., "Concepts and Applications of Finite Element Analysis", 2nd Edition, John Wiley & Sons, Inc., 1981.

[12] Coull, A. and Rao, K. S., "Analysis of Bridge Decks by Line Solution Techniques", International Symposium on the use of Electronic Digital Computers in Structural Engineering (University of Newcastle-upon-Tyne, 1966).

[13] Das, P. C., "Analysis of Curved Bridge Decks With Concentrated Loads", Ph.D. Thesis, Southampton University, 1968.

[14] DeFries-Skene, A. and Scordelis, A. C., "Direct Stiffness Solution for Folded Plates", J. Struct. Div. Am. Soc. Civ. Engrs., Vol. 90, ST4, August 1964, Pp. 15-47.

[15] Den Hartog, J. P., "Strength of Materials", Dover Publications, Inc., 1961.

[16] Desai, C. S. and Abel, J. F., "Introduction to the Finite Element Method", Van Nostrand Reinhold Company, 1972.

[17] Donnell, Lloyd Hamilton, "Beams, Plates and Shells", Mcgraw-Hill, Inc., 1976.

[18] Evans, H. R., "The Analysis of Folded Plate Structures", Ph.D. Thesis, University of Wales, Swanswa, 1967.

[19] Evans, H. R. and Rockey, K. C., "A Critical Review of the Methods of Analysis for Folded Plate Structures", Proc. Instit. Civ. Engrs., June 1971.

[20] Fertis, Demeter G., "Dynamics and Vibration of Structures", Pergamon Press Ltd., 1964.

[21] Gaafar, I., "Hipped Plate Analysis, Considering Joint Displacements", Trans. Am. Soc. Civ. Engrs., Vol. 119, 1954, Pp. 743-784.

[22] Ghali, A. and Neville, A. M., "Structural Analysis– A Unified Classical and Matrix Approach", 2nd Edition , Chapman and Hall, London, 1978.

[23] Ghali, A. and Tadros, G. S., "On Finite Strip Analysis of Continuous Plates", Research Report No. CE-72-11, Department of Civil Engineering, University of Calgary, March 1972.

[24] Goldberg, J. E. and Leve, H. L., "Theory of Prismatic Folded Plate Structures", Publs. Int. Ass. Bridge Struct. Engng., Vol. 17, 1957, Pp. 59-86.

[25] Gorman, Daniel J., "Free Vibration Analysis of Beams and Shafts", John Wiley & Son, Inc., 1975.

[26] "Hand Book of Steel Construction", 4th Edition, Canadian Institute of Steel Construction, 1985.

[27] Hsieh, Yuan Yu, "Elementary Thoery of Structures", 2nd Edition, Prentice-Hall, Inc., N. J., 1982.

[28] Jategaonkar, R., Jaeger, L. G. and Cheung, M. S., "Bridge Analysis Using Finite Elements", Canadian Society for Civil Engineering, 1985.

[29] Jenkin, R. S. and Tottenham, H., "The Solution of Shell Problems by the Matrix Progression Method", Proceedings of the World Conference on Shell Structures. (San Francisco, 1962), Washington, National Research Council, 1964.

[30] Johnson, C. D. and Lee, T., "Long Nonprismatic Folded Plate Structures", J. Struct. Div. Am. Soc. Civ. Engrs., Vol. 94, ST6, June 1968, Pp. 1457-1484.

[31] Kazmi, S. M. A. and Coull, A., "The Application of Line-soltion Technique to the Solution of Plane-stress Problems", Int. J. Mech. Sci., Vol. 6, No. 5, 1964, Pp. 391-399.

[32] Kantorovich, L. V. and Krylov, V. I., "Approximate Method of Higher Annlysis", Interscience Publishers, New York, 1958.

[33] Lapidus, Leon, "Digital Computation for Chemical Engineers", McGraw Hill Book Company, Inc., 1962, Pp. 286-288.

[34] Loo, Yew Chaye and Cusens, Anthony R., "The Finite Strip Method in Bridge Engineering", Viewpoint Publications, 1978.

[35] Loo, Y. C. and Cusens, A. R., "The Auxiliary Nodal Line Technique For The Analysis of Box Girder Bridge Decks by Finite Strip Method", Proceedings of Specialty Conference on The Finite Element Method in Civil Engineering, McGill University, Montreal, June 1972.

[36] McCormac, Jack C., "Structural Analysis", Fourth edition, Harper & Row, Publishers, Inc., New York, 1984.

[37] "Ontario Highway Bridge Design Code", Highway Engineering Division, Ministry of Transportation and Communications, 1983.

[38] Powell, G. H. and Ogden, D. W., "Analysis of Orthotropic Steel Plate Bridge Decks", Proc. ASCE, Vol. 95, No. ST5, May 1969, Pp. 909-922.

[39] Ramey, George E., "Force-Displacement Behaviour of Concrete Bridge", Journal of Structural Engineering, Vol. 109 No. 11, November 1983, Pp. 2600-2618.

[40] Rao, K. S., "The Application of Line Solution to Plate Problems, With Particular Reference to Bridge Decks", Ph.D. Thesis, Southampton University, 1966.

[41] Rockey, K. C., Bannister, J. L. and Evans, H. R., "Developments in Bridge Design and Construction", University College, Cardiff, Crosby Lockwood & Son Ltd., 1971.

[42] Scodelis, A. C., "A Matrix Formulation of the Folded Plate Equations", J. Struct. Div. Am. Soc. Civ. Engrs., Vol. 86, ST10, October 1960, Pp. 1-22.

[43] Spiegel, Murray R., "Applied Differential Equation", 3rd Edition, Prentice-Hall, Inc., 1981.

[44] Timoshenko, S. P. and Goodier, J. N., "Theory of Elasticity", 3rd Edition, McGraw Hill, 1982.

[45] Timoshenko, S. and Young, D. H., "Vibration Problems in Engineering", 3rd Edition, Van Nostrand, New York, 1955.

[46] Trockalakis, T. M., "The Analysis of Birdge Decks by the Line Solution Matrix Progression Technique", Ph.D. Thesis, Southampton University, 1968.

[47] Warburton, G. B.,"The Dynamical Behaviour of Structures", Pergamon Press Ltd., 1964.

[48] Yitzhaki, D., "The Design of Prismatic and Cylindrical Shell Roofs", Haifa, Haifa Science Publishers, 1958.

[49] Yoshida, K. and Oka, N., "A Note on The In-plane Displacement Functions of Strip Elements", Research Report, Department of Naval Architecture, Tokyo University, 1972.

[50] Zienkiewicz, O. C., "The Finite Element Method", 3rd Edition, McGraw Hill Book Company (UK) Limited, 1977.

[51] Zienkiewicz, O. C. and Cheung, Y. K., "The Finite Element Method in Structural and Continum Mechanics", McGraw-Hill, 1967.

APPENDIX A

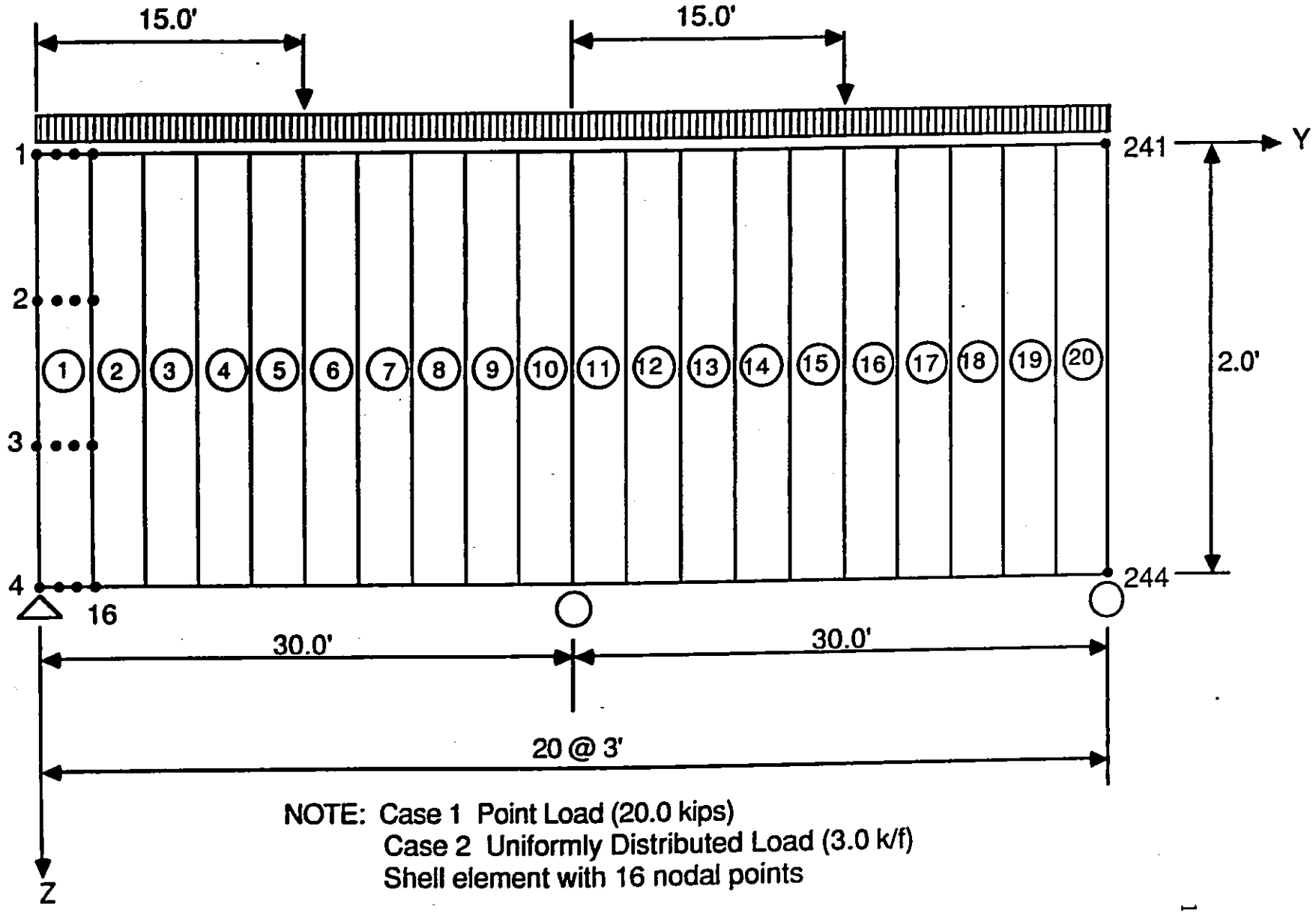

Figure A.1: ADINA MESH (20 ELEMENTS) FOR EXAMPLE 5.2.6

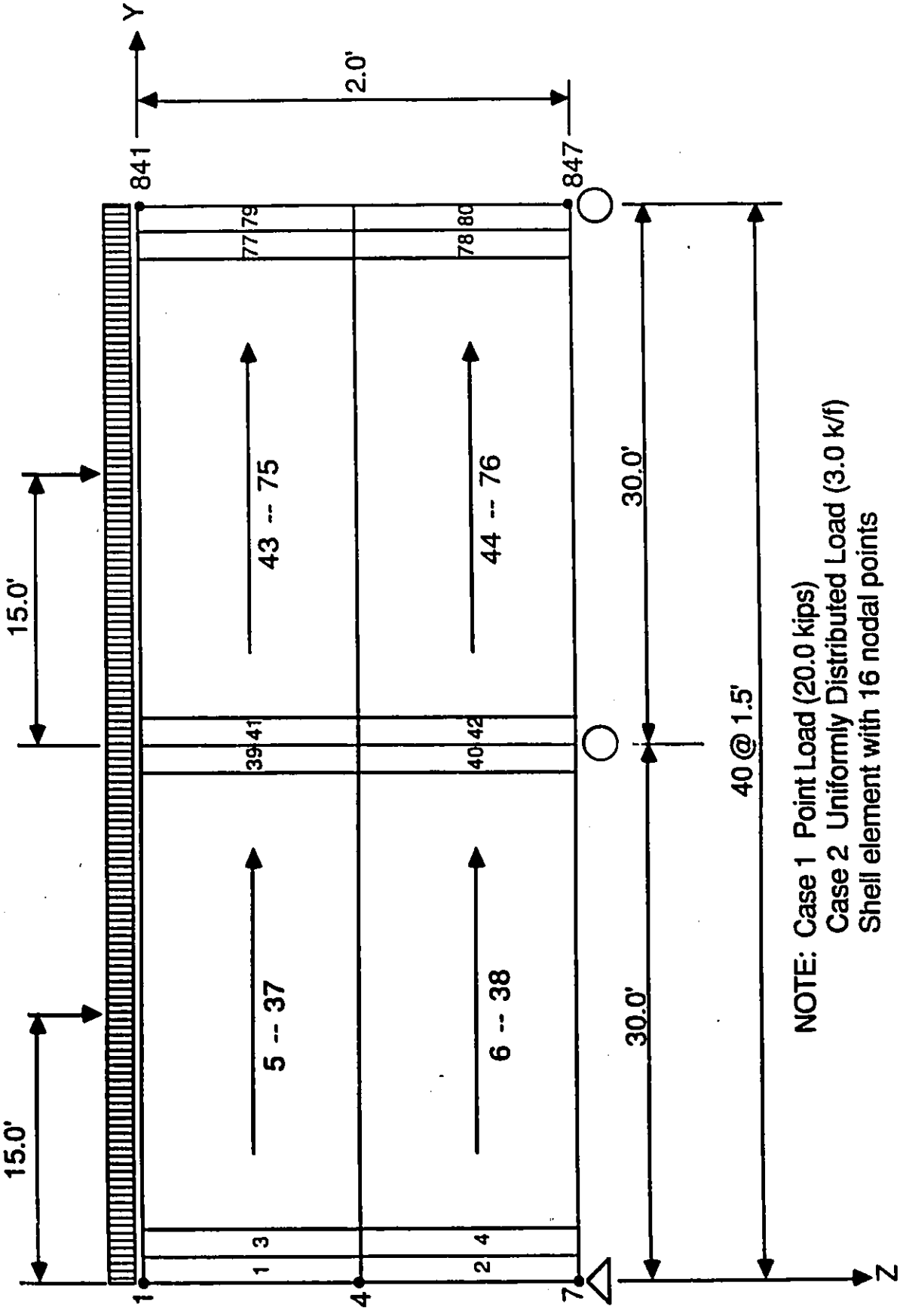

Figure A.2: ADINA MESH (80 ELEMENTS) FOR EXAMPLE 5.2.6

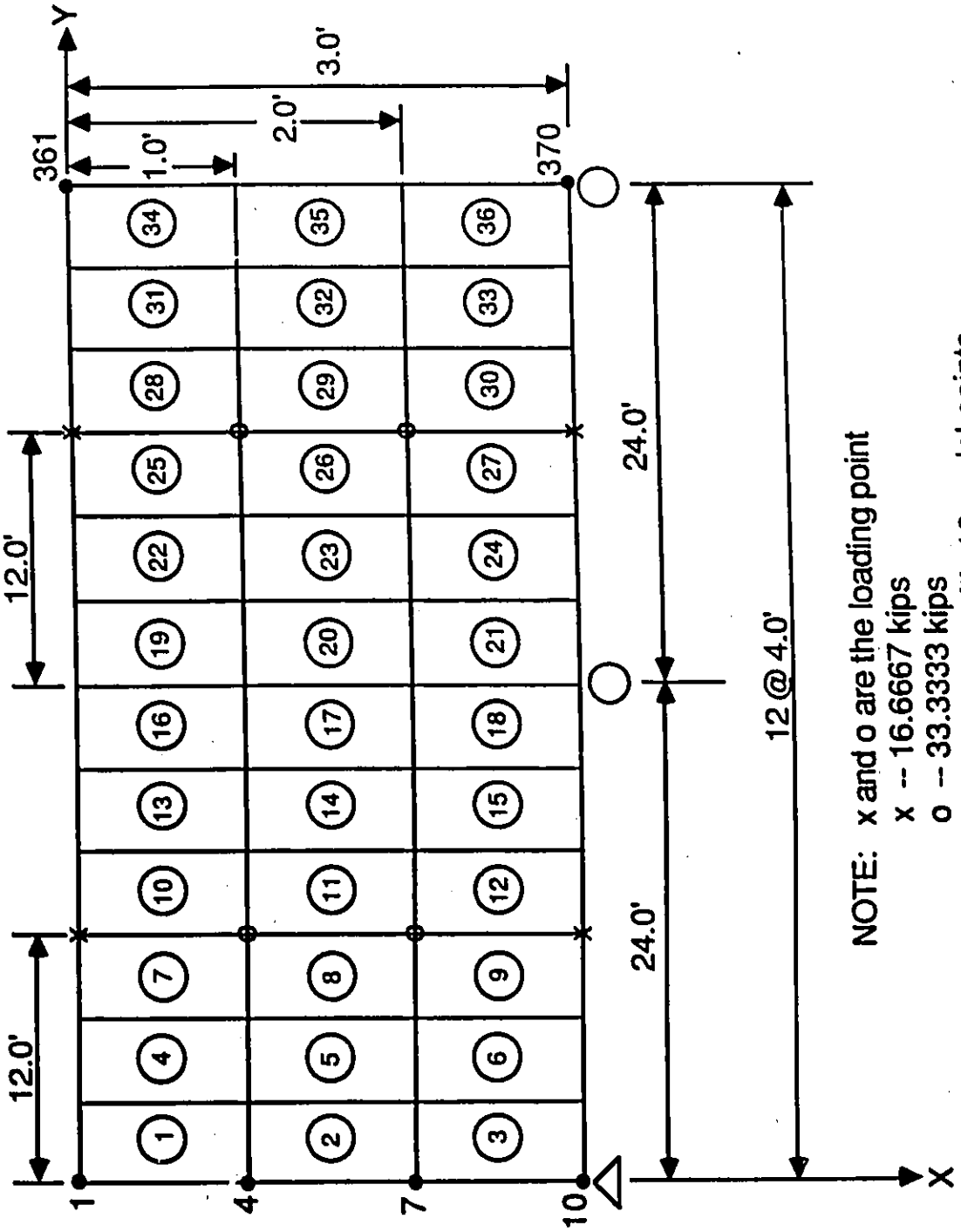

Figure A.3: ADINA MESH (36 ELEMENTS) FOR EXAMPLE 5.2.7

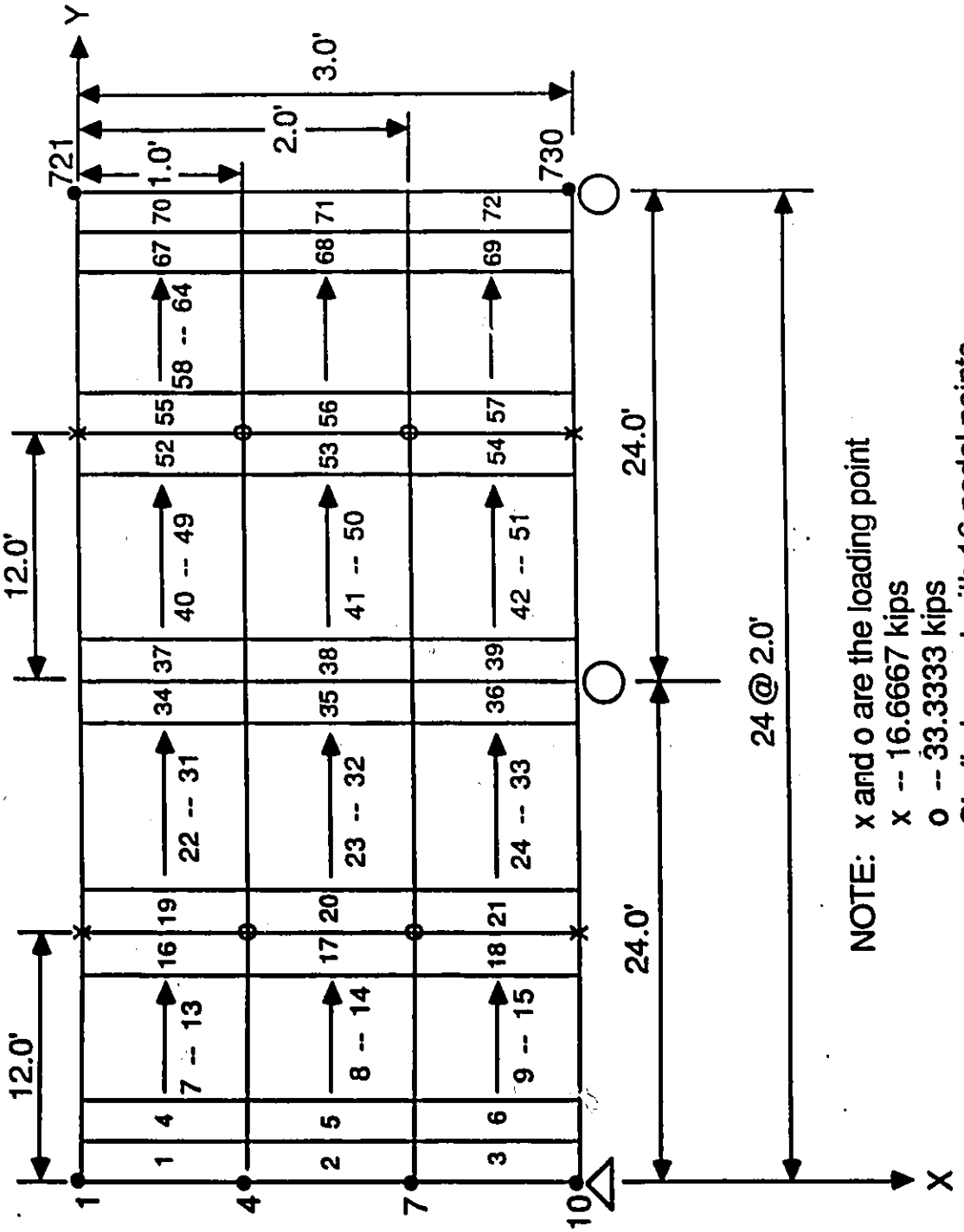

Figure A.4: ADINA MESH (72 ELEMENTS) FOR EXAMPLE 5.2.7

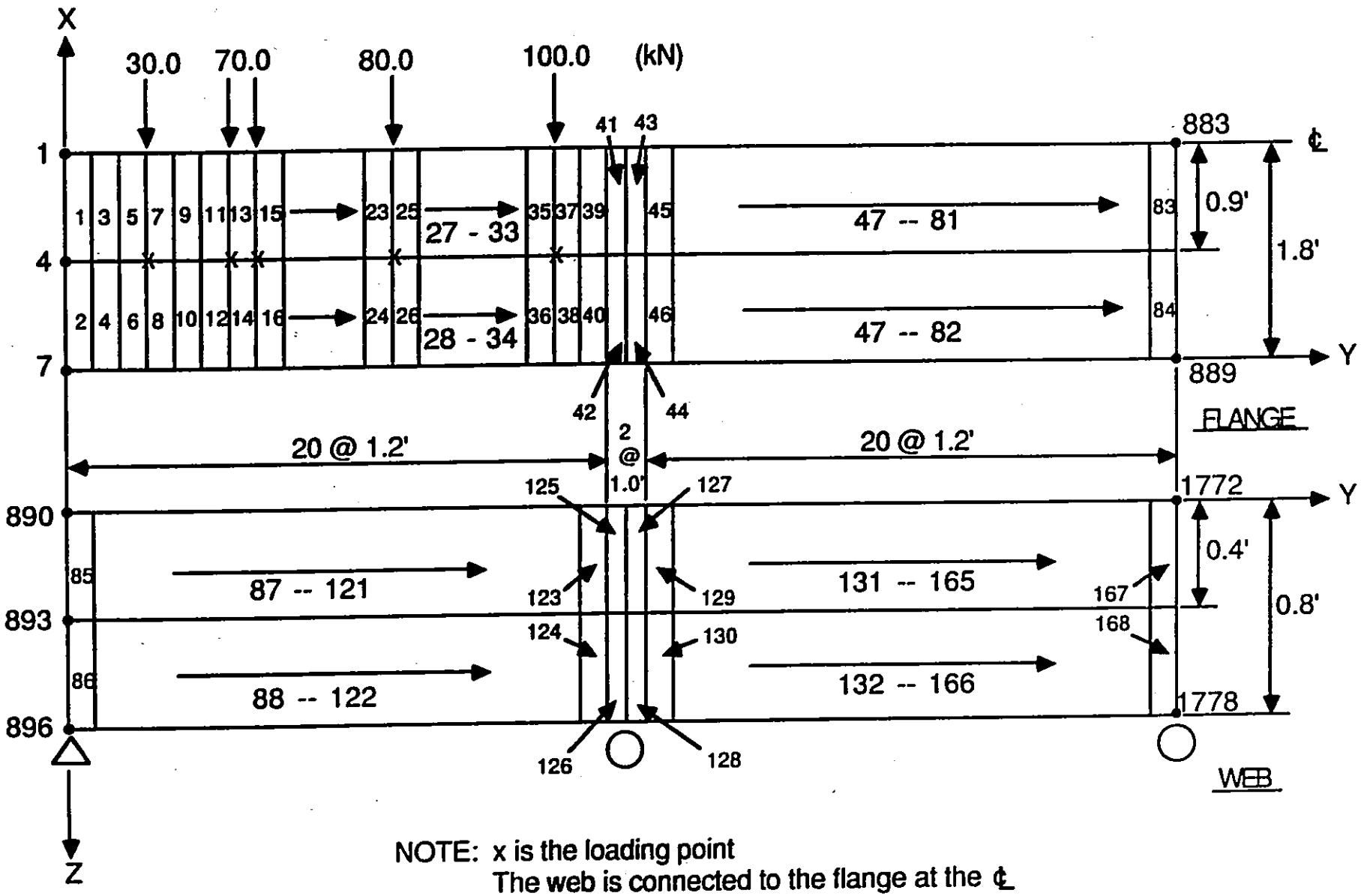

NOTE: x is the loading point
The web is connected to the flange at the ¢
Shell element with 16 nodal points

Figure A.5: ADINA MESH (168 ELEMENTS) FOR EXAMPLE 5.2.8

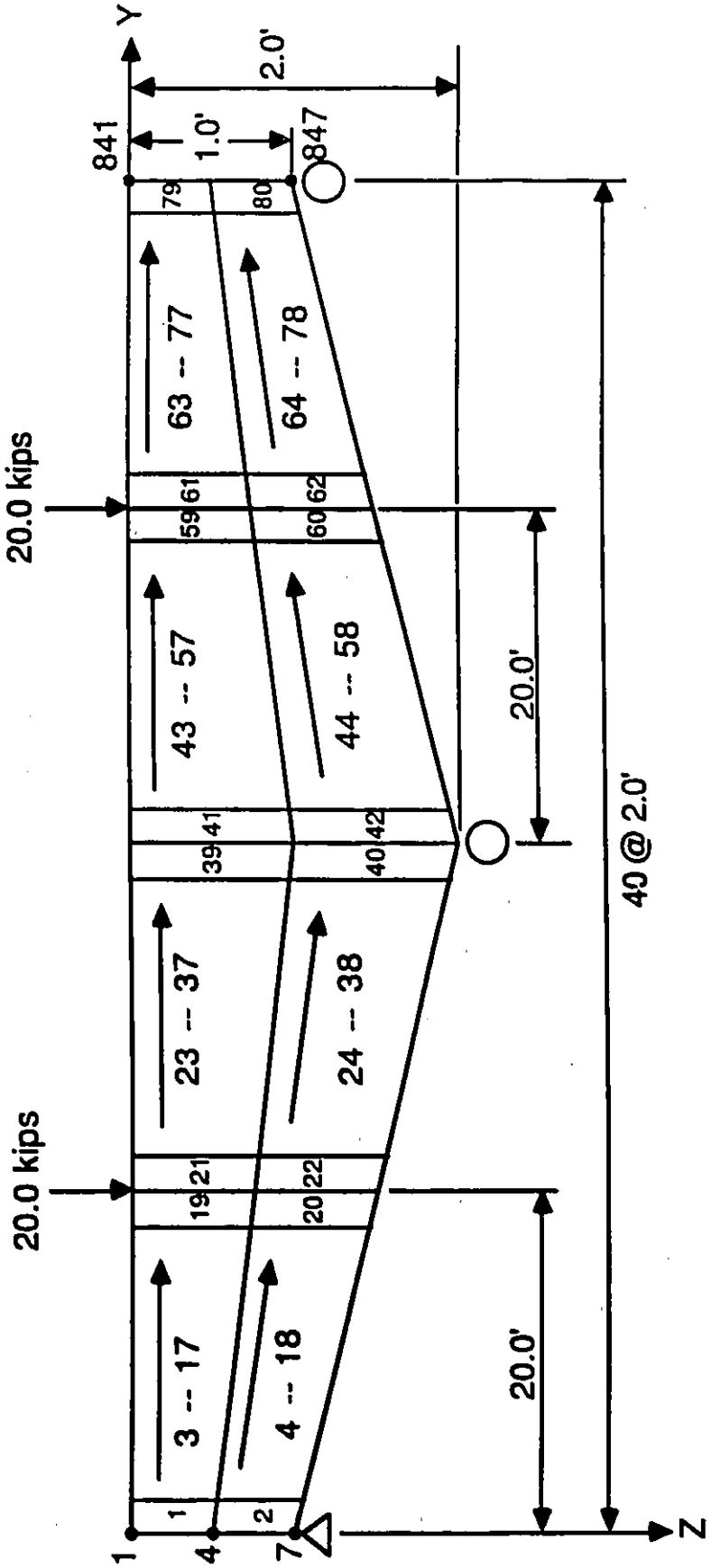

Figure A.6: ADINA MESH (80 ELEMENTS) FOR EXAMPLE 5.3.1

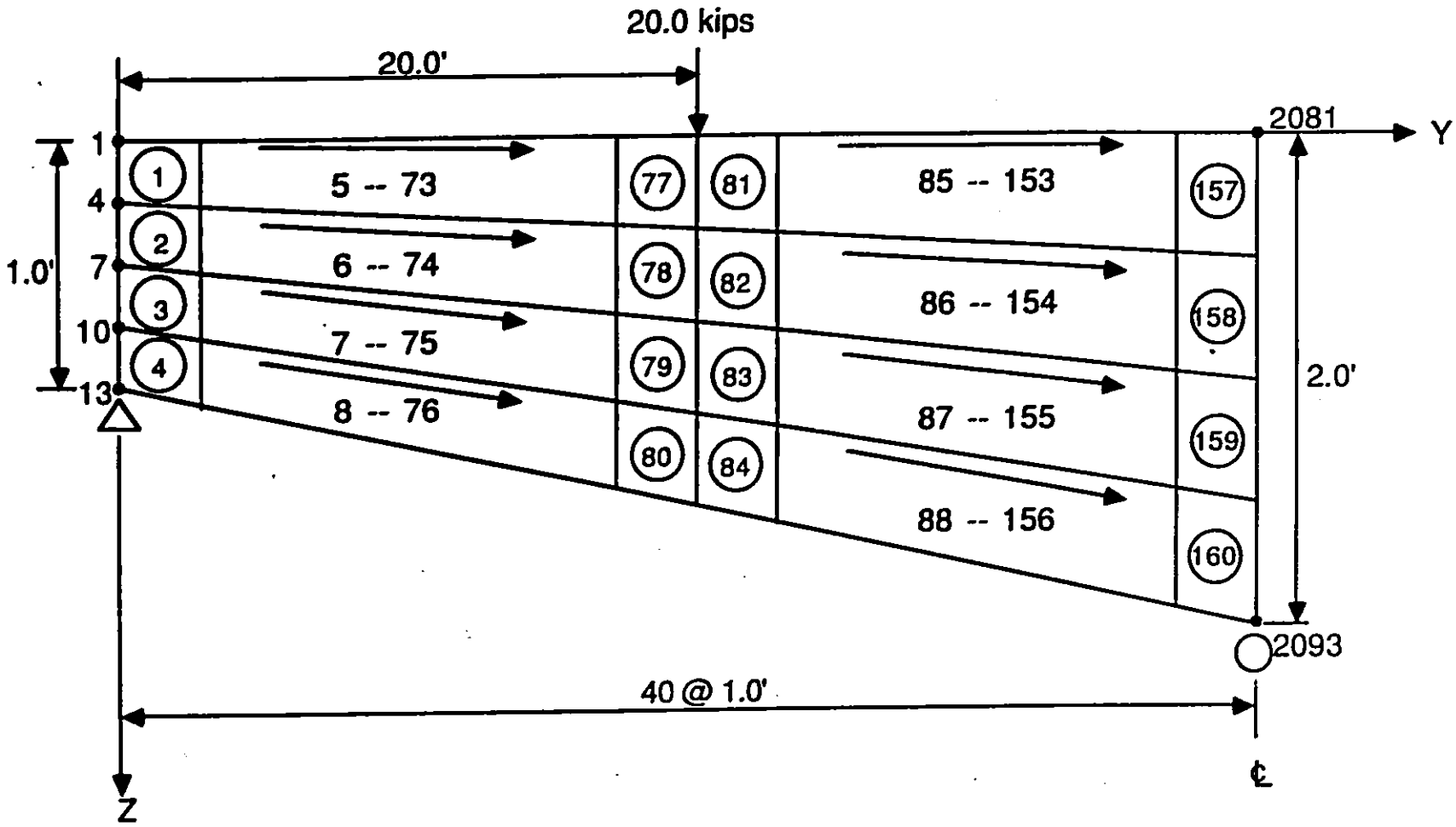

Figure A.7: ADINA MESH (160 ELEMENTS) FOR EXAMPLE 5.3.1

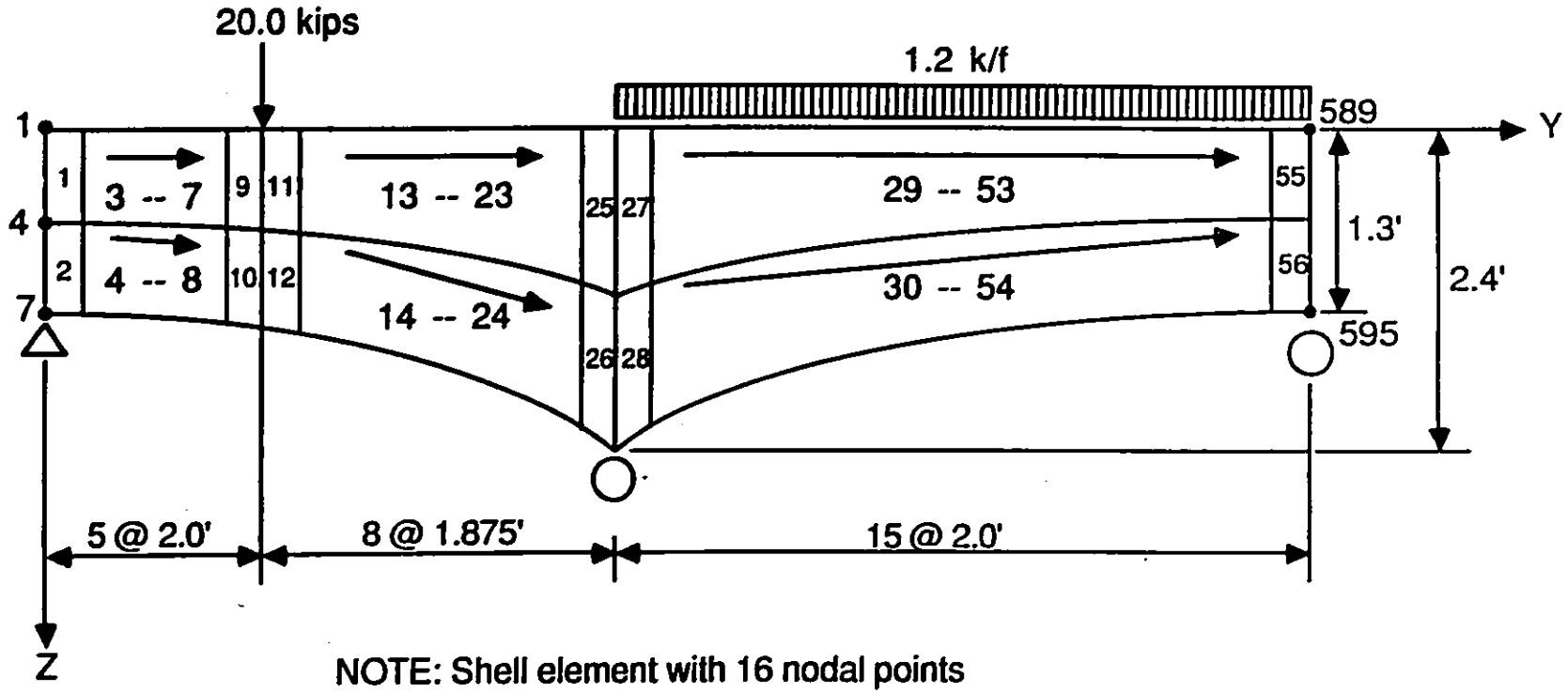

Figure A.8: ADINA MESH (56 ELEMENTS) FOR EXAMPLE 5.3.2

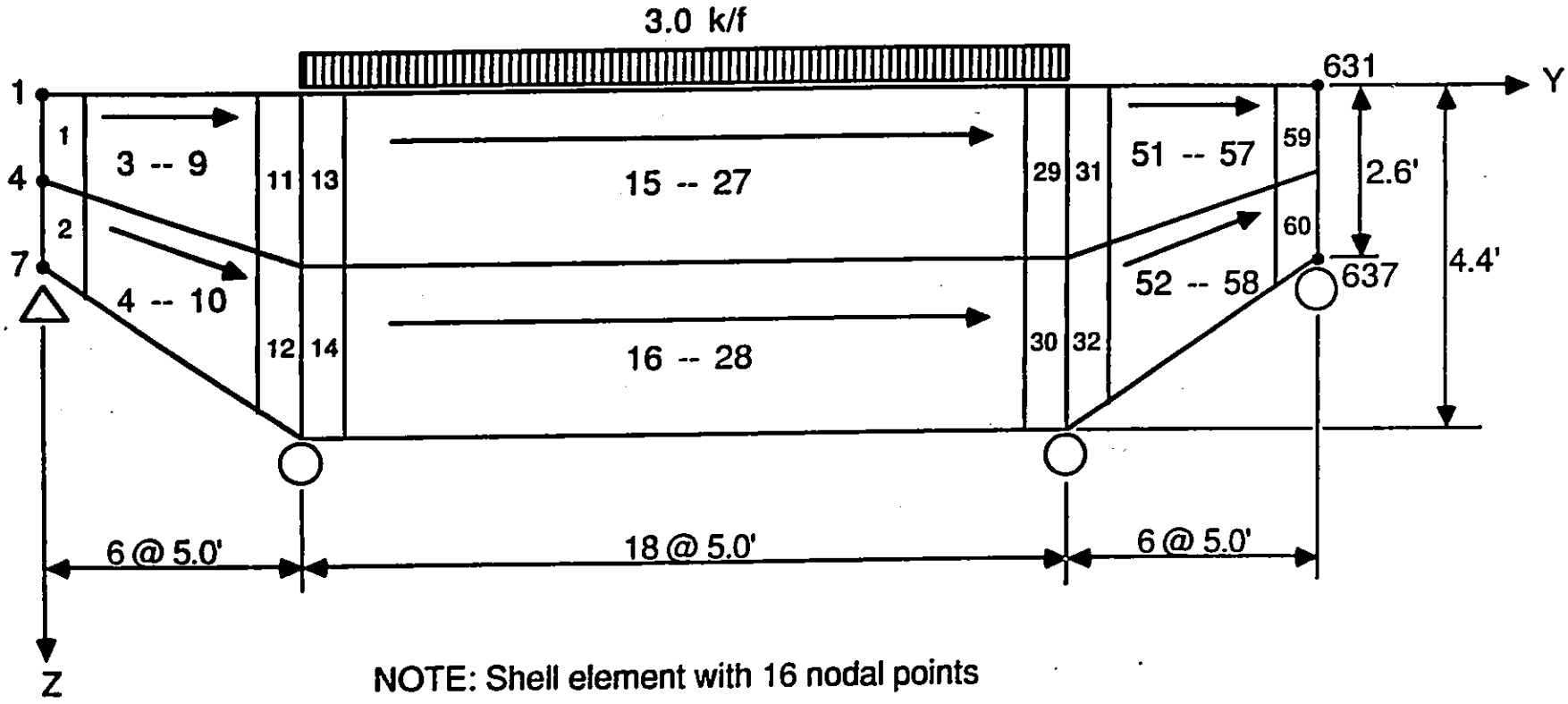

Figure A.9: ADINA MESH (60 ELEMENTS) FOR EXAMPLE 5.3.3

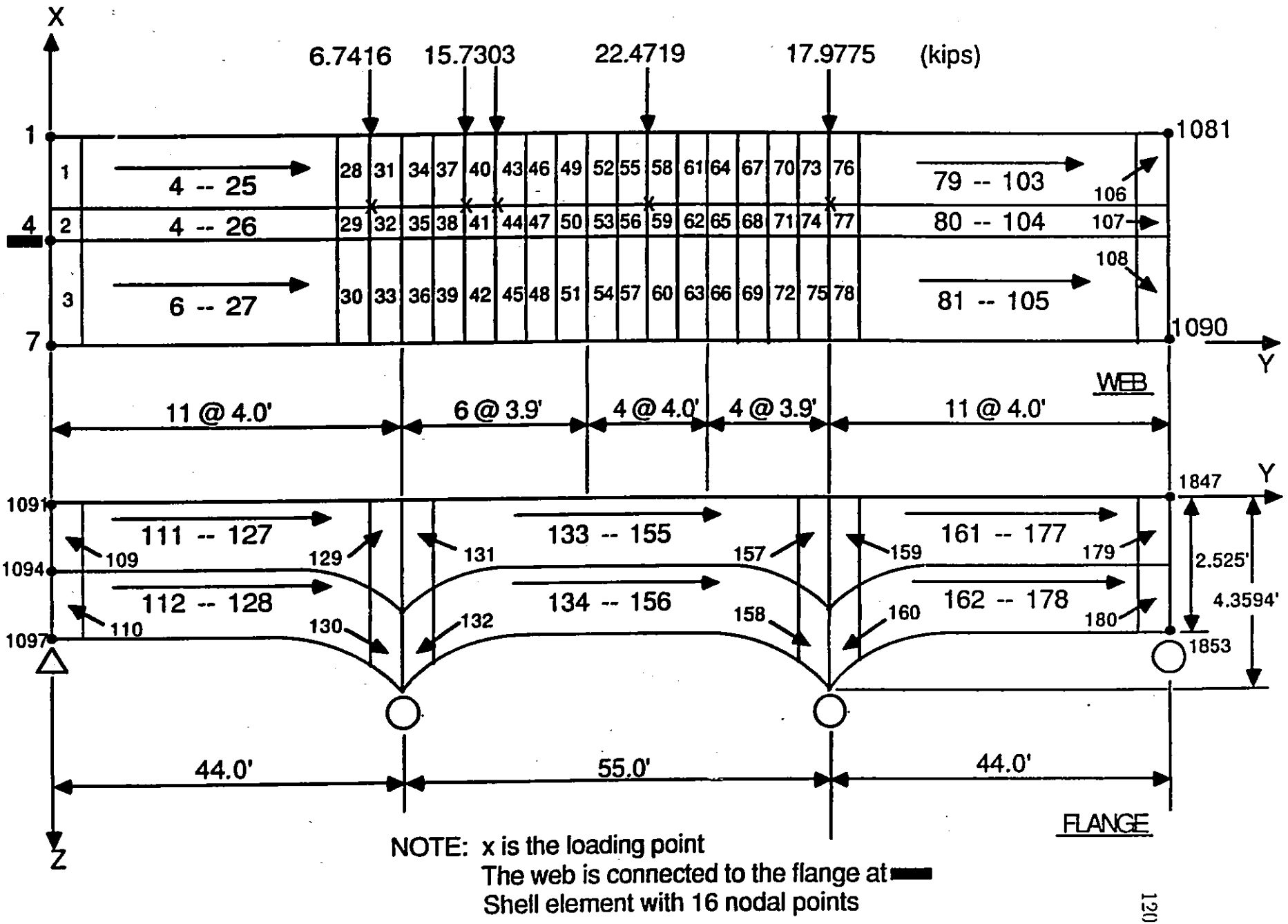

Figure A.10: ADINA MESH (180 ELEMENTS) FOR EXAMPLE 5.3.4